

**Identification and characterization of ADNP as a novel
heterochromatin component**

Dissertation

for the award of the degree

“Doctor rerum naturalium” (Dr. rer. nat.)

Division of Mathematics and Natural Sciences
of the Georg-August-Universität Göttingen

submitted by

Kerstin Mosch

from Dresden

Göttingen 2010

Members of the Thesis Committee:

Dr. Wolfgang Fischle (1st reviewer), Research group Chromatin Biochemistry

Max Planck Institute for Biophysical Chemistry, Göttingen

Prof. Dr. Herbert Jäcke (2nd reviewer), Department of Molecular Developmental Biology

Max Planck Institute for Biophysical Chemistry, Göttingen

Prof. Dr. Matthias Döbelstein, Department of Molecular Oncology

Georg-August-University Göttingen

Prof. Dr. Sigrid Hoyer-Fender, Department of Developmental Biology

Georg-August-University Göttingen

Date of the oral examination: August 11, 2010

I affirm that the presented thesis has been written independently and with no other sources and aids than quoted.

June 30, 2010, Göttingen

Kerstin Mosch

Acknowledgements

First and foremost, I would like to thank my mentor, Dr. Wolfgang Fischle, for his support and guidance. I am grateful for his constructive criticism, all the fruitful discussions, his creative and encouraging ideas that have always been a source of inspiration and motivation.

I am grateful to my thesis committee consisting of Prof. Dr. Hoyer-Fender, Prof. Dr. Herbert Jäckle, and Prof. Dr. Matthias Dobbelsstein for helpful discussions and guidance throughout my PhD project.

I want to thank Dr. Henning Urlaub and his group for their excellent mass spectrometry work, especially Uwe Plessmann and Monika Raabe for mass spectrometry and Miroslav Nicolov for data analysis.

I appreciate the GGNB “Molecular Biology of Microbial, Animal and Plant Cells” program for the constant support, informative lectures, highly supportive method courses as well as inspiring retreats.

I owe Winfried Lendeckel thanks for his trials to produce baculoviral ADNP and for his many hours of purifying histones.

I am thankful to Szabolcs Soeroes for offering me recombinant HP1 and supporting me in the generation of nucleosomal arrays.

I want to thank Kathy Gelato for reading and correcting the manuscript.

Special thanks are dedicated to the members of the Fischle lab for their help and many moments of discussion. In particular, thanks to the “first batch” of PhD students in our group, Henriette, Martina, Nora and Sabi for their friendship, the entertaining hours outside the lab, the badminton trainings and teaching me to cycle.

Lastly, I am grateful to my family, in particular to my parents Gisela und Dietmar Mosch for their constant encouragement, their belief in me, and their continuous support.

Table of contents

ACKNOWLEDGEMENTS	I
TABLE OF CONTENTS	III
LIST OF FIGURES	VII
LIST OF TABLES	VIII
ABSTRACT	IX
ABBREVIATIONS	XI
1 INTRODUCTION	1
1.1 Epigenetics	1
1.1.1 Position–effect variegation	1
1.2 Chromatin	3
1.2.1 Nucleosomes and histones	4
1.2.2 Regulatory role of chromatin	6
1.2.3 Histone modifications	7
1.2.4 Histone modifying enzymes	8
1.2.5 Distribution of histone modifications along chromosomes	9
1.2.6 Reading the histone marks	11
1.2.7 Methylation of histone H3 lysine 9	13
Establishment of H3K9 methylation	13
Biological functions of trimethylated H3K9	14
1.2.8 Heterochromatin Protein 1 (HP1)	15
HP1 chromo domain interactions	15
HP1 chromoshadow domain interactions	16
Model for heterochromatin spreading	17

1.3	Activity-dependent neuroprotective protein (ADNP).....	19
1.3.1	ADNP discovery and structure	19
1.3.2	ADNP expression and distribution	20
	Tissue specific expression.....	20
	Subcellular distribution	21
1.3.3	ADNP Function.....	22
	Neuroprotective function of ADNP	22
	ADNP function in embryogenesis	23
	Nuclear function of ADNP	23
1.4	Objective of the thesis.....	25
2	MATERIAL AND METHODS	26
2.1	Material.....	26
2.1.1	Chemicals.....	26
2.1.2	Buffers and solutions	27
2.1.3	General equipment	29
2.1.4	Antibodies	30
2.2	Molecular biological methods	32
2.2.1	Agarose gel electrophoresis	32
2.2.2	Plasmid manipulation.....	32
2.2.3	cloning.....	36
2.2.4	Preparation of genomic DNA	37
2.2.5	Southern blot analysis	37
2.2.6	RNA isolation	38
2.2.7	cDNA synthesis.....	38
2.2.8	Real time PCR.....	39
2.3	Mammalian cell culture.....	40
2.3.1	Thawing	41
2.3.2	Maintenance	41
2.3.3	Freezing.....	41
2.3.4	Generation of stable cell lines	42
2.3.5	Transfection of siRNA	42
2.4	Cell based assays	43
2.4.1	Dual luciferase assay.....	43

2.4.2	Subcellular fractionation	43
2.4.3	Immunoprecipitation	44
2.4.4	Immunofluorescence	44
2.4.5	Methyltransferase assay	45
2.5	Biochemical methods	46
2.5.1	SDS-PAGE	46
2.5.2	Western Blot	46
2.5.3	generation of oligonucleosomes	47
	Introduction of specific histone post-translational modifications	47
	Reconstitution of histone octamers	47
	Reconstitution of recombinant oligonucleosomes	48
2.5.4	Recombinant proteins	48
2.5.5	Peptide pull-down	49
2.5.6	chromatin pull-down	49
2.5.7	Mass spectrometry and analysis	50
3	RESULTS	52
3.1	Identification of factors associated with H3K9me3	52
3.2	Verification of H3K9me3 association of ADNP	55
3.2.1	ADNP associates with H3K9me3 and pericentromeric heterochromatin	55
3.2.2	ADNP is not alternatively spliced in mouse fibroblasts	60
3.3	Mode of ADNP recruitment to heterochromatin	62
3.3.1	ADNP localization to chromocenters depends on the Homeodomain	62
3.3.2	ADNP does not bind to H3K9me3 directly but is targeted to pericentromeric heterochromatin by HP1	64
3.3.3	ADNP localization to chromocenters mainly depends on HP1 binding to the PxVxL motif within the homeodomain	69
3.3.4	A possible lysine methylation in the ADNP ARKS motif is not involved in HP1 binding	73
3.4	ADNP function at pericentromeric heterochromatin	75
3.4.1	ADNP knockdown does not phenocopy the Brg1 knockout phenotype	76
3.4.2	Knockdown of ADNP does not influence the global level of histone modifications	79
3.4.3	ADNP knockdown has no influence on the localization of HP1 and repressive histone modifications	81
3.4.4	ADNP is not involved in GpG methylation	86

3.4.5	ADNP functions in silencing of major satellite repeats	87
4	DISCUSSION	91
4.1	Identification of H3K9me3 associated proteins	91
4.2	ADNP is a novel component of pericentromeric heterochromatin	92
4.3	ADNP is targeted to pericentromeric heterochromatin by HP1	94
4.4	Mapping of the HP1 – ADNP interaction interface	95
4.5	Nuclear function of ADNP	97
5	REFERENCES.....	101
6	CURRICULUM VITAE.....	112

List of figures

Figure 1-1: Position effect variegation in <i>Drosophila melanogaster</i>	2
Figure 1-2: The organization of DNA within the cell.....	3
Figure 1-3: Structure of the nucleosome core particle.....	5
Figure 1-4: Histone modifications across a typical mammalian chromosome	10
Figure 1-5: Molecular mechanisms of histone modifications.....	11
Figure 1-6: Model for the spreading of heterochromatin.....	18
Figure 1-7: phylogenetic tree of ADNP homologs in different species.....	19
Figure 3-1: experimental setup	53
Figure 3-2: Distribution of the ratios between the heavy and light samples	54
Figure 3-3: ADNP associates with H3K9me3	56
Figure 3-4 ADNP is enriched at pericentromeric heterochromatin	57
Figure 3-5: Localization of ADNP during mitosis	58
Figure 3-6: ADNP localization to pericentromeric heterochromatin depends on Suv39h59	
Figure 3-7: Only full-length ADNP mRNA is detected in mouse fibroblasts.....	61
Figure 3-8: The homeodomain of ADNP is necessary and sufficient for localization to pericentromeric heterochromatin	63
Figure 3-9 All three HP1 isoforms are able to recruit ADNP to H3K9me3.....	64
Figure 3-10: ADNP localization to pericentromeric heterochromatin is HP1 dependent. 66	
Figure 3-11: levels of HP1 γ , ADNP and H3K9me3 as well as H3K9me3 distribution are not affected by HP1 α/β knockout.....	68
Figure 3-12: The PxVxL and ARKS motifs are involved in ADNP localization.....	70
Figure 3-13: The AKRS and PxVxL pointmutations have no influence on ADNP multimerization.	71
Figure 3-14: HP1 chromoshadow domain mutation strongly reduces binding of ADNP	72
Figure 3-15: The ARKS motif of ADNP is not involved in HP1 binding.....	74
Figure 3-16: ADNP knockdown does not influence H3K9me3 localization.	77
Figure 3-17: ADNP knockdown does not influence H4K20me3 distribution.....	78
Figure 3-18: ADNP knockdown.	79

Figure 3-19: ADNP knockdown does not influence global histone modifications	80
Figure 3-20: ADNP knockdown does not influence HP1 α localization.	82
Figure 3-21: ADNP knockdown does not influence HP1 β localization.	83
Figure 3-22: ADNP knockdown does not influence HP1 γ localization.	84
Figure 3-23: ADNP knockdown does not influence H3K27me1 distribution.....	85
Figure 3-24: ADNP knockdown has no influence on CpG-methylation.	86
Figure 3-25: ADNP has silencing activity.	88
Figure 3-26: ADNP influence on major satellite repeat expression	89
Figure 4-1: Structure of mouse HP1 β chromo domain.....	97
Figure 4-2: Model for ADNP recruitment and function	100

List of tables

Table 1-1: Examples of histone marks, the responsible enzymes and their functional context in mammals	8
Table 1-2: domains of human ADNP (Q9H2P0) as predicted by UniProtKB	20
Table 2-1: Antibodies	31
Table 2-2: Cloning details.....	34
Table 2-3: Cell lines and media	40
Table 2-4: Peptides used for the pulldown experiment	49
Table 3-1: Proteins with at least 2-fold enrichment in both experiments.....	54

Abstract

In eukaryotic cells genetic information in the form of long linear DNA fibers is stored in the cell nucleus. Time and tissue specific gene expression patterns are manifested by the combination of DNA with proteins resulting in a structure called chromatin. The basic repeating element of chromatin is the nucleosome, where DNA is wrapped around an octamer of histone proteins, interconnected by sections of linker DNA. Both DNA and histones are subject to chemical modifications, which are associated with certain chromatin states. Several factors that set or recognize such modifications have been described in the recent years.

Heterochromatin is a chromatin form that is characterized by compaction, transcriptional inactivity and late replication in S-phase. It is associated with methylation of DNA and histones. Trimethylation of histone H3 lysine 9 (H3K9me3) is one hallmark of heterochromatin, and is mediated by the methyltransferase Suv39 and recognized by heterochromatin protein 1 (HP1), which has three isoforms in mammalian cells. How these and other enzymes and factors establish and maintain distinct chromatin states is not yet completely understood.

For a better understanding of factors involved with heterochromatin I used stable isotope labeling by aminoacids in cell culture (SILAC) in a H3K9me3 pull-down experiment to identify new interaction partners. Activity dependent neuroprotector (ADNP) was one such factor that had not been described in a heterochromatin context before. Association of ADNP with H3K9me3 was verified with independent experiments and the factor was further characterized.

Cell based and *in vitro* assays suggested that ADNP does not bind to H3K9me3 directly but is targeted to this modification by HP1. This recruitment of ADNP to H3K9me3 could be mediated by all three isoforms of HP1. Mapping of the interaction interface revealed a major contribution of the HP1 chromoshadow domain binding to a PxVxL motif within the ADNP homeodomain. Mutation of the PxVxL motif caused partial delocalization from heterochromatin. An additional mutation of an ARKS motif, which is

also present in the ADNP homeodomain, enhanced this effect. However, involvement of a possible lysine methylation in that motif in HP1 binding was not detected.

To determine the function of ADNP I used knock-down in cells by siRNA. I analyzed whether ADNP influences typical heterochromatin features such as distribution of histone modifications as well as HP1 localization as well as DNA methylation state. However, no effect on these properties could be detected. In luciferase reporter assays ADNP displayed transcriptional silencing potential. Knock-down and overexpression experiments suggested, that ADNP is specifically involved in silencing of major satellite repeats in pericentromeric heterochromatin. Further studies are needed to address by which mechanism ADNP exerts this silencing function.

Altogether, in this work I identified ADNP as a novel component of pericentromeric heterochromatin, which is recruited by HP1 and acts in silencing of major satellite repeats. This study deepens the understanding of how the Suv39/H3K9me3/HP1 pathway impacts chromatin function.

Abbreviations

ac	Acetylation
ADP	Adenosine diphosphate
ADNP	Activity dependent neuroprotector
BD	Bromodomain
BSA	Bovine serum albumine
C	Celsius
CD	Chromodomain
ChIP	Chromatin immunoprecipitation
cDNA	Complementary DNA
CMV	Cytomegalovirus
CSD	Chromoshadow domain
DAPI	4',6-diamidino-2-phenylindole
DIG	Digoxigenin
DMEM	Dulbecco's Modified Eagle's Medium
DMSO	Dimethylsulfoxid
DNA	Desoxyribonucleic acid
DNMT1	DNA methyltransferase 1
dNTPs	Desoxyribonucleotide triphosphates
dpt	Days post transfection
DTT	DL-1,4-dithiothreitol
E.coli	Escherichias coli
EDTA	Ethylenediaminetetraacetic acid
FDR	False discovery rate
h	Hour
H3K9me3	Histone H3 lysine 9 trimethylation
HAT	Histone acetyltransferase
HDAC	Histone deacetylase

HEK293	Human embryonic kidney 293 cell line
HeLaS3	Human cervix epithel carcinoma cell line
HEPES	2-[4-(2-hydroxyethyl)-1-piperazinyl]-ethanesulfonic acid
His	Histidine
HMT	Histone methyltransferase
HP1	Heterochromatin protein 1
HRP	Horse radish peroxidase
IF	Immunofluorescence
Ig	Immunoglobulin
IP	Immunoprecipitation
IPTG	Isopropylthio-b-D-galactoside
kDa	Kilo Dalton
me	Methylation
MEF	Mouse embryonic fibroblast cell line
min	Minutes
NAP	Neuroprotective peptide sequence in ADNP: NAPVSIPQ
NURD	Nucleosome remodeling and deacetylase complex
OD	Optical density
PBS	Phosphate buffered saline
PCR	Polymerase chain reaction
ph	Phosphorylation
PNV	Packed nuclear volume
PTM	Post translational modifications
RNA	Ribonucleic acid
rpm	Rounds per minute
RT	Room temperature
RT-PCR	Reverse transcriptase PCR
SDS	Sodium dodecyl sulfate
SDS-PAGE	Sodium docecyl sulfate polyacrylamide gel electrophoresis
SILAC	Stable isotope labeling with amino acids in cell culture
Suv39h	Suppressor of variegation 3-9 homolog

s	Second
TK	Tyrosine kinase
UAS	Upstream activator sequences
UTR	Untranslated regions
VIP	Vasoactive intestinal peptide
wt	Wild type, original sequence without mutations

1 Introduction

1.1 Epigenetics

The term epigenetics was coined by C. H. Waddington for the study of “causal mechanisms” by which “the genes of the genotype bring about phenotypic effects”. Today an epigenetic phenomenon is defined as a change in phenotype that is heritable but does not involve DNA mutation (Allis, 2007).

In principle all tissue-specific somatic cells contain the same genetic information, which is contained within the linear DNA sequence (the genome). However, each cell type is characterized by specific gene expression patterns that need to be established and inherited throughout cell division. Transcription factors and chromatin proteins that are associated with DNA play important roles for cell type-specific gene expression. Epigenetic modifications such as DNA methylation or covalent modifications to histones as well as chromatin remodeling mediate stable activation or repression of genes in specific cell types.

1.1.1 Position–effect variegation

The first description of a phenomenon with an underlying epigenetic basis has been provided by the discovery of position–effect variegation (PEV) (Muller and Altenburg, 1930). Muller described mutations of the white⁺ (w⁺) eye color gene of *Drosophila* that resulted in a variegating phenotype, with some patches of red and some patches of white facets. The mosaic phenotypes were caused by a chromosomal inversion or rearrangement in one breakpoint within the pericentromeric heterochromatin and the other adjacent to the white gene (Figure 1-1). Thus, the w⁺ gene has been displaced from its normal euchromatic location and was placed in the vicinity of heterochromatin. This

pattern of variegation suggested that a decision to express or repress the w^+ gene was made early during tissue development and was maintained in a metastable state through multiple cell divisions.

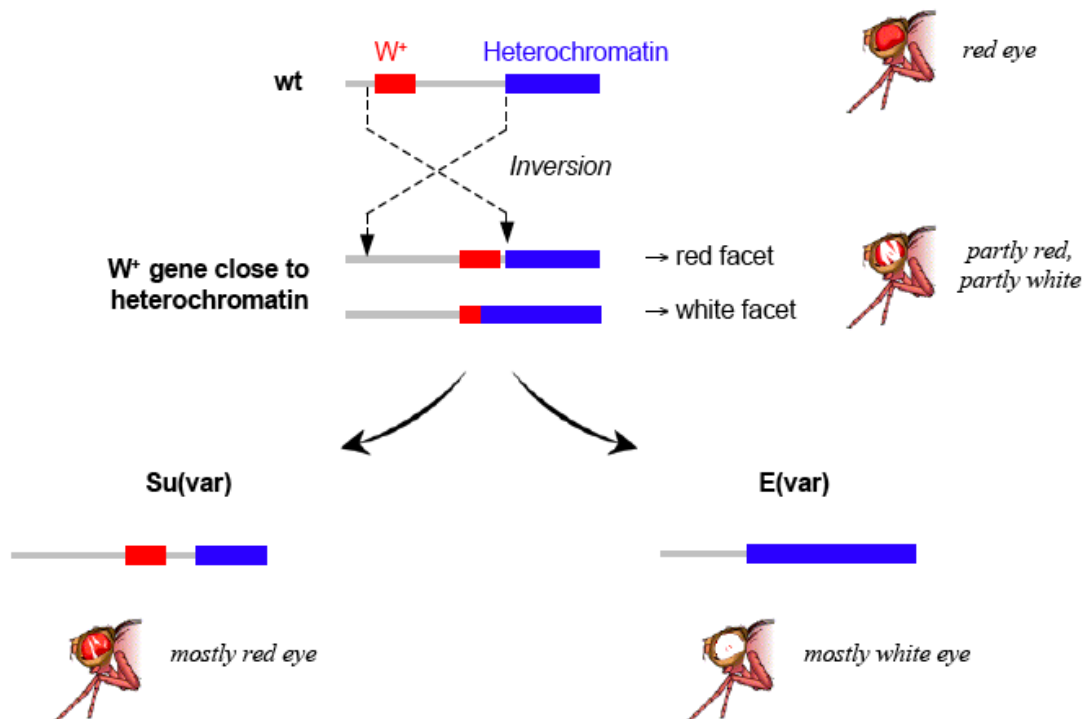


Figure 1-1: Position effect variegation in *Drosophila melanogaster*

In wild-type flies the gene responsible for the red eye pigmentation (white, w^+ , depicted in red) is located within distal euchromatin. A gene inversion relocated the gene in close proximity to pericentromeric heterochromatin, resulting in a variegating phenotype: In some cells, the white gene is still regularly expressed, normally leading to red eye facets whereas in others it is silenced by heterochromatin spreading, causing white eye facets (Dormann, 2009).

Because the variegating phenotype is caused by a change in the position of the gene within the chromosome, this phenomenon is referred to as position-effect variegation (PEV). PEV has been used as a model system to systematically screen for factors that positively or negatively regulate heterochromatin formation.

Approximately 120 loci with roles as dominant Suppressors ($Su(var)$ s) or Enhancers ($E(var)$ s) of PEV have been identified so far in genetic screens (Reuter et al., 1987; Wustmann et al., 1989), but the expected number is likely to be higher since the genome

has not yet been saturated for modifiers of PEV. Molecular analyses of several dozen modifier genes suggest diverse functions and confirm the expectation that only a subset is likely to be directly involved in heterochromatin formation.

1.2 Chromatin

The genetic information of eukaryotic cells is stored in the form of DNA, which reaches the length of 2 meters in human cells (Avery et al., 1944). To fit into the cell nucleus organization and compaction of DNA ‘fibers’ is required. Association of DNA with a set of nuclear proteins mediates this task. The resulting structures are called chromatin (Figure 1-2), the physiological form of all genetic and inheritable information in eukaryotic systems (Felsenfeld and Groudine, 2003).

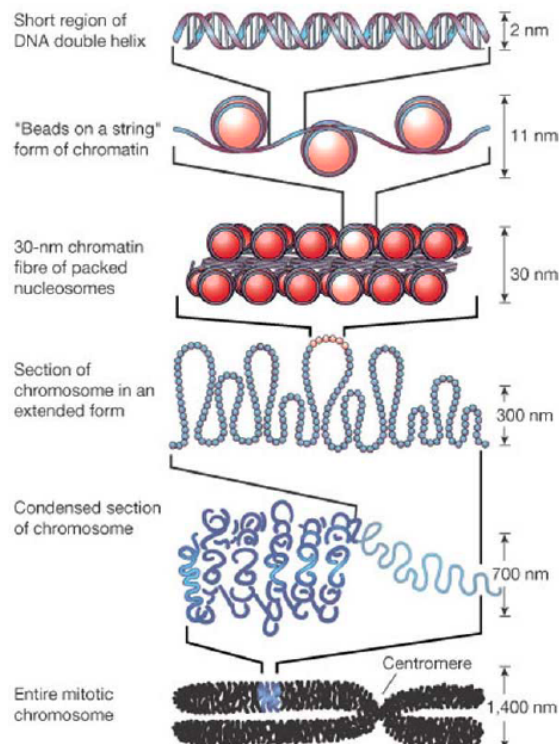


Figure 1-2: The organization of DNA within the cell

The double helix of DNA is wrapped around octamers of histone molecules, forming nucleosomes in a 'beads on a string' formation. Further folding into a 30 nm fiber and higher-order structures compacts DNA more than 10,000-fold (adapted from (Felsenfeld and Groudine, 2003).

Chromatin consists of different functional areas and domains first defined in cytological studies by Heitz et al. as euchromatin and heterochromatin (Heitz, 1928). Heterochromatin retains its deep staining, condensed appearance throughout the cell cycle, including interphase, whereas euchromatin appears diffuse during interphase. Euchromatin has an open, accessible conformation, replicates early in S-phase, and contains the majority of active genes. Heterochromatin, in contrast, is tightly compacted, replicates late in the cell cycle, and contains very few active genes. It can be divided into constitutive heterochromatin which includes regions of the genome that are heterochromatic in all types of cells and at all times (e.g. centromeres, pericentric regions and telomeres) and facultative heterochromatin, which can change its status during development or differentiation.

1.2.1 Nucleosomes and histones

The basic repeating element of chromatin is the nucleosome (Kornberg, 1974; Olins and Olins, 1974), which consists of 147 bp of DNA wrapped around an octamer of histone proteins – two copies each of the histones H2A, H2B, H3 and H4 (Figure 1-3) (Luger et al., 1997). In addition, a linker histone H1 (and, in some organisms, H5), interacts with the nucleosomal core as well as with the interconnecting linker DNA to form higher levels of chromatin organization and architecture (Thomas, 1999).

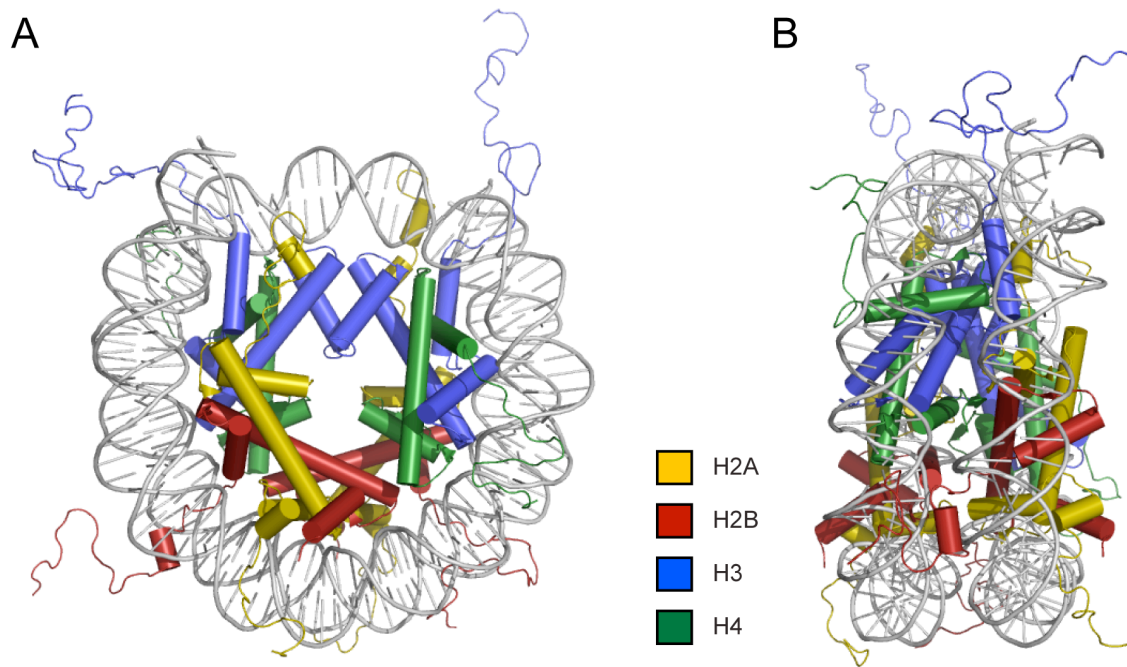


Figure 1-3: Structure of the nucleosome core particle

A, Crystal structure of the nucleosomal core particle, front view. DNA is shown in grey, core histones are depicted in the indicated colors. α -helical structures are shown as cylinders. **B**, Same structure in side view (Davey et al., 2002).

Histones represent a highly conserved family of small basic proteins containing many lysine and arginine residues in their N-terminal tails. Structurally, they consist of a ‘helix turn helix turn helix’ motif called ‘histone fold’ and relatively unstructured ‘histone-tails’. In solution histone H2A-H2B and H3-H4 heterodimers are formed by head-to-tail association of the histone-fold-helices (Arents et al., 1991). The octamer is held together by three four-helix bundles between the above mentioned histone heterodimers: one H3-H3 association forms the $(\text{H3-H4})_2$ tetramer and two H2B-H4 interactions connect the $(\text{H3-H4})_2$ tetramer with two H2A-H2B dimers. The DNA is wrapped around the resulting globular structure mainly by interaction between the basic histones and the negatively charged DNA-backbone (Luger et al., 1997). The flexible N-terminal histone tails protrude outwards from the nucleosome core (Davey et al., 2002; Luger et al., 1997) making them available for interactions with non-histone chromatin factors or with adjacent nucleosomes (Angelov et al., 2001; Bertin et al., 2007; Mangenot et al., 2002).

1.2.2 Regulatory role of chromatin

Chromatin is not only a protective and static scaffold for storage of genetic information. Dynamic changes in chromatin are involved in regulation of all genomic processes such as transcription, replication, mitotic chromosome condensation, and recombination as well as apoptosis and DNA repair (Felsenfeld and Groudine, 2003; Prigent and Dimitrov, 2003; van Attikum and Gasser, 2009).

Chromatin function is regulated by changes in chromatin structure and through the recruitment of specific effector proteins. Structural changes such as chromatin compaction or decondensation significantly affect the accessibility of DNA and thus can control various processes that require access to the DNA template (Hansen, 2002). Changes in chromatin structure can be achieved through chromatin remodeling complexes, the incorporation of histone variants and the addition or removal of posttranslational modifications of histone proteins (Allis, 2007). Several distinct posttranslational modifications on chromatin including covalent modifications of DNA and histones serve as epigenetic marks to recruit specific nuclear factors that in turn mediate downstream functions (Seet et al., 2006; Strahl and Allis, 2000; Taverna et al., 2007).

DNA methylation provides the most direct epigenetic mechanism for the maintenance of the repressed state. Methylation of DNA within the mammalian genome is catalyzed by a family of DNA (cytosine-5)-methyltransferases and occurs primarily at CpG dinucleotides. CpG methylation, especially within the promoter region of genes, is associated with stable transcriptional repression and plays important roles for X-chromosome inactivation and genomic imprinting (Bestor, 2000; Reik et al., 2001).

The N-terminal tails of histones are targets for a number of post-translational modifications (Fischle et al., 2003b). Covalent histone modifications are proposed to

provide a storage mechanism for mitotically and meiotically inheritable information that can be 'read' by various effector proteins. By regulating access to underlying DNA, histone modifications and effector proteins dictate correct cell type specific gene expression patterns (Jenuwein and Allis, 2001).

1.2.3 Histone modifications

Histones can be extensively post-translationally modified (Allfrey, 1966). Over the last decades, an enormous number of distinct posttranslational modification types and sites have been identified on histones ("marks"), especially since the introduction of mass spectrometric approaches. In particular, the histone tails have been found to be subject to a great variety and high density of posttranslational modifications. Lysine residues in histones can be modified by acetylation (Kac), (mono-, di-, or tri-) methylation (Kme1/2/3), ubiquitylation and sumoylation (Kub and Ksu); arginine residues can be (mono-, and symmetrically/asymmetrically di-) methylated (Rme1/2), serine and threonine residues can be phosphorylated (Sph and Tph), and glutamate residues can be ADP-ribosylated (Kouzarides, 2007; Peterson, 2004). Close to a hundred individual histone marks have been identified to date, about half of which have been confirmed by independent experimental methods.

The complexity of histone modifications gives an enormous potential for functional responses. Histone acetylation, for example loosens chromatin packing and correlates with transcriptional activation, whereas histone deacetylation is generally associated with transcriptional repression (Struhl, 1998). Notably, distinct histone modifications may act sequentially or in combination to form a 'histone code' that is read by other proteins to bring about distinct downstream events. Strictly speaking the histone code hypothesis predicts that a pre-existing modification affects subsequent modifications on histone tails and that these modifications serve as marks for the recruitment of different proteins or protein complexes to regulate diverse chromatin functions, such as gene expression, DNA replication and chromosome segregation (Jenuwein and Allis, 2001). Furthermore

epigenetic marks are important for mammalian telomere formation (Grunstein, 1997) and position effect variegation (Weiler and Wakimoto, 1995).

1.2.4 Histone modifying enzymes

Several distinct classes of enzymes can modify histones at several sites. Among the enzymes that establish histone marks ("writers") are histone acetyltransferases (HATs) (Sternier and Berger, 2000), histone kinases (Nowak and Corces, 2004), histone methyltransferases (HMTases) (Qian and Zhou, 2006; Zhang and Reinberg, 2001), and enzymes that mediate histone ubiquitylation (Weake and Workman, 2008), sumoylation (Nathan et al., 2006), and ADP-ribosylation (Hassa et al., 2006) (Table 1-1).

Histone	Site	Enzyme	function
H2A	K5ac	Tip60, p300	Transcriptional activation
	K119ub1	RING1B	UV damage response
H2B	S14ph	Mst1	Apoptosis
H3	K4me1	SET7/Set9	Transcriptional activation
	K4me3	SMYD3	Transcriptional activation
	K9ac	SRC1	Nuclear receptor coactivation
	K9me3	Suv39h1/H2	Transcriptional repression
	S10ph	AuroraB	Mitotic chromosome condensation
	K27me3	EZH2	X-chromosome inactivation
H4	R3me	PRMT1	Transcriptional activation
	K5ac	P300	Transcriptional activation
	K20me3	Suv4-20h1/h2	Transcriptional repression

Table 1-1: Examples of histone marks, the responsible enzymes and their functional context in mammals

Adapted from Allis et al., 2007. For references and a more complete list, see there.

Most histone marks have been shown to be reversible. Enzymes that can remove specific histone modifications ("erasers") include histone deacetylases (HDACs) (Holbert and Marmorstein, 2005), phosphatases (Nowak and Corces, 2004) and lysine demethylases (Agger et al., 2008). Arginine methylation can be reversed by demethylation or deimination (Chang et al., 2007). In addition proteolytic clipping of histone tails (Allis et al., 1980; Duncan et al., 2008) and histone replacement (Ahmad and Henikoff, 2002) result in the removal of histone marks.

1.2.5 Distribution of histone modifications along chromosomes

Large scale genome-wide approaches such as amplification of immunoprecipitated DNA and hybridization to tiling oligonucleotide microarrays (ChIP-chip) (Bernstein et al., 2006; Heintzman et al., 2009) or direct massive parallel sequencing of short fragments of ChIP DNA (ChIP-seq) (Barski et al., 2007; Mikkelsen et al., 2007) have been used to map histone modifications. In these studies, distinctive sets of modifications have been associated with different functional regions along the mammalian chromosomes (Figure 1-4). The spatial distribution can be divided in two general classes: (i) large arrays of modified nucleosomes spanning several kb (Figure 1-4); and (ii) a few highly localised modified nucleosomes occurring in punctuate peaks within 1 kb (Figure 1-4).

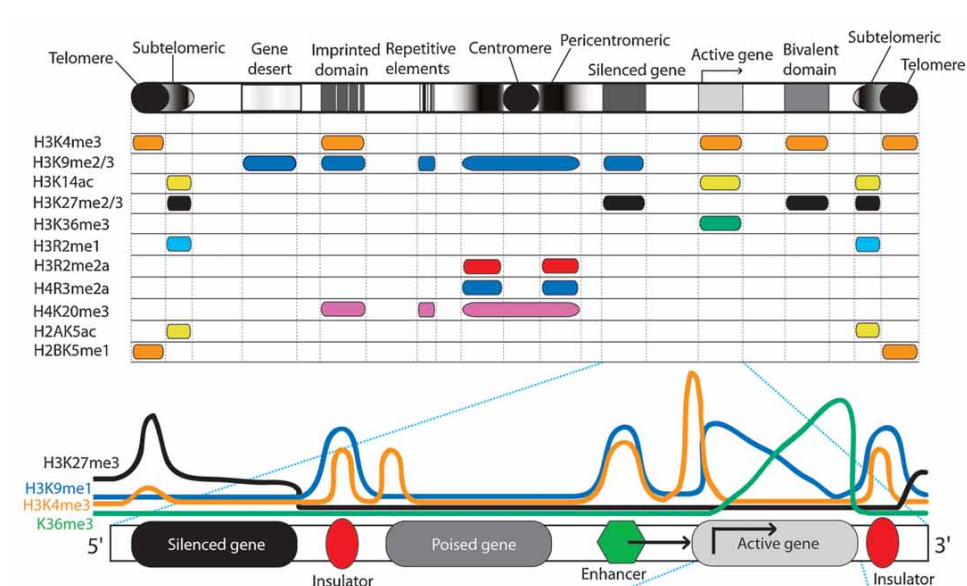


Figure 1-4: Histone modifications across a typical mammalian chromosome

Schematic representation of histone modifications across a typical mammalian chromosome and composite profile of typical histone modifications associated with silenced, poised, active genes and associated regulatory elements. Ac: acetylation, me1/me2/me3: mono/di/trimethylation, me2a: asymmetrical dimethylation (Wang et al., 2009).

A large portion of mammalian genomes is composed of non-genic chromosomal features that are derived from DNA transposons, retrotransposons, satellite repeats and structures that form telomeres and centromeres (Lander et al., 2001). These are largely constitutive heterochromatin features, associated with repressive modifications (Martens et al., 2005) (Barski et al., 2007; Mikkelsen et al., 2007).

Pericentromeric heterochromatin for example, is gene-poor, rich in repetitive satellite elements and interspersed with long and short interspersed nuclear elements (LINEs and SINEs, respectively). It is enriched in H3K9me3, H4K20me3 and H3K27me1 but is also associated with H3R2me2a and H4R3me2a (Figure 1-4 a) (Peters et al., 2003; Rosenfeld et al., 2009). Consistent with the presence of H3R2me2a, which has been reported to inhibit H3K4 methylation and binding of H3K4me3-effectors, H3K4me3 is excluded from pericentromeric regions (Guccione et al., 2007; Iberg et al., 2008).

Genic regions including genes, promoters, enhancers and insulators are characterized by complex short-range histone modification patterns. Silent genes can be distinguished from non-genic regions by a greater enrichment of H3K27me3 (Rosenfeld et al., 2009). These regions are also associated with H3K9me2/3 but lack H4K20me3 compared to centromeric regions (Rosenfeld et al., 2009). Promoters of silent CpG-rich genes are often associated with H3K27me3 in conjunction with H3K4me3, while those of inactive CpG-poor genes are devoid of H3K4me3 (Mikkelsen et al., 2007).

Transcriptionally active areas of the genome are largely associated with acetylation of lysines or methylation of H3K4 and H3K36 (Lee and Mahadevan, 2009; Wang et al., 2009). While H4K12ac and H3K36ac cover the whole gene region, other modifications are distributed only around the transcriptional start site (H3K4me, H3K9ac and H3K18ac) or the body of genes (H3K36me3) (Lee and Mahadevan, 2009; Wang et al., 2009).

1.2.6 Reading the histone marks

Histone modifications either modulate chromatin structure directly ('cis') or they act in 'trans' by recruiting binding partners that induce and direct downstream functions (Figure 1-5, (Allis, 2007)).

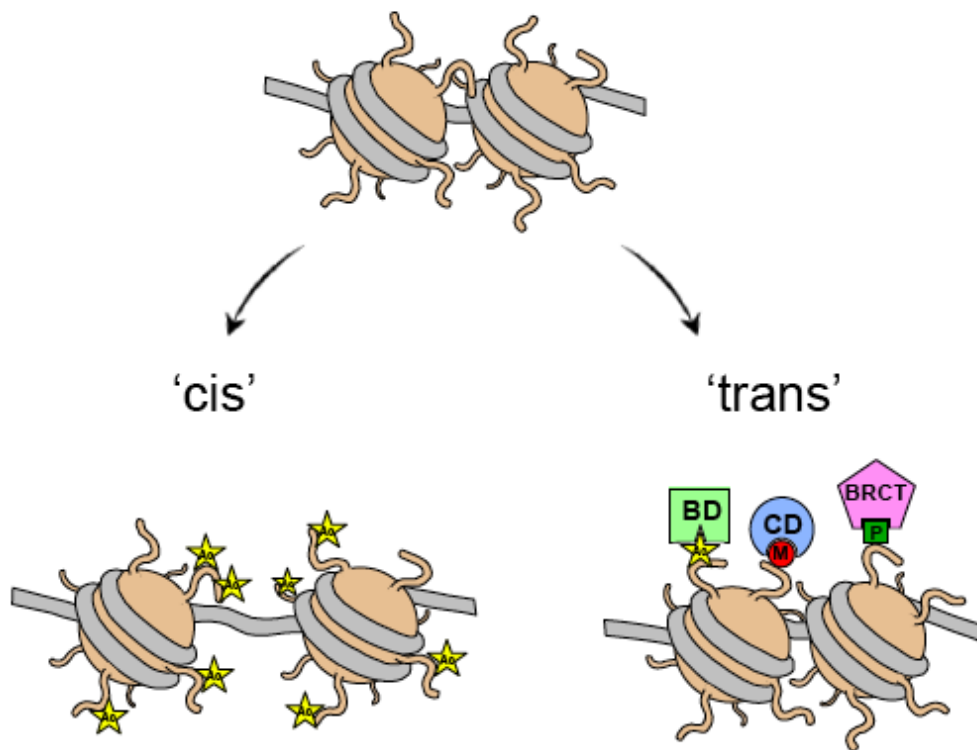


Figure 1-5: Molecular mechanisms of histone modifications

Histone modifications fulfill their function by two general mechanisms. They either change the net charge of the histone tail, which affects inter/intranucleosomal contacts and results in structural changes of the chromatin fiber ("cis" mechanisms, left). Or they recruit proteins with specific binding modules, which mediate downstream functions ("trans" mechanisms, right). Ac: acetylation. M: methylation. P: phosphorylation. BD: bromodomain. CD: chromodomain. BRCT: Breast-cancer-susceptibility protein-1 C-terminal domain (Dormann, 2009)

Modifications may affect higher-order chromatin structure by affecting the interaction of histones with DNA or the contact between different histones in adjacent nucleosomes. Acetylation has the greatest potential to unfold chromatin since it neutralizes the positive charge of the lysine residue. Chromatin condensation can be blocked by a certain amount of acetylation in general (Hansen, 2006; Hansen et al., 1998). In vitro studies have shown that acetylation of H4K16 has a negative effect on the formation of a 30-nanometer fiber and the generation of higher-order structures (Shogren-Knaak et al., 2006) whereas deacetylation of H4K16 facilitates compaction of chromatin (Johnson et al., 2009). Phosphorylation might also have consequences on chromatin compaction via charge changes (Johansen and Johansen, 2006).

In the trans mechanism, effector mediated changes are elicited in the chromatin fiber due to specific binding events that couple a particular histone modification with a cognate non-histone binding partner. Effector proteins may alter the properties of chromatin by crosslinking two or more nucleosomes (Francis et al., 2004; Nielsen et al., 2001a; Zhao et al., 2000), by affecting the RNA polymerase complex and related factors (Vermeulen et al., 2007) or by recruiting chromatin remodeling or further chemical modification activities (Jenuwein and Allis, 2001).

A number of specific binding proteins ("readers") have been identified over the last years. *Bromodomains* may specifically engage acetylated lysines, particularly in histone sequence contexts (Dhalluin et al., 1999). These are found in transcription factors and chromatin remodeling complexes that are associated with active transcription (Zeng and Zhou, 2002). Recruitment of bromodomain containing factors to promoter regions has been demonstrated to activate transcription in several model systems (Agalioti et al., 2002; Agalioti et al., 2000; Cosma et al., 1999; Mujtaba et al., 2007). *Chromo domains* act as binding modules for methylated lysines. Proteins containing a chromo domain include Heterochromatin Protein 1 (HP1), which recognizes H3K9me2/3 and Polycomb, a H3K27me3 binding factor. HP1 is involved in gene silencing and heterochromatinization (Jacobs and Khorasanizadeh, 2002; Jacobs et al., 2001; Lachner et al., 2001). Polycomb mediates repression and has important functions in development

(Fischle et al., 2003c).

Plant homeo domains (PHD), *Tudor domains (TD)* and *malignant brain tumor(MBT) repeat domains*, which belong, along with the Chromo domains, to the ‘*royal family*’ represent additional methyl-lysines binding modules (Adams-Cioaba and Min, 2009). Furthermore, proteins/domains that recognize phosphorylation such as the 14-3-3 protein family and WD40 domains (Seet et al., 2006), as well as ubiquitin binding domains (Hofmann, 2009) have been characterized as histone modification binding proteins.

The abundance of post-translational modifications on the histone tail makes ‘crosstalk’ between modifications very likely. First, the binding of a protein can be affected by an adjacent modification as has been shown for the H3K9me3 binding of HP1, which is disrupted by H3S10 phosphorylation (Fischle et al., 2005). Second, the modification of the recognition site may influence substrate recognition or the catalytic activity of an enzyme. For example the acetyltransferase GCN5 recognizes H3 more effectively when it is phosphorylated at H3S10 (Clements et al., 2003). Also cis/trans isomerization of H3P38 affects methylation of H3K36 by Set2 (Nelson et al., 2006). Communication between modifications can also occur when modifications are on different histone tails as in the case of H2B ubiquitination being required for H3K4 and H3K79 methylation.

1.2.7 Methylation of histone H3 lysine 9

Establishment of H3K9 methylation

H3K9 is methylated by diverse HMTases which can interact with a variety of factors. In mammals, the histone methyltransferases G9a and G9a-like protein GLP monomethylate lysine 9 of histone H3 (Collins et al., 2008). Di- or trimethylation of histone H3 lysine 9 is mediated by Suv39h1/h2 as well as ESET/SETDB1 histone methyltransferase (Kouzarides, 2007; Wang et al., 2003). Interaction of the histone methyltransferases with DNA-binding proteins as well as with small RNAs is also involved in the methylation process (Grewal and Elgin, 2007). SETDB1 is mainly found in euchromatic regions,

where it participates in gene silencing (Schultz et al., 2002). In contrast, Suv39-like enzymes mainly localize to pericentromeric heterochromatin. Suv39h1/h2 double knockout mice fail to show H3K9 trimethylation at these loci (Aagaard et al., 1999; Peters et al., 2003). Therefore, it is likely that Suv39h1/h2 is the main HMTase establishing H3K9 trimethylation at heterochromatic regions.

The first demethylating enzyme of H3K9 methylation that has been described is LSD1, which acts in a complex with the androgen receptor and activates transcription (Metzger et al., 2005). Other H3K9 demethylases include the jumonji proteins JHDM2A, JMJD2A/JHDM3A, JMJD2B, JMJD2C/GASC1 and JMJD2D (Kouzarides, 2007). The exact mechanism and occurrences of these demethylation events are not well understood so far.

Biological functions of trimethylated H3K9

H3K9 methylation has mainly been linked to heterochromatic domains and gene silencing. For example, Suv39h1 mediated methylation is associated with transcriptionally inert regions at pericentric heterochromatin in mammals (Lachner et al., 2001; Peters et al., 2001). Loss of the Suv39h HMTase activities in mutant mice impairs pericentric H3K9 methylation but does not affect the broad methylation at the chromosome arms (Peters et al., 2001). Mice lacking Suv39h1/h2 enzymes display impaired viability, overall genomic instability in both mitotic and meiotic cells, an increased risk for B-cell lymphomas and complete spermatogenic failure, suggesting a potential role in tumor suppression, mitosis and meiosis (Peters et al., 2001).

H3K9 methylation is not restricted to constitutive heterochromatin. The Suv39h1 HMTase is also recruited to euchromatic targets, through interaction with HP1 and by the tumor suppressor retinoblastoma protein (pRb), where it is also involved in gene repression (L. Vandel, 2001; Nielsen et al., 2001b).

Notably, H3K9 methylation has been shown to have a direct impact on DNA

methylation. One of the three mammalian isoforms of HP1, HP1 α interacts with the DNA methyltransferase DNMT3b and targets it to heterochromatic foci. However, in Suv39h1/h2 double-null cells it fails to localize to these regions. Consistently, Suv39h1/h2 knockout cells display an altered DNA methylation profile at major satellite repeats but not at other repeat sequences (Lehnertz et al., 2003).

How one modification can be involved in regulating so many functions at such distinct chromatin environments is not well understood. The induction of an H3K9 HMTase-dependent chromatin configuration could require the combination of two or more signals that involve a defined pre-existing modification pattern of the associated nucleosomes and/or the presence of a 'specific' DNA or RNA sequence. Subsequently, the overall density of methylated nucleosomes might contribute to the distinct qualities of H3K9 methylation in constitutive versus facultative heterochromatin and in euchromatin (Maison et al., 2002; Peters et al., 2001).

1.2.8 Heterochromatin Protein 1 (HP1)

HP1 proteins consist of an N-terminal chromo domain (CD), a flexible hinge region and a C-terminal chromoshadow domain (CSD).

HP1 chromo domain interactions

The chromo domain was originally described as a domain of about 40 amino acids that was present in various proteins involved in chromatin organization and gene regulation (Koonin et al., 1995). The CD of HP1 is a binding module for H3K9me3 (Bannister et al., 2001; Jacobs et al., 2001; Lachner et al., 2001). Interestingly, the amino acid context of H3K9 ("ARKS") is found in identical or similar form at multiple other sites in histones and other proteins. The corresponding lysines have been found to be methylated in several of these instances: H3K27: ARKmeS binds Polycomb (Fischle et al., 2003c), H1K26: ARKmeS binds HP1 (Daujat, 2005), G9aK165: ARKmeT binds HP1 (Sampath

et al., 2007). Additional modifications such as lysine acetylation and serine phosphorylation occurring in this sequence stretch suggest that ARKS and related sequences might act as "modification cassettes" which confer the ability for the recruitment of specific binding partners (Fischle et al., 2003a).

Disruption of the H3K9me_{2/3} – HP1 interaction by mutations in the CD or removal of the H3K9me mark results in mislocalization of HP1 in flies, *S. pombe* and mammals (Fischle et al., 2003c; Platero J.S., 1995; Platero et al., 1995; Stewart et al., 2005; Thiru et al., 2004). Thus, binding of the chromo domain to the modified H3 tail is essential for recruitment of HP1 to chromatin.

HP1 chromoshadow domain interactions

The structure of the chromoshadow domain bears some resemblance to the chromo domain (a three-stranded β sheet packed against two α helices; (Cowieson et al., 2000). However, it does not engage a histone modification, but rather mediates a wide array of protein interactions. The HP1 CSD mediates homodimerization with the same HP1 isoform as well as heterodimerization between different HP1 isoforms (Brasher et al., 2000; Cowieson et al., 2000; Gaudin et al., 2001; Thiru et al., 2004).

A phage display screen carried out with the HP1 CSD identified a pentapeptide motif PXVXL (X = any amino acid) that interacts specifically with the chromo shadow domain (Smothers and Henikoff, 2000). Binding of proteins with the PXVXL motif to HP1 requires dimerization of the CSD, which generates a hydrophobic groove that the peptide motif associates with (Thiru et al., 2004). The peptide motif has been shown to be present in many reported interaction partners of the HP1 CSD, for example in KAP-1 (Brasher et al., 2000), Su(var)3-7 (Delattre et al., 2000), CAF-1 p150 (Brasher et al., 2000), the TAFII130 component of TFIID (Vassallo and Tanese, 2002), and AF10 (Linder et al., 2001). This HP1 binding to transcriptional repressors could provide the means for initial recruitment of HP1 to specific regions of chromatin. Rb, for example, has been reported to recruit HP1 β to the cyclin E promoter and induce tri-methylation of H3K9 by Suv39h1

(Nielsen et al., 2001b). Suv39h1 itself also interacts physically with HP1 via interaction with the CSD (Aagaard et al., 1999; Melcher et al., 2000).

The binding of HP1 to a variety of interaction partners such as DNA methyltransferases, histone methyltransferases and transcriptional repressors (Brasher et al., 2000; Lehnertz et al., 2003; Schotta et al., 2004) suggests a role of HP1 is to serve as a platform for the recruitment of downstream factors to H3K9me3. However, as for the modification itself it is unclear how HP1 distinguishes between different interaction partners to exert its function in the different contexts.

Model for heterochromatin spreading

As described above, Suv39h1 functionally interacts with the chromo domain of HP1. Suv39h1 methylates H3K9 and thus generates a binding site for the HP1 CD that is essential for HP1 recruitment to chromatin. The interaction between Suv39h1 and the HP1 CSD suggests a mechanism for the spreading and maintenance of heterochromatic structures and epigenetic gene silencing. According to this model, Suv39h1, the histone H3 tail and HP1 collaborate to form a self-sustaining loop. Methylated H3K9me recruits HP1, which in turn directs more Suv39h1 histone methyltransferase to chromatin, enabling further methylation (Figure 1-6).

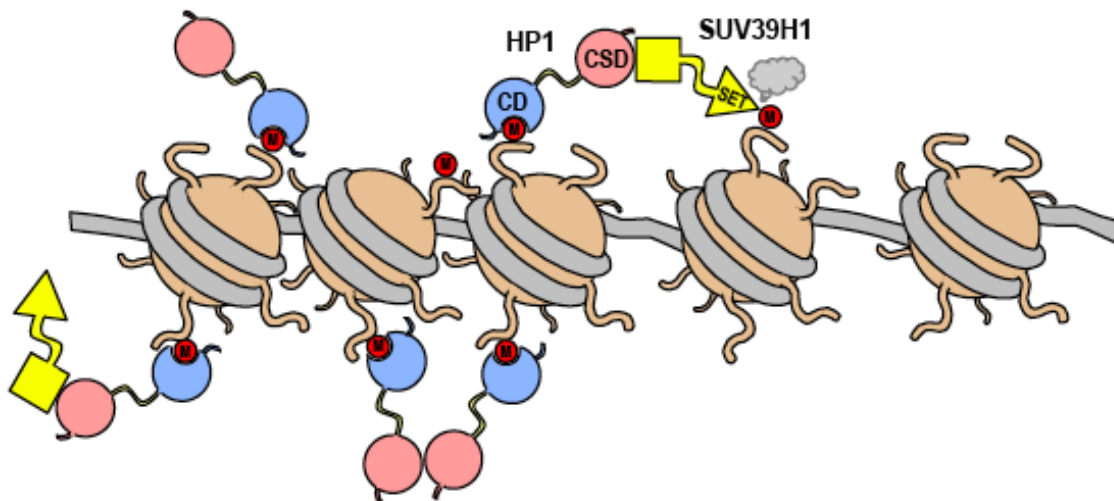


Figure 1-6: Model for the spreading of heterochromatin

The histone mark H3K9me (small red circle "M") recruits the effector protein HP1 via its chromo domain (CD) to chromatin. HP1 crosslinks nucleosomes and recruits effector proteins such as the HMTase Suv39h1 (in yellow). Upon recruitment to chromatin, Suv39h1 methylates through its SET domain adjacent unmethylated H3 tails at lysine 9, forming new H3K9me binding sites for HP1. Thus, this three-component system could explain spreading and maintenance of heterochromatic gene silencing (Dormann, 2009).

Subsequently, H3K9me3 bound HP-1 dimerizes and interacts with many nuclear proteins via its chromoshadow domain. That may lead to downstream functions either directly by interconnecting nucleosomes to compact chromatin (Soeroes, 2010) or indirectly by recruiting factors such as Suv4-20 (trimethylates H4K20), TRIM28 (involved in transcriptional repression) and DNMT3a/b (a DNA methyltransferase) (Lehnertz et al., 2003; Schotta et al., 2004).

1.3 Activity-dependent neuroprotective protein (ADNP)

1.3.1 ADNP discovery and structure

ADNP was originally cloned from P19 mouse carcinoma cells, differentiated into neuroglial cells (Bassan et al., 1999). The hADNP gene spans 40 kb and includes 5 exons and 4 introns with alternative splicing of an untranslated second exon. Protein variants resulting from alternative splicing have not yet been reported. Sequence comparison with human ADNP from a fetal brain cDNA library (Zamostiano et al., 2001) indicated 90% identity at the mRNA level, suggesting a very high evolutionary conservation, which also extends to the clade of euteleostomi (<http://www.ncbi.nlm.nih.gov/homologene>, Figure 1-7).

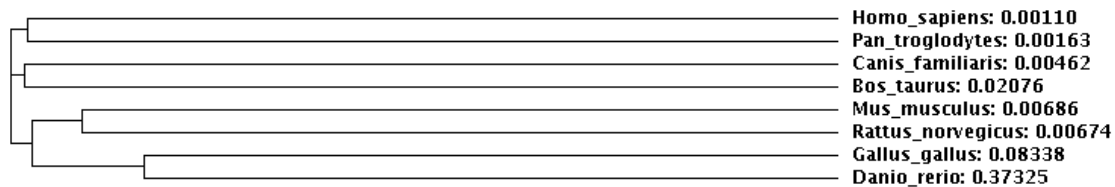
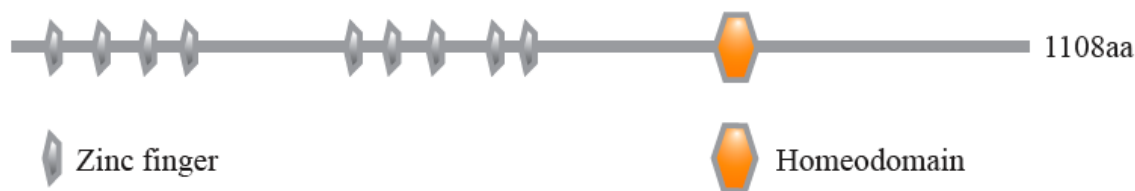


Figure 1-7: phylogenetic tree of ADNP homologs in different species.

(<http://www.ncbi.nlm.nih.gov/homologene>)

The predicted structure of the 124 kDa protein contains 9 zinc fingers, a proline-rich region, a nuclear bipartite localization signal, cellular export and import signals, and a homeobox domain profile (Table 1-2). ADNP exhibits sequence homology to the engrailed homeoprotein, containing a leucine-rich sequence within the homeobox profile that has been shown to be necessary for nuclear export and secretion (Furman et al., 2004; Gozes and Brenneman, 2000; Gozes et al., 2000). Therefore, ADNP may play a role in transcription, cytoplasmic and extracellular pathways. Besides zinc fingers and the

homeodomain, no other regions of similarity are predicted. Therefore it is impossible to derive assumptions about the protein function from domain structure.



Feature key	Position(s)	Length	Description
Zinc finger	74 – 97	24	C2H2-type 1
Zinc finger	107 – 129	23	C2H2-type 2; atypical
Zinc finger	165 – 188	24	C2H2-type 3
Zinc finger	221 – 244	24	C2H2-type 4
Zinc finger	447 – 469	23	C2H2-type 5; atypical
Zinc finger	489 – 510	22	C2H2-type 6; atypical
Zinc finger	512 – 535	24	C2H2-type 7
Zinc finger	622 – 647	26	C2H2-type 8; atypical
Zinc finger	662 – 686	25	C2H2-type 9; atypical
DNA binding	754 – 814	61	Homeobox
Region	354 – 361	8	Neuroprotective peptide (NAP)

Table 1-2: domains of human ADNP (Q9H2P0) as predicted by UniProtKB

(http://www.uniprot.org/uniprot/Q9H2P0#section_comments)

1.3.2 ADNP expression and distribution

Tissue specific expression

Human ADNP mRNA shows higher expression in the heart, skeletal muscle, kidney, placenta, microvascular endothelial cells and brain as compared to other tissues such as the colon or the small intestine (Zamostiano et al., 2001). Serial analysis of gene expression suggests increased expression in tumor tissues.

In mice, Northern blot hybridizations have identified a unique 5.5-kb ADNP mRNA in the brain. Comparison of tissues reveals enrichment in brain-derived structures and low abundance in the lung, kidney, and intestine with slight increases in the testis (Bassan et al., 1999).

Subcellular distribution

Cell fractionation, gel electrophoresis, immunoblotting, and immunocytochemistry reveal ADNP-like immunoreactivity in both the cytoplasmic and in the nuclear cell fractions of astrocytes (Furman et al., 2004).

In the extracellular milieu of astrocytes, ADNP-like immunoreactivity is detected as well. Its content is increased with the vasoactive intestinal peptide (VIP), which is known to activate astrocytes to secrete neuroprotective/neurotrophic factors. This observation suggests that ADNP constitutes part of this VIP-stimulated protective pathway (Furman et al., 2004).

Homology between the engrailed cytoplasmic import sequence and ADNP indicates ADNP may be internalized by other cells, such as neurons after being secreted from glial cells (Furman et al., 2004).

ADNP-like immunoreactivity in the cytoplasm colocalizes with tubulin/microtubule-like immunoreactivity, which correlates with microtubules being key components of the neuron/brain (Furman et al., 2004). Neuroprotection by ADNP is conferred by NAP, an 8-amino acid fragment of ADNP (Bassan et al., 1999). Further studies identified tubulin as an NAP target for astrocyte (Divinski et al., 2004) and neuronal protection (Divinski et al., 2006). NAP appears to show some selectivity in binding to the neuron enriched beta III isoform (Burkhart et al., 2001; Divinski et al., 2006; Katsetos et al., 2003) and interacts with brain tubulin but not with tubulin from fibroblasts (Divinski et al., 2006).

In the nucleus, ADNP has been identified as one of the proteins that interact with the interferon-alpha promoter (Qu et al., 2005). Interferon-alpha has been associated with immunomodulation/autoimmunity and is used as a therapeutic agent against hepatitis C virus (Selmi et al., 2006). Association of ADNP with nuclear compartments such as nucleoli or pericentromeric heterochromatin has not yet been investigated.

1.3.3 ADNP Function

Neuroprotective function of ADNP

To test ADNP function in neuronal systems it has been fused to VP22, a viral protein that facilitates penetration through cellular membranes, potentially enhancing the intrinsic cellular penetration signal in ADNP (Steingart and Gozes, 2006). When incubated with pheochromocytoma cells (PC12), a neuronal model system, VP22-ADNP protects against beta amyloid peptide toxicity and oxidative stress (H_2O_2). Furthermore, the p53 level decreases in the stressed cells, whereas in non-treated cells a p53 increase under oxidative stress has been observed. Interestingly, VIP analogues that provide protection to PC12 cells against H_2O_2 induce a parallel increase in ADNP expression (Sigalov et al., 2000). These results suggest that exposure of postmitotic cells (such as neurons) to environmental stress and injurious conditions results in p53 increases and enhances cellular demise which may be rescued by increased ADNP levels.

An increase in ADNP in injured brains is suggested to be a part of an endogenous compensatory mechanism and VIP treatment of a mouse macrophage cell line causes an increase of ADNP expression (Beni-Adani et al., 2001; Quintana et al., 2006). Thus, ADNP may be activated as a protective mechanism of neuroimmune interactions.

ADNP function in embryogenesis

Mouse ADNP has been detected at the time of neural tube closure at E7.5 and increased on E9.5. Expression is augmented in the brain (E12.5), sustained throughout embryogenesis and regulated by VIP (Pinhasov et al., 2003). Analysis in ADNP knockout mice reveals failure of cranial neural tube closure and death on E8.5–9.5 (Pinhasov et al., 2003). In turn, the neuroprotective peptide motif of ADNP, NAP (Bassan et al., 1999; Gozes et al., 2005) has been shown to enhance neural tube closure, which is compromised in the case of alcohol exposure, as observed in conditions of fetal alcohol intoxication (Chen and Charness, 2008; Sari and Gozes, 2006).

The expression of Oct4, a gene associated with germ-line maintenance is down regulated and the expression of Pax6, a gene crucial for cerebral cortex formation, is abolished in the brain primordial tissue in ADNP knockout embryos. This observation indicates a mechanism of ADNP action on brain formation, inhibiting germ-line division while activating morphogenesis (Pinhasov et al., 2003).

Nuclear function of ADNP

Down-regulation of ADNP up-regulates the tumor suppressor p53 and causes reduced cell viability. Thus, ADNP is implicated in maintaining cell survival, perhaps through modulation of p53 (Zamostiano et al., 2001).

Co-immunoprecipitation experiments identify BRG1, BAF250a, and BAF170, all components of the SWI/SNF (mating type switching/sucrose nonfermenting) complex, as interaction partners of ADNP. Mammalian SWI/SNF is a multiprotein chromatin-remodeling complex that is composed of at least 10 elements existing in two distinct forms that contain either BAF250 and BRG1 or BRM (termed BAF) or BAF180 and BRG1 (termed PBAF) (Simone, 2006). ADNP associates with the BAF complex containing the BRG1 core motor subunit. ADNP down-regulation in HEK293 cells

results in reduced cell viability and microtubule reorganization and changes in cell morphology. These morphological changes are closely associated with the SWI/SNF complex multifunctionality. In addition, ADNP association with neuronal maturation in pluripotent p19 cells that are differentiated into neuronal/glial phenotype (Mandel et al., 2007) correlates well with BRG1 (and by inference the SWI/SNF complex) being an essential regulator of neuronal differentiation (Eroglu et al., 2006) with direct interaction with Neurogenin1 and Neurod (Seo et al., 2005).

In addition to its transcriptional activator functions, the SWI/SNF complex has been described to interact with the retinoblastoma tumor suppressor (RB) in transcriptional repression at euchromatic sites in concert with the Suv39h1/HP1 complex (Nielsen et al., 2001b). At heterochromatic sites, Brg1 knockout causes a disruption of pericentromeric heterochromatin domains as shown with DNA, H3K9me3 and H4K20me3 stainings (Bourgo et al., 2009). Whether ADNP is involved in these heterochromatin functions has not been reported so far.

Morphological changes after ADNP down-regulation are also in line with a SWI/SNF complex function that is associated with cellular differentiation. BRG1 loss induces an altered cellular morphology and disruption in the organization of the actin cytoskeleton (Rosson et al., 2005). Mutations in the SWI/SNF complex result in changes in cell size and attachment area (Hill et al., 2004).

1.4 Objective of the thesis

A main focus in chromatin research is trying to understand how enzyme systems that mediate histone modifications, histone modification marks, specific binding proteins of such marks, and other factors/components interplay to establish and maintain distinct functional domains of chromatin such as euchromatin and heterochromatin. Parts of this process have been described. For example, Suv39h1 (the H3K9me3 methyltransferase), the H3K9me3 mark, and HP1 (a H3K9me3 binding protein) seem to be involved in the formation of heterochromatin. However, our insights into the biochemistry of the different states of chromatin and the complement of factors that mediate these states are still very limited.

To get a more detailed picture of the Suv39h/H3K9me3/HP1 pathway I used modern mass spectrometric methods to identify effector proteins and accessory factors that are associated with H3K9me3 modified chromatin. Factors that had not been described in a heterochromatin context so far were chosen for further characterization.

First, the mechanism by which such a protein is recruited to heterochromatin was investigated. I tested whether binding to H3K9me3 occurs either by direct binding to that modification or indirectly by interaction with another H3K9me3 recognizing protein. Domains and interaction interfaces were then mapped to deepen the understanding of how specific factors are targeted to heterochromatin to mediate distinct functions.

In the second part, I addressed the function of the selected protein at pericentromeric heterochromatin. Therefore, the knockdown phenotype was analyzed for defects in heterochromatin features such as chromatin density, the level and distribution of histone modifications, DNA methylation and transcriptional inactivity.

These studies aimed to broaden our knowledge about how histone modifying enzymes, histone modifications and their binding partners interact to finally mediate distinct biological functions.

2 Material and Methods

2.1 Material

2.1.1 Chemicals

Chemical	Manufacturer	Chemical	Manufacturer
2-Mercaptoethanol	Sigma, Steinheim	Luciferin	PJK, Rehovot (Israel)
4-(2-Hydroxyethyl)-1-piperazineethanesulfonic acid (HEPES)	VWR, Poole	Magnesium chloride (MgCl ₂)	Merck, Mannheim
4,6-Diamidino-2-phenylindole (DAPI)	Sigma, Steinheim	Magnesium sulfate (MgSO ₄)	Roth, Karlsruhe
Acetic acid	Merck, Mannheim	Maleic acid	Sigma, Steinheim
Acrylamide / Bisacrylamide (37.5:1)	Merck, Mannheim	Methanol	Sigma, Steinheim
Adenosine 5'-triphosphate (ATP)	Sigma, Steinheim	Milk powder	Regilait, Saint-Martin-Belle-Roche (France)
Agar	Roth, Karlsruhe	Mowiol	Calbiochem, Darmstadt
Agarose	Serva, Heidelberg	Non essential amino acids	Gibco, Muenchen
Albumin, bovine (BSA)	New England Biolabs, Ipswich	Nonidet P-40 (NP-40)	Roche, Penzberg
Ammonium persulfate (APS)	AppliChem GmbH, Darmstadt	Normal goat serum	Bioscience International, Maine (USA)
Ampicillin	AppliChem GmbH, Darmstadt	Paraformaldehyde	Sigma, Steinheim
Benzyl mercaptan	Sigma, Steinheim	Penicillin Streptomycin 100x	Gibco, Muenchen
Boric acid	Merck, Mannheim	Peptone	Roth, Karlsruhe
Bromophenol blue	Serva, Heidelberg	Phenol	Sigma, Steinheim
Calcium chloride (CaCl ₂)	Roth, Karlsruhe	Phenol/Chloroform/Isoamyl alcohol	Roth, Karlsruhe
Chloramphenicol	Amresco, Solon (USA)	PLB buffer	Promega, Madison
Chloroform	Merck, Mannheim	Polyethylene glycole 8000	Merck, Mannheim
Coelenterazine	Invitrogen, Karlsruhe	Ponceau S	Sigma, Steinheim
Coenzyme A	Invitrogen, Karlsruhe	Potassium chloride (KCl)	Roth, Karlsruhe
Coomassie brilliant blue	BIO-RAD, Muenchen	Potassium dihydrogen phosphate (KH ₂ PO ₄)	Roth, Karlsruhe
Dimethylsulfoxid (DMSO)	Sigma, Steinheim	Potassium monohydrogen phosphate (K ₂ HPO ₄)	Merck, Mannheim
Dithiothreitol (DTT)	Alexis Biochemicals	Protease Inhibitor	Roche, Penzberg
DMEM GlutaMAXII [-Pyruvate]	Gibco, Muenchen	Puromycin	InvivoGen, San Diego (USA)

Chemical	Manufacturer	Chemical	Manufacturer
dNTPs	Invitrogen, Karlsruhe	S-[3H]adenosylmethionine	GE Healthcare, Buckinghamshire
Ethanol	Merck, Mannheim	Sodium azide (NaN ₃)	Alfar Aesar, Karlsruhe
Ethidium bromide	Roth, Karlsruhe	Sodium chloride (NaCl)	Merck, Mannheim,
Ethylene glycol-bis (b-aminoethylether)N,N,N',N' tetraacetic acid (EGTA)	Roth, Karlsruhe	Sodium citrate	VWR, Poole
Ethylenediaminetetraacetate (EDTA)	Roth, Karlsruhe	Sodium dihydrogen phosphate (NaH ₂ PO ₄)	Merck, Mannheim
Fetal calf serum 10x (FCS)	Sigma, Steinheim	Sodium pyruvate	Gibco, Muenchen
Geneticindisulfat (G418)	Roth, Karlsruhe	Sodium sulfate (Na ₂ SO ₄)	Merck, Mannheim
Glucose	Merck, Mannheim	Sodium tetraborate	VWR, Poole
Glycerol	Merck, Mannheim	Streptavidin-coated beads	Promega, Madison
Glycine	Merck, Mannheim	Tetramethyl ethylenediamine (TEMED)	Sigma, Steinheim
Glycylglycine	AppliChem GmbH, Darmstadt	Thiophenol	Sigma, Steinheim
Guanidin hydrochlorid	Sigma, Steinheim	Triethanolamine	VWR, Poole
Hydrochloric acid (HCl)	Merck, Mannheim	Tris (hydroxymethyl)amino ethane (Tris)	Roth, Karlsruhe
Hygromycin	Roth, Karlsruhe	Triton X-100	Merck, Mannheim
Isoamylalcohol	Sigma, Steinheim	Tween 20	Sigma, Steinheim
JetPEI	Biomol, Hamburg	Urea	Merck, Mannheim
L-Glutamine 100 x	Gibco, Muenchen	Yeast extract	MOBIO, Hamburg
Lipofectamine 2000	Invitrogen, Karlsruhe		

2.1.2 Buffers and solutions

Blocking solution: 1x PBS, 2% BSA, 0.2% Triton X100 (v/v), 5% Normal goat serum (v/v)

Coomassie solution: 2.5% Coomassie Brilliant Blue, 10% acetic acid, 50% methanol

CPD buffer: 20mM Hepes (7.9), 100mM KCl, 10% Glycerol, 0.1% Triton, 1mM DTT + 1x Protease Inhibitor

Destaining solution: 10% acetic acid (v/v), 7.5% methanol (v/v)

DMEM, complete: 1x DMEM GlutaMAX II [-Pyruvate], 1x LGlutamine, 1x Pencillin Steptomycin, 10% FCS

DNA loading buffer, 10x: 10 mM EDTA, 30% w/v glycerol, 100 µg/ml bromphenol blue

DNase I buffer, 10x: 100 mM Tris-HCl (pH 7.5), 2.5 mM MgCl₂, 0.5 mM CaCl₂

Fixation solution (I): 3% Paraformaldehyde (w/v) in 1x PBS

Fixation solution (II): 10% glacial acetic acid (v/v), 30% methanol (v/v)

Freezing medium: DMEM cell culture medium, 10% (v/v) DMSO

Laemmli buffer 1x: Tris 63 mM (pH 6.8), 0.1% 2-Mercaptoethanol (v/v), 0.0005% Bromophenol blue (w/v), 10% glycerol (v/v), 2% SDS (w/v)

LB agar: 1.5 % (w/v) Agar in LB medium

LB Ampicillin medium/agar: LB medium or agar with 100 µg/ml Ampicillin

LB medium: 1 % (w/v) Peptone, 0.5 % (w/v) Yeast extract, 0.5 % NaCl % (w/v), pH 7,5, autoclaved

Luciferase assay reagent “Firefly”: 25 mM Glycylglycine, 15 mM K₂HPO₄ (pH 8.0), 4 mM EGTA, 15 mM MgSO₄, 4 mM ATP pH 7.0, 1.25 mM DTT, 0.1 mM Coenzyme A, 80 µM Luciferin

Luciferase assay reagent “Renilla”: 1.1 M NaCl, 2.2 mM Na₂EDTA, 0.22 M K₂HPO₄ (pH 5.1), 0.5 mg/ml BSA, 1.5 mM NaN₃, 1.5 µM Coelenterazine

Mounting medium: Mowiol including 50 µg/ml DAPI

NE buffer A: 10 mM Hepes-KOH (pH 7.9), 1.5 mM MgCl₂, 10 mM KCl, 0.34 M Sucrose, 10% Glycerol (v/v), 1x Protease Inhibitor

NE buffer B: NE Buffer A including 0.2% NP-40 (v/v)

NM buffer: 50 mM Tris-HCl (pH 8.0), 50 mM NaCl, 10 mM MgCl₂, 0.5 mM DTT, 10% sucrose (w/v), protease inhibitors

PBS 1x: 137 mM NaCl, 2.7 mM KCl, 4.3 mM Na₂HPO₄ (pH 7.4), 1.47 mM KH₂PO₄

PBST: PBS including 0,1% of Tween 20 (v/v)

PD150: 20 mM Hepes NaOH (pH 7.9), 20% glycerol, 150 mM KCl, 0.2% Triton X100 (v/v), 1x Protease Inhibitor

Peptide ligation buffer: 100 mM potassium phosphate (pH 7.9), 3 M guanidine-HCl, 0.5% benzyl mercaptan (v/v), 0.5% thiophenol (v/v)

Permibilization solution: 1xPBS, 0.2% Triton X100 (v/v),

Ponceau: 5% acetic acid (v/v), 0.1% ponceau S (w/v)

Precipitation solution: 1% glycerol (v/v), 10% PEG 8.000 (w/v)

Proteinase K buffer: 100 M NaCl, 10 mM Tris-HCl (pH 8.0), 25 mM EDTA (pH 8.0), 0.5 % SDS, 0.1 mg/ml proteinase K (added freshly)

RB high buffer: 10 mM Tris-HCl (pH 7.5), 1 mM EDTA, 2 M NaCl, 1 mM DTT

RB low buffer: 10 mM Tris-HCl (pH 7.5), 1 mM EDTA, 10 mM NaCl, 1 mM DTT

SAU-200 buffer: 7 M deionized urea, 20 mM sodium acetate (pH 5.2), 1 mM EDTA, 1 mM DTT, 200 mM NaCl

SB washing buffer: 0.1 M maleic acid, 0.15 M NaCl, pH 7.5, 0.3 % Tween 20 (v/v)

SB maleic acid buffer: 0.1 M maleic acid, 0.15 M NaCl, pH 7.5

SB detection buffer: 0.1 M Tris-HCl (pH 9.5), 0.1 M NaCl

SDS-Running buffer: 25 mM Tris, 200 mM glycine. 0.1% SDS (w/v)

SSC, 20x: 3 M NaCl, 0.3 M Na₃citrate (pH 7.0)

TBE: 90 mM Tris, 90 mM Sodiumtetraborate, 2 mM EDTA (pH 8.0)

TEAE buffer: 10 mM triethanolamine-HCl (pH 7.5), 0.1 mM EDTA

Transferbuffer: 200 mM glycine, 25 mM Tris-HCl, 0,04% SDS (w/v), 20% Methanol (v/v)

Unfolding buffer: 7 M guanidinium-HCl, 20 mM Tris-HCl (pH 7.5), 10 mM DTT

Wash buffer: 1x PBS, 0.1% Triton X100 (v/v)

2.1.3 General equipment

Bioruptor	Diogenode, Liège (Belgium)
Centrifuge 5415 R	Eppendorf, Hamburg
Centrifuge 5810 R	Eppendorf, Hamburg
Cryo Freezing controller	Nalgene, Ohio (USA)
DNA Engine OPTICON real-time PCR	BIO-RAD, Muenchen
Freezer -150°C	Thermo Scientific, Braunschweig
Freezer -80°C	Thermo Scientific, Braunschweig
Gel Doc 2000	BIO-RAD, Muenchen
Gel dryer Model 583	BIO-RAD, Muenchen
Hereaus Heracell 240 Incubator	Thermo Scientific, Braunschweig

Hereaus Kelvitron® Incubator	Thermo Scientific, Braunschweig
Kodak X OMAT 2000 proprocessor	Carestream Health, New York (USA)
Leica TCS SP5	Leica, Wetzlar
Microscope Axiovert 40CFL	Zeiss, Jena
Mini-PROTEAN 3 Cells	BIO-RAD, Muenchen
MiniTrans-Blot®	BIO-RAD, Muenchen
Multitron shaker (Bacteria)	HT Infors, Braunschweig
Nanodrop ND-1000	Peqlab, Erlangen
Neubauer chamber BRAND,	Wertheim
Orbitrap XL mass spectrometer	Thermo Scientific, Braunschweig
PCR machine eppgradient S	Eppendorf, Hamburg
PlateChameleon Hidex,	Turku (Finnland)
Scanner Perfection V750 PRO	Epson, Meerbusch
Stuart Gyrorocker SSL3	Sigma, Steinheim
Sub-Cell-GT® Agarose gel electrophoresis	BIO-RAD, Muenchen
Thermomixer comfort	Eppendorf, Hamburg

2.1.4 Antibodies

Antibody	Host	Supplier	Application	Dilution
α ADNP	Mouse, mc	BD Biosciences	IF	1:70
			WB	1:1.000
$\alpha\beta$ -tubulin	Mouse, mc	Sigma	WB	1:20.000
α CDYL	Rabbit, pc	Abcam	WB	1:1.000
α Digoxigenin-AP	Mouse, mc	Roche	SB	1:1.000
α FLAG-M2	Mouse, mc	Sigma	WB	1:1.000
α GFP	Mouse, mc	Roche	IP	5 μ l / sample
α H3	Rabbit, pc	Abcam	WB	1:25.000
α H3K27me1	Rabbit, pc	Thomas Jenuwein	IF	1:500
			WB	1:1.000
α H3K9me3	Rabbit, pc	Upstate/Millipore	IF	1:500
			WB	1:1.000

Antibody	Host	Supplier	Application	Dilution
α H3K9me3S10ph	Rabbit, pc	Upstate/Millipore	WB	1:1.000
α H3K9ac	Rabbit, pc	Upstate/Millipore	WB	1:1.000
α H4	Rabbit, pc	Abcam	WB	1:1.000
α H4K20me3	Rabbit, pc	Upstate/Millipore	IF	1:500
			WB	1:1.000
α HP1 α	Mouse, mc	Chemicon/Millipore	IF (MAB3584)	1:2.500
			WB (MAB3446)	1:1.000
α HP1 β	Mouse, mc	Chemicon/Millipore	IF	1:7.500
			WB	1:10.000
α HP1 γ	Mouse, mc	Chemicon/Millipore	IF	1:15.000
			WB	1:20.000
α mouse-IgG-Alexa 555	Goat	Molecular Probes	IF	1:1.000
α mouse-IgG -HRP	Goat	DakoCytomation	WB	1:3.000
α mouse-IgG magnetic beads	Sheep	DYNAL Biotech	IP	40 μ l / sample
α rabbit-IgG -Alexa 488	Donkey	Molecular Probes	IF	1:1.000
α rabbit-IgG -HRP	Swine	DakoCytomation	WB	1:3.000

Table 2-1: Antibodies

List of antibodies, suppliers, the application for which they are used and the dilutions. mc: monoclonal; pc: polyclonal; Applications: IF: Immunofluorescence staining; IP: Immunoprecipitation; WB: Western Blot analysis; SB: Southern blot analysis

2.2 *Molecular biological methods*

2.2.1 Agarose gel electrophoresis

Agarose gel electrophoresis of DNA was carried out according to (Sambrook and Russel, 2001). Typically, 0.5% to 2.0% agarose gels (w/v agarose in TBE) were used. Gels were poured and run using the Sub-Cell GT horizontal electrophoresis system (Bio-Rad). Samples were mixed with 10x DNA loading buffer and run on agarose gels for 45 min at a constant voltage of 110 V in TBE buffer at RT. 1 kb Plus DNA Ladder (Fermentas) was used as size reference. DNA was visualized by staining of the agarose gels after electrophoresis with 1 µg/ml ethidium bromide for 20 min at RT.

2.2.2 Plasmid manipulation

Constructs were generated by standard techniques of DNA cloning (Sambrook and Russel, 2001). Restriction endonucleases and ligase from NEB and PfuII Ultra polymerase (Stratagene) were used according to the manufacturers instructions.

ADNP was amplified by PCR from an EST (expressed sequence tag) clone (I.M.A.G.E. Consortium Clone ID 3448801). PCR products were then cloned into the destination vectors via the restriction sites given in (Table 2-2).

Site directed mutagenesis was performed by fusion PCR. In a first step two fragments of ADNP were generated by PCR using either the forward or the reverse primers for cloning and overlapping mutagenesis primers containing the point mutation. These fragments were fused by PCR using both fragments as template and the cloning primers.

Plasmid name	Parental vector	Source	Insert	primer	Restriction sites
pADNP-FIFI-HAHA	pCDNA-	N.	Koester-	ADNP	BamHI-ADNP
					BamHI

CHAPTER 2 – Material and Methods

pADNP-FIFL-HAHA	FIFL-HAHA	Eiserfunke (Koester-	ADNP	ADNP-NotI	NotI
pADNPK767R-FIFL-HAHA		Eiserfunke, 2010)	ADNP (K767R)	1. K767R-f/K767R-r 2. BamHI-ADNP ADNP-NotI	
pADNPV821A-FIFL-HAHA			ADNP (V821A)	1. V821E-f/V821E-r 2. BamHI-ADNP ADNP-NotI	
pADNPK767R/V821A-FIFL-HAHA			ADNP (K767R/V821E)	1. K767R-f/K767R-r 2. V821E-f/V821E-r 3. BamHI-ADNP ADNP-NotI	
pECFP-ADNP	pECFP-C1	Clontech	ADNP	Sall-ADNP ADNP-BamHI	Sall BamHI
pECFP-ADNP-ΔHD			ADNP-Δ741-846	1. ADNP-1-r ADNP-2-f 2. Sall-ADNP ADNP-BamHI	Sall BamHI
pECFP-ADNP-HD			ADNP-701-846	1. Del2-f/Del3-r 2. Sall-ADNP ADNP-BamHI	Sall BamHI
pGal4-ADNP	DBD-Gal4-null	Judd Rice	ADNP	BamHI-ADNP ADNP-Sall	BamHI Sall
pGene-YFP	pGene	Invitrogen	EYFP	no PCR; direct subcloning	NheI HindIII
pGene-YFP-ADNP	pGene-YFP		ADNP	Sall-ADNP ADNP-BamHI	Sall BamHI
pGene-YFP-ADNPK767R			ADNP (K767R)	1. K767R-f/K767R-r 2. Sall-ADNP ADNP-BamHI	Sall BamHI
pGene-YFP-ADNPV821E			ADNP (V821A)	1. V821E-f/V821E-r 2. Sall-ADNP ADNP-BamHI	Sall BamHI
pGene-YFP-ADNPK767R/V821E			ADNP (K767R/V821E)	1. K767R-f/K767R-r 2. V821E-f/V821E-r 3. Sall-ADNP ADNP-BamHI	Sall BamHI

Table 2-2: Cloning details

For vector information see

pCDNA-FIF1-HAHA: (Koester-Eiserfunke, 2010)

pECFP-C1: www.clontech.com/images/pt/dis_vectors/PT3259-5.pdf

DBD-Gal4-null: (Kalakonda et al., 2008)

pGene: toolszh.invitrogen.com/content/sfs/vectors/pgenev5his_map.pdf

Primers:

ADNP-1-r: 5'-CAGCCACTCAGCATCAAAATCAAAGCAGCTAGGGGAATCAGC-3'

ADNP-2-f: 5'-GCTGATTCCCCTAGCTGCTTTGATTTTGATGCTGAGTGGCTG-3'

ADNP-BamHI: 5'-TCCGGTGGATCCCTAGGCTTGCTGGCTGCTC-3'

ADNP-NotI: 5'-GTATGCGGCCGCGGCTTGCTGGCTGCTCAGC-3'

ADNP-SalI: 5'-GCTCGAGTCGACGCTAGGCTTGCTGGCTGCTCAGC-3'

BamHI-ADNP: 5'-GAATTGGGATCCATGTTCCAACCTTCCTGTCAAC-3'

Del2-f: 5'-TGGTACGTCGACGCACCTTCTCGGCTCAATC-3'

Del3-r: 5'-TCCGGTGGATCCCTATTCAAACAGCCACTCAGCATC-3'

K767R-f: 5'-CTTATGAGGCTAGGAGAAGCTTTCTCAC-3'

K767R-r: 5'-GTGAGAAAGCTTCTCCTAGCCTCATAAG-3'

SalI-ADNP: 5'-TGGTACGTCGACATGTTCCAACCTTCCTGTCAAC-3'

V821E-f: 5'-GTACAAGCCTGGTGAGCTGCTAGGTTTAAAC-3'

V821E-r: 5'-ACCTAGCAGCTCACCAGGCTTGTAACCTTTTACAG-3'

Insert sequences:

The EYFP was subcloned from pEYFP-C1 (Clontech):

ATGGTGAGCAAGGGCGAGGAGCTGTTACCGGGGTGGTGCCATCCTGGTCGAGCTGGACGG
CGACGTAAACGGCCACAAGTTCAGCGTGTCCGGCGAGGGCGAGGGCGATGCCACCTACGGCA
AGCTGACCCTGAAGTTCATCTGCACCACCGGCAAGCTGCCCCGTGCCCTGGCCACCCTCGTGA
CCACCTTCGGCTACGGCCTGCAGTGCTTCGCCCCGCTACCCCGACCACATGAAGCAGCAGCACT
TCTTCAAGTCCGCCATGCCCCGAAGGCTACGTCCAGGAGCGCACCATCTTCTTCAAGGACGACG
GCAACTACAAGACCCGCGCCGAGGTGAAGTTCGAGGGCGACACCCTGGTGAACCGCATCGAG
CTGAAGGGCATCGACTTCAAGGAGGACGGCAACATCCTGGGGCACAAGCTGGAGTACAATA
CAACAGCCACAACGTCTATATCATGGCCGACAAGCAGAAGAACGGCATCAAGGTGAACTTCA
AGATCCGCCACAACATCGAGGACGGCAGCGTGCAGCTCGCCGACCACTACCAGCAGAACACC
CCCATCGGCGACGGCCCCGTGCTGCTGCCCCGACAACCACTACCTGAGCTACCAGTCCGCCCTG

AGCAAAGACCCCAACGAGAAGCGCGATCACATGGTCCTGCTGGAGTTCGTGACCGCCGCCGG
GATCACTCTCGGCATGGACGAGCTGTACA

The ADNP sequence was derived from the I.M.A.G.E. Consortium Clone ID 3448801:

ATGTTCCAACCTTCCTGTCAACAATCTTGGCAGTTTAAGAAAAGCCCGGAAAACCTGTGAAAAA
ATACTTAGTGACATTGGGTTGGAATACTGTAAAGAACATATAGAAGATTTTAAACAGTTTGAA
CCTAATGACTTTTATTTGAAAAACACTACATGGGAGGATGTAGGACTGTGGGACCTTCTCTT
ACGAAAAATCAGGACTATCGGACAAAACCTTTTTGCTGCAGTGCTTGTCCGTTTTCTCAAAA
TTCTTCTCTGCCTACAAAAGTCATTTCCGGAATGTCCATAGTGAAGACTTTGAAAATAGGATTC
TCCTTAACTGCCCTTACTGTACCTTCAATGCAGATAAAAAGACTTTGAAAACACACATTAAAA
TATTTTCATGCTCCAAACTCCGGCGCACCAAGTAGCAGCCTCAGCACTTTCAAAGATAAAAACA
AAAACGATGGCCTTAAACCTAAGCAGGCTGACAATGTAGAGCAAGCCGTGTATTACTGCAAG
AAGTGCACCTACCGAGACCCTCTCTACGAGATCGTCAGGAAGCACATCTACAGGGAACATTTT
CAACACGTGGCAGCACCTACATAGCAAAAGCAGGAGAAAAATCACTCAATGGTGCAGTCTC
CCTGGGCACAAATGCCCAGAGGAGTGTAACATCCACTGCAAGCGATGCCTTTTCATGCCCAA
GTCCTATGAAGCTTTGGTACAGCATGTCATTGAGGACCATGAACGGATAGGCTATCAGGTCAC
TGCCATGATCGGACACACAAATGTTGTAGTTCCCCGAGCCAAGCCCTTGATGCTGATAGCTCC
CAAACCTCAAGACAAAAAGGGCATGGGACTCCACCACGAATCAGCTCCCTTGCTTCTGGAA
ATGTCCGGTTCGTTGCCATCACAGCAGATGGTAAACCGATTGTCAATACCAAAGCCCAACTCAA
ATTCAACGGGAGTCAACATGATGTCCAATGTTTACCTGCAGCAAAACAACCTATGGAGTCAAAT
CTGTGGGCCAGAGCTATGGTGTGGCCAGTCAGTGAGGCTGGGACTAGGTGGCAATGCTCCA
GTTTCCATCCCTCAACAGTCTCAGTCCGTGAAACAGTTACTTCCAAGTGGGAATGGGAGGTCT
TTTGGGCTAGGTGCTGAGCAGAGGCCCCAGCAGCAGCCAGGTACTCCCTGCAGACTGCCAA
CACCTCTCTACCCCCAGGCCAAGTGAAGTCTCCCTCTGTGTCTCAGTCACAGGCATCTAGAGT
ATTAGGTCAAGTCCAGTTCTAAACCTCCACCAGCCGCCACAGGCCCTCCTCCAAGCAACCACTG
TGCCACTCAGAAGTGGAATCTGTACAATCTGTAACGAGCTTATCCCTGAGAATGTCTATAG
CGTTCACCTCGAAAAGGAGCATAAAGCTGAGAAAGTCCCAGCCGTAGCTAACTACATTATGA
AAATACACAATTTTACTAGCAAATGCCTCTACTGTAATCGCTATTTGCCTACAGATACCCTACT
CAACCATATGTTAATTCATGGTCTGTCTTGTCCGTATTGCCGTTCACCTTCAATGATGTAGAG
AAGATGGCAGCACACATGCGAATGGTTCATATTGATGAAGAGATGGGGCCTAAAACGGATTC
TACTTTGAGCTTTGATTTGACATTGCAACAGGGCAGTCACACCAACATTCATCTCCTGGTGACC
ACATAAACCTGAGGGATGCCCCGGCTGAATCAGTTGCTTACCATGCCCAAAATAATGCCCA
GTTCTCCAAAGCCACAACCAAAAGTTCAGGAAAAAGCAGATGTCCCGGTTAAAAGTTCACC
TCAAGCTGCAGTGCCCTATAAAAAAGATGTTGGGAAGACCCTTTGCCCTCTTTGCTTTTCAATA
CTAAAAGGACCCATATCTGATGCACTTGACATCATTTACGAGAAAGACACCAAGTTATTAG
ACAGTTCATCCGGTTGAGAAAAAGCTAACTTACAAATGTATCCATTGCCTTGGTGTGTATACT

AGCAACATGACAGCCTCAACCATCACTCTGCATCTAGTCCACTGCAGGGGTGTTGGAAAAACC
 CAGAATGGCCAGGACAAGACAAACGCACCTTCTCGGCTCAATCAGTCTCCAGGCCTGGCCCCCT
 GTGAAGCGCACGTATGAGCAGATGGAGTTTCCACTGCTAAAAAAGCGGAAGCTGGAGGAGGA
 TGCTGATTCCCCTAGCTGCTTTGAAGAGAAGCCAGAAGAGCCTGTTGTTTTAGCTTTAGACCC
 CAAGGGTCATGAAGATGATTCTTATGAGGCTAGGA^AAAGCTTTCTCACAAAGTACTTCAACAA
 ACAGCCCTATCCCACCAGGAGAGAAATTGAGAAGTTAGCTGCCAGTCTATGGCTATGGAAGA
 GTGACATTGCCTCCCATTTCAGTAACAAGAGGAAGAAGTGTGTCCGCGACTGTGAAAAGTAC
 AAGCCTGGTG^TGCTGCTAGGTTTTAACATGAAAGAATTAAATAAAGTCAAACACGAGATGGA
 TTTTGATGCTGAGTGGCTGTTTGAAAATCACGATGAGAAAGACTCAAGAGTCAATGCTAGCAA
 GACTGTTGACAAAAAGCATAACCTTGGGAAAAGAAGATGATAGCTTCTCAGATAGTTTTGAAC
 ATTTGGAAGAAGAATCCAATGGAAGCGGGAGTCCTTTTGACCCTGTCTTTGAAGTTGAGCCTA
 AAATTCCCAGTGATAATTTAGAGGAGCCTGTACCGAAGGTTATTCCGGAAGGTGCTTTGGAAT
 CTGAGAAGCTAGACCAAAAAGAGGAGGAGGAGGAGGAGGAGGAGGAGGATGGTTCAAAATA
 TGAAACTATCCATTTGACTGAGGAACCAGCCAAATTAATGCATGATGCCTCTGATAGTGAGGT
 AGACCAAGATGATGTAGTTGAGTGGAAGATGGTGCTTCACCATCTGAGAGTGGGCCTGGTTC
 CCAACAAATCTCAGACTTTGAGGATAATACATGTGAAATGAAACCAGGAACCTGGTCTGATG
 AGTCTTCCCAGAGTGAAAGATGCAAGGAGCAGTAAGCCAGCTGCCAAAAAAAAGGCTACAGTG
 CAAGATGACACAGAGCAGTTAAAATGGAAGAATAGTTCCTATGGAAAAGTTGAAGGGTTTTG
 GTCCAAGGACCAGTCACAGTGGGAAAATGCATCTGAGAATGCAGAGCGCTTACCAAACCCAC
 AGATTGAGTGGCAGAATAGCACAAATTGACAGTGAGGACGGGGAGCAGTTTGACAGCATGACT
 GACGGAGTTGCTGATCCCATGCATGGCAGCTTAAGTGGAGTGAAGCTGAGCAGCCAGCAAGC
 C

Labeled in red are the two bases A, which are mutated to G to achieve the K767R mutation and to T for the V821E mutation respectively.

2.2.3 cloning

To 100 µl chemically competent *E.coli* DH5α ~100 ng transforming DNA was added. The tubes containing these cells were stored for on ice 20 min, transferred for 1 min into a preheated 42°C waterbath and rapidly cooled on ice for 2 min. Thereafter the transformation-mix was suspended in prewarmed 37°C LB-medium and the cells were allowed to recover for 45 min at 37°C and 1000 rpm in a thermomixer. 100 µl of the cell suspension were plated on agar-plates, containing 33,34 µg/ml kanamycin or 100 µg/ml ampicillin respectively and grown over night at 37°C. Single colonies were picked into 5 ml LB medium containing 50 µg/ml kanamycin or 100µg/ml ampicillin respectively and

incubated at 37°C overnight. Plasmids were purified using a MiniPrep Kit (Qiagen, Hilden). To screen for positive colonies, 10% of the purified plasmids were digested with the cloning restriction enzymes and separated by electrophoresis on a 1 % agarose gel in TBE buffer. Plasmids showing the right insert size were sequenced by MWG (Ebersberg) or Seqlab (Goettingen).

2.2.4 Preparation of genomic DNA

Genomic DNA was prepared from cell aliquots (2.3.5) as described (Ausubel et al., 1998). Briefly, cell pellets were resuspended in Proteinase K buffer and digested overnight at 50°C. The samples were extracted with an equal volume of phenol/chloroform/isoamylalcohol by centrifugation for 10 min at 1.700xg. The aqueous (top) layer was transferred into a new tube. DNA was precipitated with ½ vol of 7.5 M ammonium sulfate and 2 vol of 100 % Ethanol. After centrifugation for 2 min at 1.700xg and one washing step with 70 % Ethanol the pellet was dried and resuspended in 10 mM Tris-HCl (pH 8.0) and stored at -20°C.

2.2.5 Southern blot analysis

The DNA prepared in 2.2.4 was digested with *Tai*I (NEB) according to the manufacturers instructions. The samples were separated on a 1 % agarose gel and stained as described in 2.2.1.. Southern blot was performed according to (Ausubel et al., 1998) with modifications: The gel was rinsed in H₂O, depurinated for 20 min in 0.25 M HCl and neutralized for 30 min in 0.4 M NaOH. Downward transfer of the DNA onto a positively charged nylon transfer membrane (GE Healthcare) was performed overnight using 0.4 M NaOH as transfer buffer. Major satellite DNA was detected using the DIG High Prime DNA Labeling and Detection Starter Kit I (Roche Diagnostics GmbH, Mannheim) as described by the manufacturer. Briefly, the major satellite probe was generated by PCR using DIG-labeled dUTP : dTTP 1:3, genomic DNA of NIH 3T3 cells as template and major satellite repeat primers (5'-ATATGTTGAGAAAAGTGAATCACG-3'; 5'-

CCTTCAGTGTGCATTTCTCATTTTTCAC-3'). After washing the membrane twice in 2x SSC for 10 min at RT it was prehybridized in DIG Easy Hyb for 30 min at 37°C. 25 ng/ml DIG-labeled DNA probe was denatured by boiling for 5 min and rapidly cooling in ice water. The probe was mixed with prewarmed DIG Easy Hyb and hybridized overnight at 42°C. Two post-hybridization washes for 5 min in 2x SSC, 0.1 % SDS at RT were followed by 2 washes in 0.5x SSC, 0.1 % SDS at 65-68° C. The membrane was rinsed in SB washing buffer, blocked in 1x Blocking solution in SB washing buffer for 30 min and incubated with Anti-Digoxigenin-AP antibody in Blocking solution in SB washing buffer for another 30 min at RT. Thereafter, the membrane was washed twice in SB washing buffer for 15 min at RT and equilibrated for 2 – 5 min in SB detection buffer. For detection, 200 µl of NBT/BCIP stock solution were added to 10 ml of SB detection buffer and applied to the membrane. The color reaction was performed in the dark until bands became visible and then stopped by washing the membrane in H₂O for 5 min.

2.2.6 RNA isolation

Cell aliquots prepared in 2.3.5 were resuspended in 1 ml TRIzol® reagent. 0.2 ml chloroform were added and mixed vigorously for 15 s. After 2-3 min incubation at RT the samples were centrifuged for 15 min at 12.000xg, 4°C. The upper aqueous phase was transferred into a new tube, mixed with 0.5 ml isopropanol and incubated for 10 min at RT. Thereafter the RNA precipitate was centrifuged for 10 min at 12.000xg, 4°C. The pellet was washed in 75 % Ethanol and centrifuged for 10 min at 7.600xg, 4°C. Then the pellet was dried and redissolved in 100 µl RNase-free water. The concentration was measured using the Nanodrop ND 1000.

2.2.7 cDNA synthesis

First strand synthesis of cDNA was performed using the Superscript II Kit (Invitrogen, Karlsruhe) according to the manufacturers protocol. Before cDNA synthesis

contaminating genomic DNA was removed from the RNA by digesting DNase I mix for 30 min at 37°C. The reaction was stopped by adding 0.4 µl 100 mM EDTA and DNase I inactivation for 10 min at 75°C. 1 µl random hexamers and dNTPs were added and incubated for 5 min at 65°C. After rapid cooling the samples in ice water the Superscript II mix was added. Reverse transcription was performed at 25°C for 10 min followed by a 50°C incubation for 10 min and terminated for 5 min at 85°C. RNA was digested by addition of 1 µl RNase H and incubation at 37°C for 20 min. The cDNA was stored at -20°C for further use.

DNase I mix:

RNA:	3 µg
DNase I buffer:	0.8 µl
DNase I (NEB):	0.8 µl
RNase OUT:	1 µl
H2O (RNase-free):	to 8 µl

Superscript II mix:

RT buffer:	2 µl
MgCl ₂ :	4 µl
0.1 M DTT:	2 µl
RNase OUT:	1 µl
Superscript II:	1 µl

2.2.8 Real time PCR

To quantify the relative amount of major satellite repeat transcripts real time PCR was performed. All PCR were done in triplicate. 2 µl of 1:4 diluted cDNA (2.2.7) were added to 18 µl master-mix (1.25 µM of each primer, 10 µl 2x iQ SYBR® Green Supermix (BIO-RAD, Muenchen), H₂O to 18 µl) and processed in a DNA Engine OPTICON real-time PCR machine with the following program: 15 min at 95°C – [15 s at 94°C – 55 s at 55°C – 30 s at 72°C – read plate]_{40x} – perform melting curve from 60°C to 95°C, read every 0.3°C. To calculate the relative expression levels, the major satellite signals were normalized to the signals of GAPDH as follows: $Ct_{\text{major satellite repeat}} - Ct_{\text{GAPDH}} = \Delta Ct$. The average of the $2^{-\Delta Ct}$ values from the triplicates were blotted with the standard deviation of the triplicate as error bars.

Primers:

Major satellite repeats:

Fwd: 5'-ATATGTTGAGAAAAGTGAATTCACG-3'

Rev: 5'-CCTTCAGTGTGCATTTCTCATTTTTCAC-3'

GAPDH:

Fwd: 5'-AGGTCGGTGTGAACGGATTTG-3'

Rev: 5'-TGTAGACCATGTAGTTGAGGTCA-3'

2.3 Mammalian cell culture

Cell line	Origin	Medium	Supplier
HEK 293	Human, embryonic kidney	DMEM, complete	Wolfgang Fischle
HEK TK22	Human, embryonic kidney	DMEM, complete + 5 µg/ml Puromycin	Judd Rice
MEF (isogenic to MEF Suv39h1/h2 -/-)	Mouse, embryonic fibroblast	DMEM, complete + 1x non essential amino acids, 1x sodium pyruvate	Thomas Jenuwein
MEF Suv39h1/h2 -/-	Mouse, embryonic fibroblast	DMEM, complete + 1x non essential amino acids, 1x sodium pyruvate	Thomas Jenuwein
MEF (isogenic to MEF HP1α -/-; HP1β -/-; HP1γ -/-; HP1α/β -/-)	Mouse, embryonic fibroblast	DMEM, complete + 1x non essential amino acids, 1x sodium pyruvate	Prim Singh
MEF HP1α -/-; HP1β -/-; HP1γ -/-; HP1α/β -/-	Mouse, embryonic fibroblast	DMEM, complete + 1x non essential amino acids, 1x sodium pyruvate	Prim Singh
NIH 3T3	Mouse, fibroblast	DMEM, complete	DMSZ
GeneSwitch NIH 3T3	Mouse, fibroblast	DMEM, complete + 100 µg/ml Hygromycin	Invitrogen

Table 2-3: Cell lines and media

2.3.1 Thawing

To thaw cells from frozen stocks 10 ml of the appropriate medium was equilibrated to 37°C and 5 % CO₂. The cells were thawed in a 37°C water bath, resuspended with 1 ml prewarmed medium (Table 2-3), added dropwise to the equilibrated medium and grown at 37°C and 5 % CO₂ until they reached ~80 % confluency.

2.3.2 Maintenance

The cell lines were grown in the medium given in Table 2-3 at 37°C and 5 % CO₂. At 90 % confluency cells were washed with prewarmed PBS and trypsinized for 10 min in 0.05 % Trypsin-EDTA. Supplemented medium was added to stop the reaction. The cells were subsequently plated in 1:10 (wild type) or 1:5 (knockout cell-lines) dilution to be 90 % confluent after three days (NIH3T3, HEK293, GeneSwitchNIH3T3) or five days (wild type and knockout MEF cells).

2.3.3 Freezing

The cells at 70 % confluency were washed with PBS and trypsinized as described above. The number of viable cells was determined by mixing of the cells with one volume 0.4 % Trypan blue and counting in a Neubauer chamber. After centrifugation for 5 min at 250xg and room temperature the cells were resuspended in 4°C freezing medium (culture medium with 5 % DMSO) in an appropriate volume to obtain 1×10^6 cells /ml. 1 ml cell suspension was aliquoted per cryotube on ice. These tubes were stored in a precooled Cryo Freezing Controller at -80°C for 48 h to allow a cooling by approximately 1°C per min. Thereafter the cells were transferred to -150°C for long time storage.

2.3.4 Generation of stable cell lines

One day prior to transfection GeneSwitchNIH3T3 cells were seeded in 10 cm dishes to reach ~50 % confluency at the day of transfection. Transfection was performed using JetPEI reagent (Biomol, Hamburg) in accordance with the instructions of the manufacturer. Typically 16 µl JetPEI reagent and 8 µg of pGeneYFP, pGeneYFP-ADNP, pGeneYFP-ADNP(K767R), pGeneYFP-ADNP(V821E) and pGeneYFP-ADNP(K767R/V821E) were used per dish. One day after transfection, the cells were trypsinized and transferred to 15 cm dishes containing medium supplemented with 400 µg/ml zeocin (Invitrogen). To remove dead cells the medium was exchanged after two days. Untransfected cells were treated at the side as a control to verify that the treatment was working. Two weeks post transfection separate colonies were visible. Expression of YFP/YFP-ADNP was induced with 10 ng/ml Mifepristone. The cells were washed with PBS and covered with 37°C warm 0.5 % low melting agarose in PBS. After the agarose polymerized at room temperature YFP/YFP-ADNP expressing cells were picked using cloning cylinders and transferred into 24 well plates. Stable inducible colonies were analyzed by fluorescence microscopy (Axiovert 40 CFL) and Western Blot. Two colonies of moderately overexpressing cell-lines for each construct were frozen for long term storage.

2.3.5 Transfection of siRNA

NIH3T3 cells were seeded in 6-well plates one day prior to transfection to be 30-50 % confluent at the day of transfection. 100 µg siRNA was transfected with 5 µl Lipofectamine2000 as described by the manufacturer (Invitrogen, Karlsruhe). One day post transfection the cells were trypsinized and transferred to a 10 cm dish where the transfection was repeated with 600 µg siRNA and 30 µl Lipofectamine2000. The next day the cells were washed with ice cold PBS, scraped off the plates and aliquoted into 3 samples for protein, DNA and RNA extraction.

2.4 Cell based assays

2.4.1 Dual luciferase assay

HEK293 and HEK293 TK22 (Kalakonda et al., 2008) cells were seeded at a density of 1.5×10^5 cells/well into 12-well plates 24 h prior treatment. On the next day a total amount of 1.2 μ g DNA per well was transfected using Lipofectamine2000 (Invitrogen, Karlsbad) according to the manufacturers protocol. For transfection of HEK293 cells the total DNA contained 100 ng of the targeting plasmid UAS TK, which contains Gal4 binding sites and a tyrosine kinase promotor, 2 ng of CMV Renilla, a transfection control under CMV promotor control, the Gal4-tagged protein of interest in different amounts (2 ng -50 ng), and empty pcDNA3.1 vector to reach 1.2 μ g in total. In the case of HEK293 TK22 cells no UAS TK and 10-200 ng Gal4-tagged protein expressing plasmid were transfected. HEK293 cells were incubated for 24 h and HEK293 TK22 cells were incubated for 48 h at 37°C/ 5% CO₂. Then the cells were detached from the wells by pipetting in medium and transferred to 1.5 ml Eppendorf tubes. Cells were pelleted by centrifugation for 5 min at 3000 rpm, RT. The pellets were resuspended in 100 μ l of 1x PLB buffer and incubated for 15 min at RT under constant agitation at 1400 rpm. The lysates were centrifuged for 1 min at 14000 rpm. 20 μ l of the supernatant was pipetted into one well of a 96-well Optiplate, which was inserted into the PlateChameleon. There 100 μ l of the “Firefly” solution and afterwards 100 μ l “Renilla” solution were then added to each well. The luminosity was counted after each step. The measured values were transferred into Microsoft Excel and the Firefly signals were normalized against the Renilla signal and the control transfected cells.

2.4.2 Subcellular fractionation

NIH3T3 cells were washed once with ice cold PBS and scraped into 3 ml ice cold PBS per 15 cm dish. Next the cells were pelleted for 10 min at 300xg, 4°C and resuspended in

4 ml/ 10^7 cells NE buffer A. After 10 min incubation on ice an equal volume NE buffer B was added, mixed and incubated for another 10 min on ice. Nuclei were pelleted by centrifugation for 10 min at 500xg, 4°C. Afterwards the supernatant was saved as cytoplasmic fraction and the nuclear pellet was resuspended in one packed nuclear volume NE buffer C and was transferred to a dounce homogenisator. The suspension was dounced every 5 min for 20 times until 90 % of nuclei were broken. After centrifugation for 10 min at 20.000xg, 4°C the nuclear soluble fraction was transferred to a new tube whereas the pellet was used as nuclear insoluble (chromatin) fraction. Subsequently, the fractions were separated by SDS-PAGE followed by Western Blot analysis.

2.4.3 Immunoprecipitation

GeneSwitch NIH3T3 YFP/YFP-ADNP cells were induced with 10 ng/ml Mifepristone over night. Nuclei of these cells were prepared as in (2.4.2). To solubilize the chromatin fraction, the nuclei were resuspended in 1 ml/ 10^8 nuclei PD150 + 10 mM CaCl_2 and 10 U/ml micrococcal nuclease (Calbiochem) and rotated 37°C for 30 min. The reaction was stopped with 1 mM EGTA. The nuclei were broken by sonication for 30min with on/off cycles of 30 s/30 s. The insoluble fraction was pelleted at 10.000xg for 1 h. The supernatant was split into an input, control (no antibody) and immunoprecipitation (anti-GFP) sample. 40 μl dynabeads (sheep anti mouse) per sample were 3x washed in PBS. 5 μl mouse anti-GFP antibody were added to the beads and rotated for 3 h at 4°C. The beads were then washed 3x with PD150 buffer and added to the samples. Proteins were immunoprecipitated over night at 4°C. The antibody/protein complex bound beads were washed 6 times with PD150, separated by SDS-PAGE and analyzed by Western Blot.

2.4.4 Immunofluorescence

Cells were seeded on glass coverslips in 6-well plates. For ADNP staining in interphase cells, they were treated with nocodazole (200 nM, in DMSO) for 5 min prior to fixation.

Before staining they were washed 2 times with PBS and fixed for 10 min in fixation solution (I) at 37°C. The coverslips were washed once with PBS and permeabilized for 7 min with permeabilization solution. Cells were washed again once with PBS and blocked for 30 min with blocking solution. Primary and fluorescently labeled secondary antibodies were applied in blocking solution for 1 h at room temperature / over night at 4°C followed by three washing steps with PBS. Thereafter the coverslip was washed three times in water and mounted in mounting medium. Slides were dried overnight at RT and analysed with the confocal microscope Leica TCS SP5.

2.4.5 Methyltransferase assay

NIH3T3 cell nuclei were prepared as described in the immunoprecipitation section. The methyltransferase assay was performed according to (Fischle, 2005). Briefly, aliquots of $5 \cdot 10^6$ nuclei were centrifuged at 500xg, 4 °C, resuspended in 20 µl of cold NM buffer and incubated at room temperature for ca. 5 min. 5 µl of 5-S-adenosyl-L-[methyl³H]methionine in NM buffer were added to start the reaction. After 60 min incubation at 30 °C under constant agitation the nuclei were treated with micrococcal nuclease and immunoprecipitated as described in that section (2.4.3). 15 % of the samples were used for Western Blot and 85 % for autoradiography. For autoradiography enhancement EN3HANCE (PerkinElmer) was used as described by the manufacturer. The gel was stained for 10 min with coomassie solution, incubated 30 min in destaining solution and another 30 min in fixation solution (II). The gel was impregnated with scintillators in EN3HANCE for 1 h and then incubated in precipitation solution for 1 h at RT. After drying over night in a gel dryer (BIO-RAD) the gel was exposed to an ECL Hyperfilm (GE Healthcare, Buckinghamshire, UK) for 6 months at -80°C and signals were detected using the Kodak X-OMAT 2000.

2.5 Biochemical methods

2.5.1 SDS-PAGE

Polyacrylamide gel electrophoresis of proteins in the presence of sodium dodecyl sulfate (SDS-PAGE) was based on the method of Laemmli (Laemmli, 1970). Typically, Tris-glycine gels with 10 or 15 % acrylamide-bisacrylamide separating gels were poured and run using the Mini-PROTEAN electrophoresis system (Bio-Rad). Cell pellets, immunoprecipitates and samples from pull-down experiments were resuspended in 1x Laemmli-buffer and boiled for 5 min. For cell extracts 100 U/ml Benzonase was included in the 1xLaemmli-buffer and the sample was incubated for 5 min at room temperature prior to boiling. SeeBlue Plus2 Pre-Stained protein standard (Invitrogen, Karlsbad) was used as size reference. The gel was run in SDS running buffer at 100 V until the loading dye (bromphenolblue) had left the stacking gel and then at 200 V until the tracking dye reached the end of the gel.

2.5.2 Western Blot

A nitrocellulose membrane, two blot papers and the filter pads were equilibrated in 1x transfer buffer for 15 min and the gel was equilibrated in 1x transfer buffer for 5 min. The sandwich was assembled and fit into a BioRad tank blot chamber which was filled with 1x transfer buffer. Transfer was run for 1 h at 100 V and 4°C. To check for successful transfer, the membrane was stained for 5 min with Ponceau S Red and washed with water until protein bands became visible. Unspecific protein binding sites of the membrane were blocked in 5 % milk powder in PBS for 1h at room temperature. The primary antibody and subsequently the secondary antibody were applied in 2.5 % milk powder in PBST (Table 2-1). Afterwards the membrane was washed three times for 10 min in PBST. Excess of antibody solution was removed by washing three times in PBST. The membrane was developed by chemiluminiscence using the ECL detection kit (Amersham

Biosciences). The signals were detected on Amersham ECL Hyperfilms using the Kodak X OMAT.

2.5.3 generation of oligonucleosomes

For reconstitution of oligonucleosomes, a biotinylated array of twelve 200 bp long DNA fragments was used, with each subunit containing the 601 nucleosome-positioning sequence (12x200-601). These DNA fragments as well as the scavenger DNA used to prevent oversaturation of the DNA template with histone octamers during assembly (Huynh et al., 2005) were provided by Szabolczs Soeroes (Soeroes, 2010). Histones were expressed according to (Luger et al., 1999) and provided by Winfried Lendeckel.

Introduction of specific histone post-translational modifications

Specific lysine 9 trimethylation of histone H3 was achieved by native protein ligation according to (Shogren-Knaak and Peterson, 2004). Briefly, 0.2 mM of truncated H3 protein (amino acids 21 to 135) with a point mutation of alanine 21 to cysteine (H3 Δ 1-20 A21C) and 1 mM of an N-terminal H3 peptide fragment with the desired H3K9me3 mark and a C-terminal thioester group were ligated in peptide ligation buffer for 24 h at 25°C with vigorous mixing. The reaction mix was diluted 50-fold into SAU-200 buffer, applied to a 5 ml Hi-Trap SP-Sepharose high performance cation exchange column (GE Healthcare), and eluted with a linear NaCl gradient from 200 to 600 mM in 10 column volumes. Fractions, containing the ligated product were identified by SDS-PAGE and Coomassie staining and verified by ESI mass spectrometry. The protein was dialyzed extensively against 2 mM DTT at 4°C, lyophilized and stored at -80°C.

Reconstitution of histone octamers

Core histone octamers were reconstituted as described in (Luger et al., 1999). Briefly, lyophilized purified wt core histones H2A, H2B, H4 and wt or modified H3 were dissolved in unfolding buffer and mixed to equimolar ratios. The histone mix was dialyzed at 4°C against RB high buffer with at least three changes of dialysis buffer. Histone octamers were concentrated to 10-20 mg/ml using an Amicon Ultra centrifugal filter unit (Millipore) and purified over a HiLoad 16/60 Superdex 200 prep grade gel-filtration column (GE Healthcare) on a ÄKTA Purifier or ÄKTA Explorer FPLC instrument (GE Healthcare) from H2A-H2B dimers. Peak fractions with pure histone octamers were pooled, concentrated to at least 2 mg/ml ($OD_{276} = 0.9$) and stored in 50 % v/v glycerol at -20°C.

Reconstitution of recombinant oligonucleosomes

Reconstitution of oligonucleosomes was carried out according to (Huynh et al., 2005; Luger et al., 1999) at 4°C. Firstly, glycerol was removed from the octamers by dialyzing for at least 3 h against RB high buffer. For reconstitution of oligonucleosomes, 12x200-601 DNA templates (in the presence of equimolar scavenger DNA) were mixed with histone octamers in a molar ratio of 1.0 to 1.1 octamers per DNA in 500 µl RB high buffer. Reaction mixture was first dialyzed against RB high buffer using a dialysis tube with a molecular weight cutoff of 3500. Nucleosome assembly was performed by continuously replacing RB high buffer against RB low buffer for 72 h using a peristaltic pump as described in (Luger et al., 1999). Reconstituted oligonucleosomes were extensively dialyzed against TEAE buffer and stored at 4°C.

2.5.4 Recombinant proteins

ADNP-FLAG was expressed using the TNT® Quick Coupled Transcription/Translation System (Promega, Madison, USA). The TNT® Quick Master Mix was thawed on ice. 20 µl master mix, 0.5 µl methionine, 0.5 µg pADNP-F1F1-HAHA – DNA and H₂O to 25 µl were mixed per precipitation and incubated for 90 min at 30°C.

Recombinant HP1 variants were obtained from Szabolcs Soeroes (Soeroes, 2010).

2.5.5 Peptide pull-down

To detect binding of proteins to modified histone peptides, 1 µg of the biotinylated peptides was bound to 40 µl streptavidin coated beads for 3 h at RT, 1400 rpm. To remove excess peptides the beads were washed 3x with PBS. 0.5 ml of nuclear extract (prepared as in 2.4.3) or 20 µl of a *in vitro* transcription and translation reaction (TNT Quick coupled Transcription/Translation System) +/- recombinant HP1 in 0.5 ml PD150 were incubated with the peptide-bound beads overnight at 4°C under constant rotation. On the next day the beads were washed 6x with 1 ml PD150 at 4°C. Proteins, which were bound to the beads were analyzed by SDS-PAGE followed by Western Blot analysis.

Name	Protein (aa)	Sequence
H3unmod	Histone H3 (1-20)	MARTKQTARKSTGGKAPRKQ
H3K9me3	Histone H3 (1-20)	MARTKQTARKme3STGGKAPRKQ
ADNPunmod	ADNP (759-778)	EDDSYEARKSFLTKYFNKQP
ADNPK767me3	ADNP (759-778)	EDDSYEARKme3SFLTKYFNKQP

Table 2-4: Peptides used for the pulldown experiment

2.5.6 chromatin pull-down

SILAC HeLa S3 nuclear extracts (unlabeled, light or labeled with Arg-13C15N(+10) and Lys-13C(+6), heavy) were prepared as described (Ong and Mann, 2006) and provided by the Group of Prof. Dr. Reinhard Lührmann at the Max Planck Institute for Biophysical Chemistry.

50 µg of biotinylated nucleosomal arrays were pre-incubated with 200 µl of streptavidin coated magnetic beads (Promega) in CPD buffer for 4 h at 4°C. Unbound

oligonucleosomes were removed by three washes for 5 min with CPD buffer. Immobilized nucleosomal arrays were incubated with 5 ml SILAC HeLa S3 nuclear extracts (first experiment: unmodified nucleosomal arrays with light extract and H3K5me3 arrays with heavy extract; second experiment vice versa) for 4 hr at 4°C. Beads were then washed 6 times with CPD buffer and bound proteins were eluted by boiling the beads in Laemmli buffer. The heavy and light samples were mixed, run on SDS-PAGE gels, stained with Coomassie and analyzed by mass spectrometry.

For Western Blot analysis 10 µg of biotinylated oligonucleosomes were bound to 40 µl of streptavidin coated magnetic beads (Promega) and incubated with nuclear extract (prepared as for 2.4.3) as described above. CPD buffer was replaced by PD150.

2.5.7 Mass spectrometry and analysis

The mass spectrometry analysis was performed by the mass spectrometry facility of Dr. Henning Urlaub at the Max Planck Institute for Biophysical Chemistry.

Entire gel lanes of the SDS PAGE gels from 2.5.6 were cut into 23 slices of equal size. Proteins within the slices were digested according to (Shevchenko et al., 1996). Peptides were extracted and analyzed by LC-coupled tandem MS on an Orbitrap XL mass spectrometer (Thermo Fisher Scientific). Data analysis was performed as described (Sharma et al., 2009). Briefly, raw data files analyzed with the MaxQuant software (version 1.0.12.31), which performs peak list generation, SILAC-based quantitation, false discovery rate (FDR) determination, peptide to protein group assembly and data filtration. Data were searched against a concatenated forward and reversed version of the human International Protein Index (IPI) database (version 3.52) Mascot (Matrix Science). The accepted FDR was 1 % for the proteins and peptides. For peptides shared among different identified proteins, SILAC ratios were only considered for the ratio of the protein identified with the highest number of unique peptides. Output files were subtracted according to the gi-numbers (NCBI) of the found proteins with the help of the

statistical program R. An arbitrary cut-off of at least 2 fold enrichment in both experiments per protein was used.

R program used for data analysis:

open “R” (D1=experiment1 , D2=experiment2 with reversed ratio)

```
D1=read.table("/Users/kmosch/Desktop/exp1.txt", sep="\t", header=T)
```

```
D2=read.table("/Users/kmosch/Desktop/exp2.txt", sep="\t", header=T)
```

```
D1_D2=merge(D1,D2, by.x=1, by.y=1) ##### combining tables by GI number
```

3 Results

3.1 Identification of factors associated with H3K9me3

To gain insight into mechanisms for heterochromatin formation and maintenance I tried to identify proteins involved in heterochromatin formation by quantitative mass spectrometry analysis of a chromatin pulldown experiment. In vitro reconstituted chromatin consisting of 12 nucleosomes assembled on an artificial nucleosome positioning sequence (Lowary and Widom, 1998; Thastrom et al., 1999), trimethylated or unmodified at lysine 9 of histone H3 was immobilized on magnetic beads. These beads were incubated with stable isotope (Arg- $^{13}\text{C}^{15}\text{N}$ and Lys ^{13}C = heavy) labeled and normal (= light) HeLa S3 nuclear extracts respectively. The bound proteins, separated by SDS-PAGE were digested with trypsin and subjected to MS/MS analysis. The stable isotope labeling of amino acids in cell-culture (SILAC) (Ong and Mann, 2005, 2006) allowed for quantitative determination of factors enriched at the H3K9me3 oligonucleosomes. To exclude factors that are enriched in either the heavy or the light extract or which do not bind reproducibly to the modified oligonucleosomes, a reverse experiment using light HeLa S3 nuclear extract for unmodified H3 and light extract for the oligonucleosomes trimethylated at lysine 9 was conducted. The overlap of proteins with a greater than 2-fold enrichment in the H3K9 trimethylated sample was determined and further analyzed (Figure 3-1).

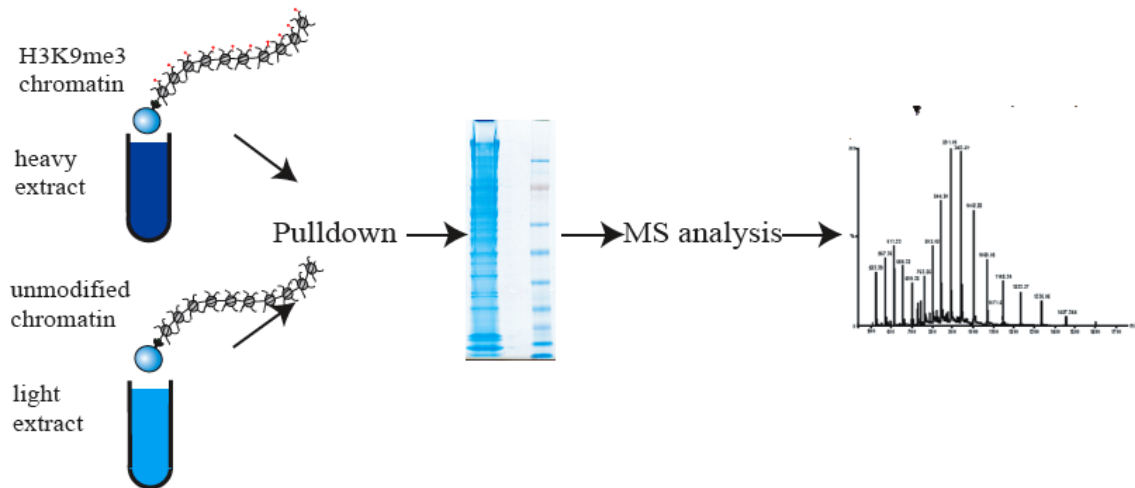


Figure 3-1: experimental setup

Arg- $^{13}\text{C}^{15}\text{N}$ and Lys- ^{13}C labeled (heavy) and unlabeled (light) nuclear extracts were used for pulldown experiments with nucleosomal arrays biotinylated at one end and immobilized on streptavidin coated beads. Red dots represent lysine 9 trimethylation on H3. The two samples were mixed and separated by SDS-PAGE. Proteins in gel slices were proteolytically fragmented and analyzed by LC-MS/MS.

In the initial experiment 490 proteins were identified but only for 355 of them a heavy to light (H/L) ratio could be determined. 208 of those factors displayed less than 2-fold enrichment in either the modified or unmodified sample. 106 proteins with more than 2-fold enrichment were detected in that pulldown experiment (Figure 3-2 A). In the reverse experiment 535 proteins were identified, 405 of those with an calculatable H/L ratio. 248 proteins were not enriched more than 2-fold at modified or unmodified chromatin whereas 79 proteins were enriched in the H3K9me3 fraction (Figure 3-2 B).

The overlap of both experiments consists of 20 proteins including known H3K9me3 interaction partners such as all isoforms of HP1 (CBX1, 3 and 5) and ICBP90 (UHRF 1 and 2) (Table 3-1).

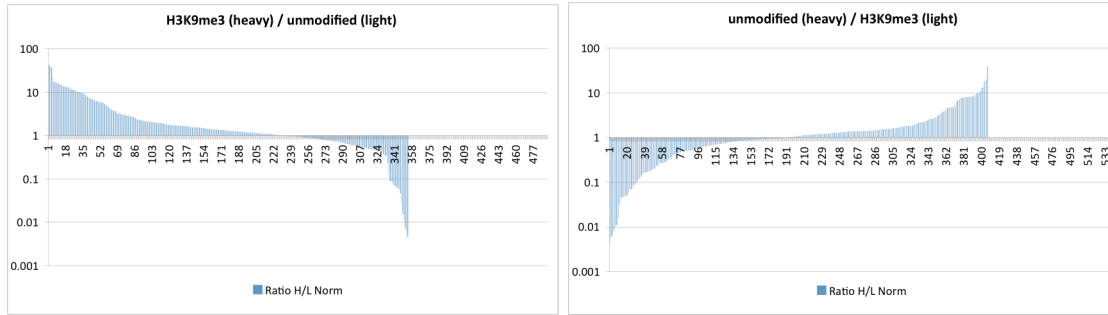


Figure 3-2: Distribution of the ratios between the heavy and light samples

The ratios between the heavy and light samples were calculated for each protein, ordered by value and plotted beginning with the proteins enriched at H3K9me3.

name	ratio H3K9me3 heavy unmodified light	ratio H3K9me3 light unmodified heavy
CBX5	14	5
UHRF1	12	4
UHRF2	12	5
MED31	10	4
UBP7	8	6
CBX1	8	6
DNMT1	7	6
CBX3	7	7
ADNP	4	12
CAF1B	4	13
POGZ	4	6
ZN580	4	3
JHD1A	3	3
CA103	3	7
DYL1	3	3
CIR1A	2	4
WDR75	2	4
NOL11	2	2
WDR43	2	3
UTP15	2	4

Table 3-1: Proteins with at least 2-fold enrichment in both experiments

One factor that which had so far not been identified as associated with heterochromatin was the activity dependent neuroprotector ADNP. Therefore this protein was selected for further studies.

3.2 Verification of H3K9me3 association of ADNP

3.2.1 ADNP associates with H3K9me3 and pericentromeric heterochromatin

In order to verify the enrichment of ADNP at oligonucleosomes trimethylated at H3K9, I repeated the chromatin pulldown experiment described above. Western Blot analysis with an ADNP specific antibody showed specific binding to H3K9me3 but not to unmodified oligonucleosomes (Figure 3-3 A). The detection of one ADNP band instead of two was not reproducible and might be due to low pulldown efficiency. Detection of histone H4 served as a loading control for the unmodified and methylated oligonucleosomes. To test if this specificity depends only on the trimethylation of H3K9 or on the DNA/nucleosome context, I performed a peptide pulldown. In this experiment peptides containing the first 21 amino acids of histone H3 were used instead of oligonucleosomes. Again specific binding of ADNP to H3K9me3 in contrast to the unmodified peptides was observed (Figure 3-3 B).

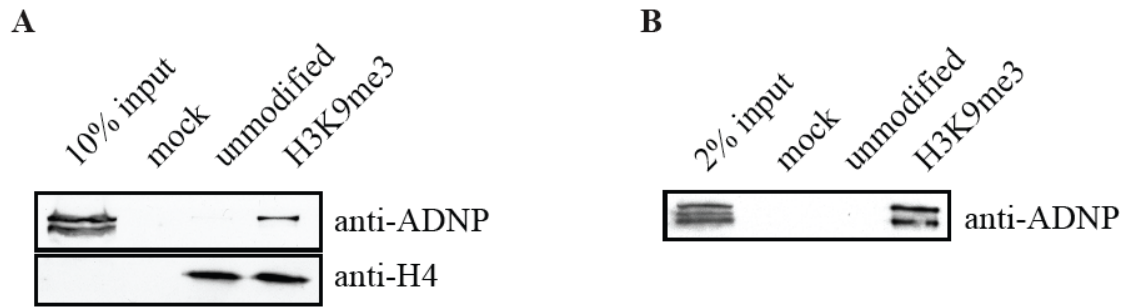


Figure 3-3: ADNP associates with H3K9me3

A, Chromatin pulldown. Recombinant 12-mer oligonucleosomal arrays reconstituted with the indicated H3 species were immobilized on magnetic beads and incubated with HeLa S3 nuclear extract. Beads without coupled oligonucleosomes were used as control (mock). Western Blots with the indicated antibodies are shown. **B**, Peptide pulldown. Histone H3 peptides (aa 1-21) unmodified or trimethylated at lysine 9 were bound to magnetic beads and incubated with HeLa S3 nuclear extract. Beads without immobilized peptides served as a control (mock). Western Blot with anti-ADNP antibody is shown.

In vivo the localization of ADNP was analyzed by immunostaining using an anti-ADNP antibody. DNA was counterstained with DAPI to visualize heterochromatic areas, which are mainly pericentromeric heterochromatin. The ADNP staining in interphase cells revealed a speckled distribution in the cell nucleus with enrichment at DAPI-dense regions. In the cytoplasm, a tubulin-like staining was observed (Figure 3-4 A). During mitosis and until telophase ADNP is largely displaced from chromatin. The tubulin-like staining however, does not allow conclusions about whether ADNP is completely excluded from chromatin or remains at microtubuli attachment sites (Figure 3-5). Furthermore, the distribution of ADNP in fibroblasts was investigated by subcellular fractionation. The cytoplasm and the nuclear soluble (nucleoplasm) and insoluble (chromatin) fractions were probed with an anti-ADNP antibody. β -tubulin was used as cytoplasmic marker and the transcription factor TBP and histone H3 as nuclear/chromatin markers. ADNP was enriched in the nuclear/chromatin fraction. However, no ADNP could be detected in the cytoplasmic fraction with β -tubulin (Figure 3-4 B).

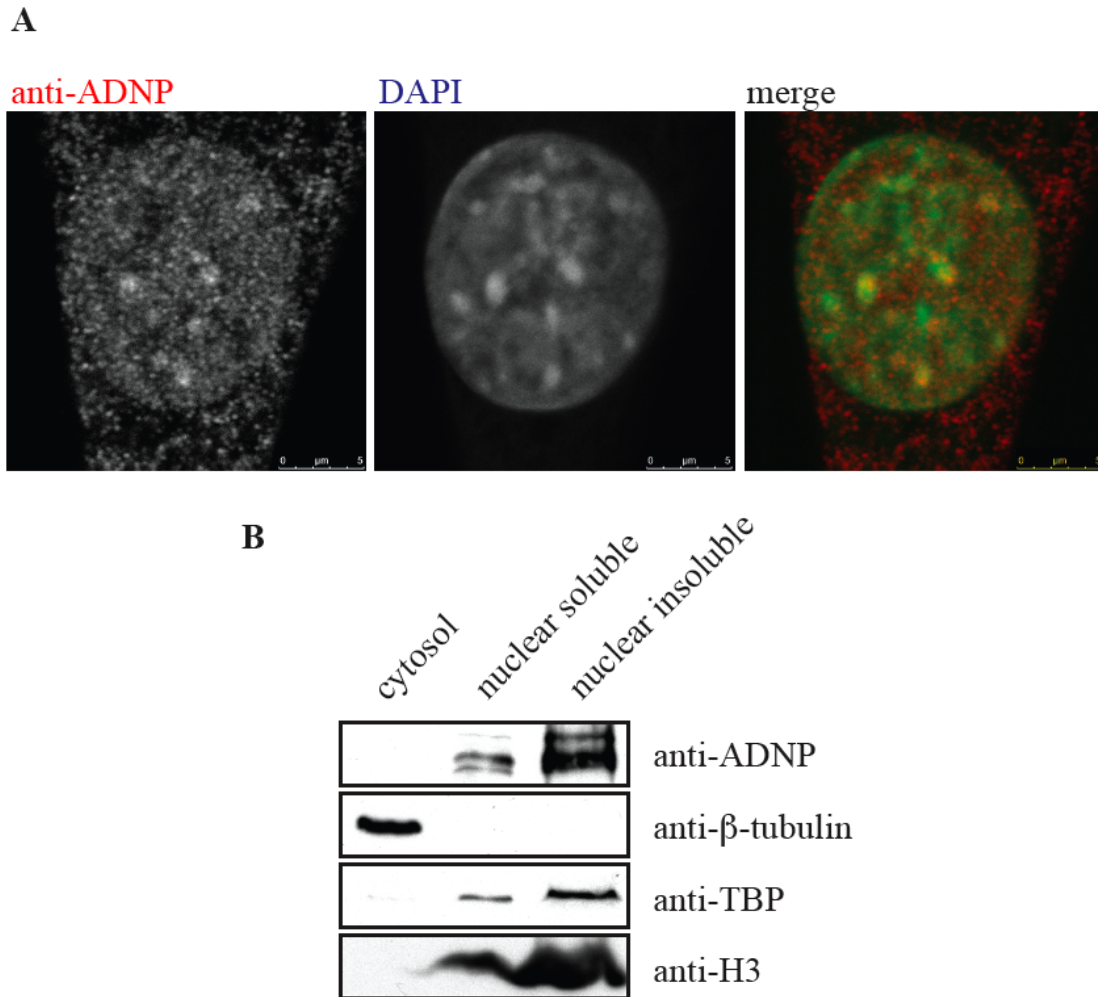


Figure 3-4 ADNP is enriched at pericentromeric heterochromatin

A, Immunofluorescence. NIH3T3 cells were stained with anti-ADNP antibody and DNA was visualized using DAPI. Bars represent 5 μ m. **B**, Subcellular fractionation. The cytoplasmic fraction of NIH3T3 cells was extracted with 0.1% Triton X-100. Nuclei were lysed under salt-free conditions and the soluble and insoluble fractions were separated by centrifugation. Western Blots with the indicated antibodies are shown.

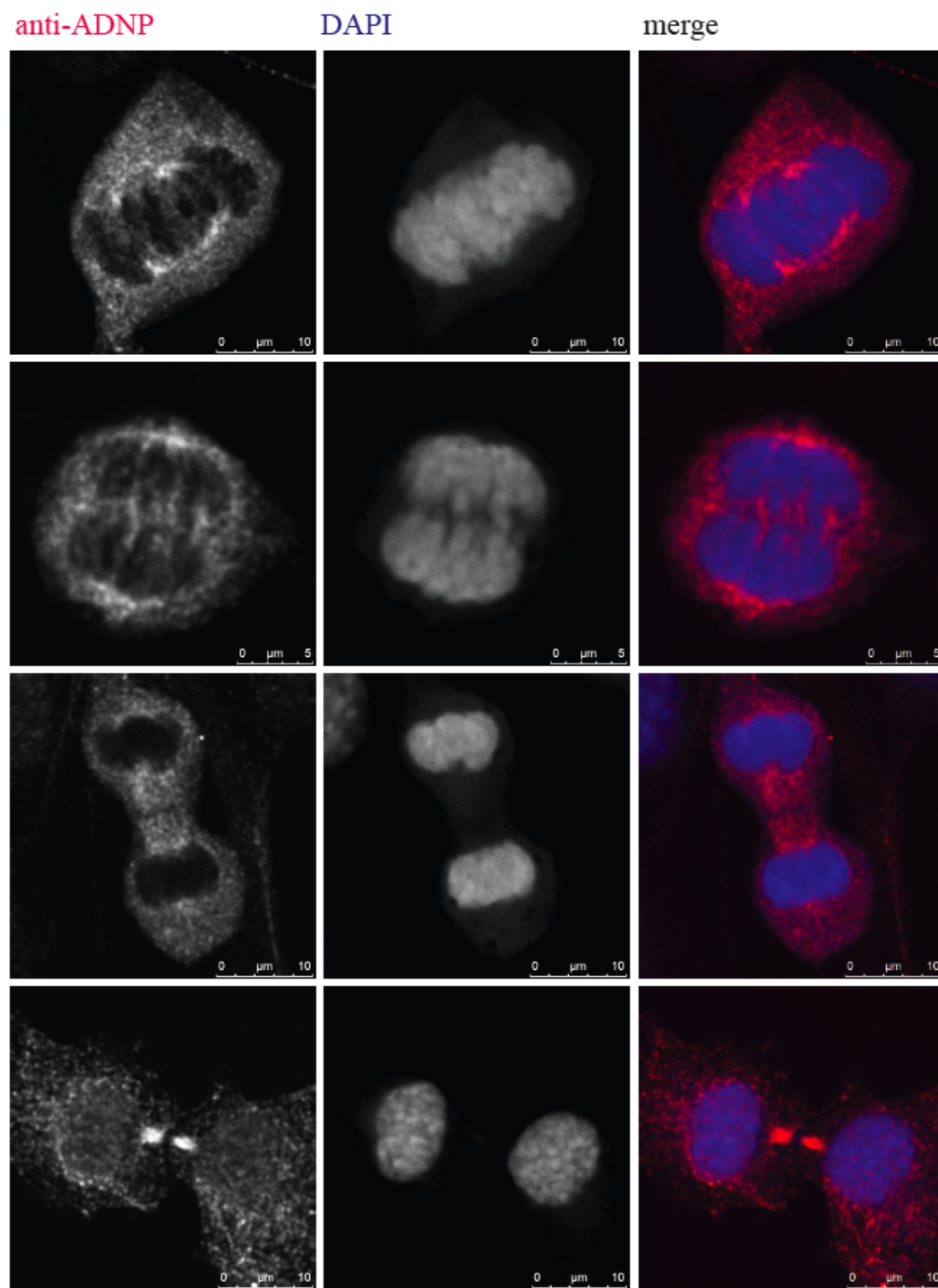


Figure 3-5: Localization of ADNP during mitosis

Immunofluorescence. NIH3T3 cells were stained with an anti-ADNP antibody. DNA was visualized using DAPI. Bars represent 10 μm (rows 1, 3, 4) and 5 μm (row 2).

Returning to the initial observation that ADNP associates with H3K9me3, I investigated their co-localization in cells. Co-staining with anti-ADNP and anti-H3K9me3 antibodies in mouse embryonic fibroblast (MEF) cells showed co-localization at DAPI-dense regions. Since trimethylation of H3K9 cannot be removed from the cells directly, I repeated the staining in Suv39h1/h2 double knockout cells. Suv39 is the methyltransferase that is responsible for H3K9me2/3 at pericentromeric heterochromatin (Peters et al., 2001). Consequently, no enrichment of H3K9me3 at DAPI-dense areas could be seen in those cells. Interestingly, ADNP was found removed from pericentromeric heterochromatin whereas the speckled distribution in the nucleus remained (Figure 3-6).

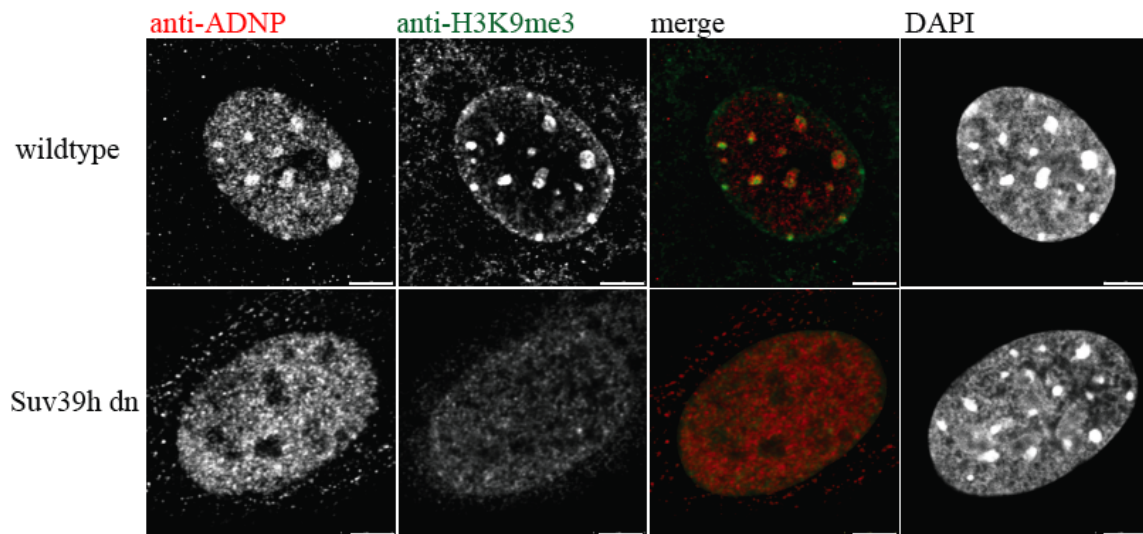


Figure 3-6: ADNP localization to pericentromeric heterochromatin depends on Suv39h

Immunofluorescence. MEF wildtype and Suv39h1/h2 double knockout cells were stained with the indicated antibodies. DNA was visualized using DAPI. Bars represent 5µm.

In conclusion, ADNP associates with H3K9me3 oligonucleosomes and histone peptides in vitro. The protein is localized to the cell nucleus, where it co-localizes with H3K9me3 at pericentromeric heterochromatin. This localization depends on the H3K9 methyltransferase Suv39.

3.2.2 ADNP is not alternatively spliced in mouse fibroblasts

Western Blots with anti-ADNP antibodies showed a double band after a 15 % SDS-PAGE (Figure 3-3) which could be further resolved by 10% SDS-PAGE (Figure 3-7 B). Therefore, I tested whether alternative splicing occurs in mouse fibroblasts. Figure 3-7 A shows a schematic representation of the genomic structure of ADNP. An untranscribed exon is followed by two small (108 bp and 93 bp) and one major exon. To see if one of the two smaller exons is removed by alternative splicing, I designed primers surrounding each of these exons. mRNA was extracted from MEF and NIH3T3 cells, reverse transcribed and analyzed by PCR. Primer-pair 1 surrounding exon 2 amplifies a 199 bp fragment from the full-length transcript and a 91 bp fragment if exon 2 is lacking. Primer-pair 2 amplifies a 198 bp or a 105 bp fragment from a transcript with or without exon 3 respectively. In both cases only the PCR product corresponding to the full-length transcript could be detected (Figure 3-7 C).

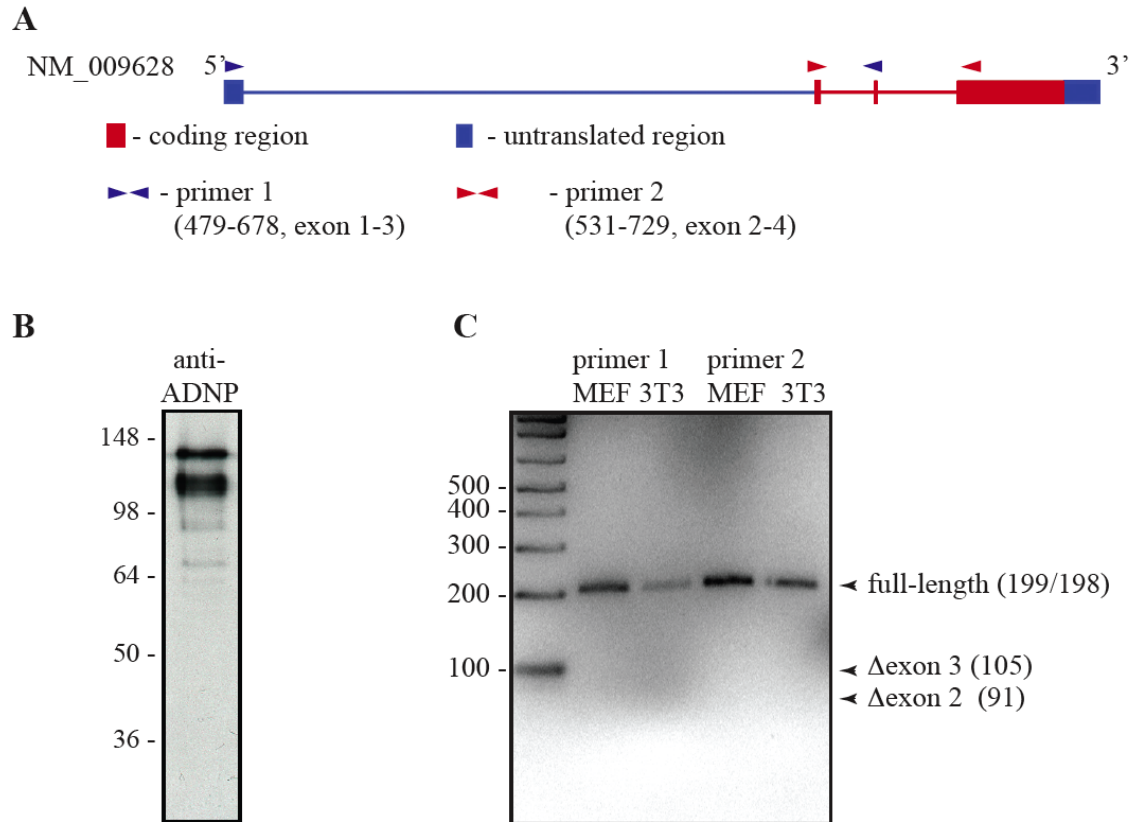


Figure 3-7: Only full-length ADNP mRNA is detected in mouse fibroblasts.

A, Schematic representation of the genomic structure of ADNP. Exons are drawn as boxes while introns are shown as lines. Red and blue arrowheads indicate the location of the primers used in **C**. **B**, Western Blot. Whole cell extract was separated by 15 % SDS-PAGE and analyzed by Western Blotting using an anti-ADNP antibody (BD Biosciences). **C**, RT-PCR. cDNA from NIH3T3 (3T3) cells and mouse embryonic fibroblasts (MEF) was used as template for the PCR reaction with the primers shown in **A**. The PCR products separated on a 1% agarose-gel stained with ethidium bromide are shown. Expected sizes of the full-length cDNA and the alternatively spliced variants are indicated.

From this experiment, I concluded that there are no alternatively spliced ADNP transcripts in mouse fibroblasts.

3.3 Mode of ADNP recruitment to heterochromatin

ADNP does not contain a chromo domain or another known domain that is known to bind histone modifications. However, ADNP was reported to interact with the SWI/SNF complex via its C-terminal domain (Mandel and Gozes, 2007). Brg1, one component of that complex was recently shown to have functions in pericentromeric heterochromatin (Bourgo et al., 2009). Co-precipitation of ADNP with HP1 α has also been reported (Mandel et al., 2007). The ADNP homeodomain contains a PxVxL motif, a known HP1 interaction motif. It also includes an ARKS sequence, similar to that of the histone H3 tail, which can be trimethylated at lysine 9 and then be bound by HP1. Therefore the homeodomain is likely to be an HP1 interaction domain, allowing indirect targeting of ADNP to pericentromeric heterochromatin by HP1.

To determine how ADNP is recruited to pericentromeric heterochromatin I used deletion mutants, which identified the homeodomain as necessary and sufficient for localization. Peptide pull-down experiments with ADNP expressed in reticulocyte lysate showed that ADNP does not bind to H3H9me3 directly but only in the presence of HP1. The ADNP-HP1 interaction could be mapped to the PxVxL but not the ARKS motif.

3.3.1 ADNP localization to chromocenters depends on the Homeodomain

To identify the domain that is responsible for ADNP localization, I cloned different deletion constructs. Shown in Figure 3-8 are CFP-ADNP constructs containing full-length ADNP, the protein lacking the homeodomain, and the homeodomain alone, all containing the nuclear localization signal (NLS). These constructs were co-expressed with RFP-HP1 β as a heterochromatin marker in NIH3T3 cells. Full-length ADNP and the homeodomain alone co-localized with HP1 whereas the mutant lacking the homeodomain did not display an enrichment at any particular site in the nucleus.

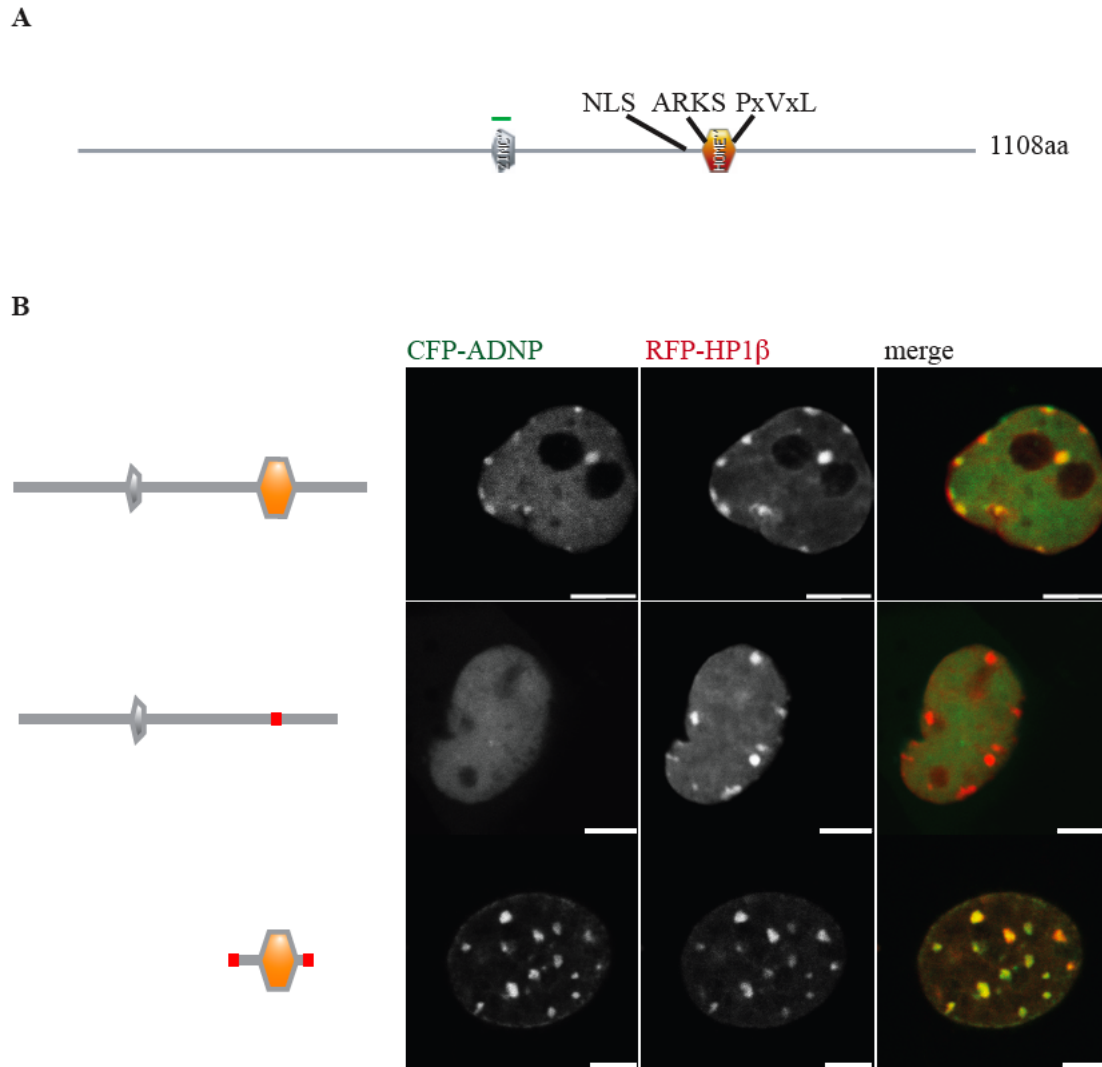


Figure 3-8: The homeodomain of ADNP is necessary and sufficient for localization to pericentromeric heterochromatin

A, Schematic representation of the ADNP protein structure as predicted by PROSITE (www.expasy.ch/cgi-bin/prosite). Positions of the zinc-finger (grey), the homeodomain (orange), the nuclear localization signal (NLS) and the ARKS and PxVxL motifs are indicated. **B**, Live cell imaging. NIH3T3 cells were transfected with CFP-ADNP, CFP-ADNP Δ 741-846 (homeodomain deletion), CFP-ADNP-701-846 (NLS and the homeodomain) and RFP-HP1 β . Bars represent 5 μ m.

3.3.2 ADNP does not bind to H3K9me3 directly but is targeted to pericentromeric heterochromatin by HP1

Since the homeodomain contains the putative HP1 interaction motifs, I asked whether ADNP is able to bind to H3K9me3 directly or only in the presence of HP1. I performed a peptide pull-down experiment using H3K9me3 and unmodified H3 peptides immobilized to magnetic beads, and beads without peptides as a control. FLAG-tagged ADNP was expressed in TNT reticulocyte extract and incubated with these beads in the absence and presence of recombinant HP1. In the absence of HP1, ADNP did not bind to the beads or peptides. When co-incubated with HP1 α , HP1 β and HP1 γ , ADNP bound specifically to the methylated peptide bound beads together with each of the HP1 isoforms (Figure 3-9).

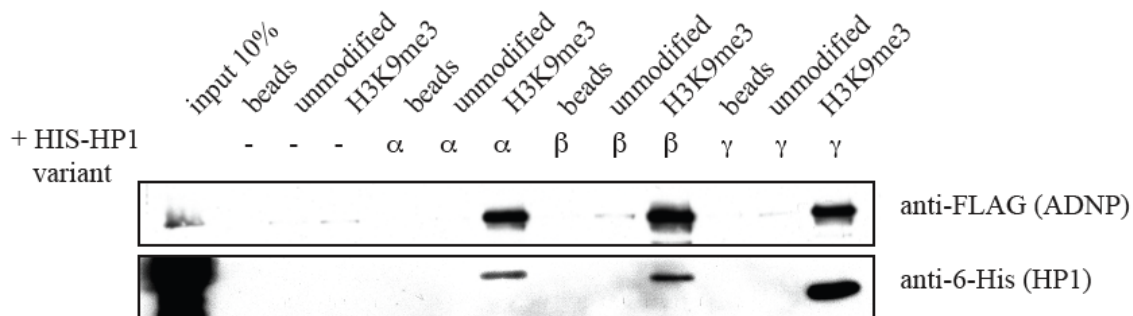


Figure 3-9 All three HP1 isoforms are able to recruit ADNP to H3K9me3

Peptide pulldown. Flag-tagged ADNP was expressed in TNT-reticulocyte extract and incubated with histone H3 peptides (unmodified or trimethylated at lysine 9), immobilized on magnetic beads. 1 μ g recombinant, HIS-tagged HP1 was added as indicated. Beads without peptide served as a control. The pulldown was analyzed by Western Blotting using anti-FLAG and anti-6-HIS antibodies.

To test whether the isoform independent recruitment of ADNP by HP1 *in vitro* is also reflected *in vivo*, I used HP1 knockout cells. Antibody staining of ADNP and visualization of DNA with DAPI in HP1 α , HP1 β and HP1 γ single knockout MEF cells showed that ADNP localization is not affected by the lack of one HP1 isoform (Figure 3-10 A). In HP1 α/β double knockout MEF cells HP1 γ is the only isoform expressed, and HP1 γ did not localize to chromocenters in these HP1 α/β knockout cells. Also in these cells, no enrichment of ADNP at pericentromeric heterochromatin could be detected (Figure 3-10 B).

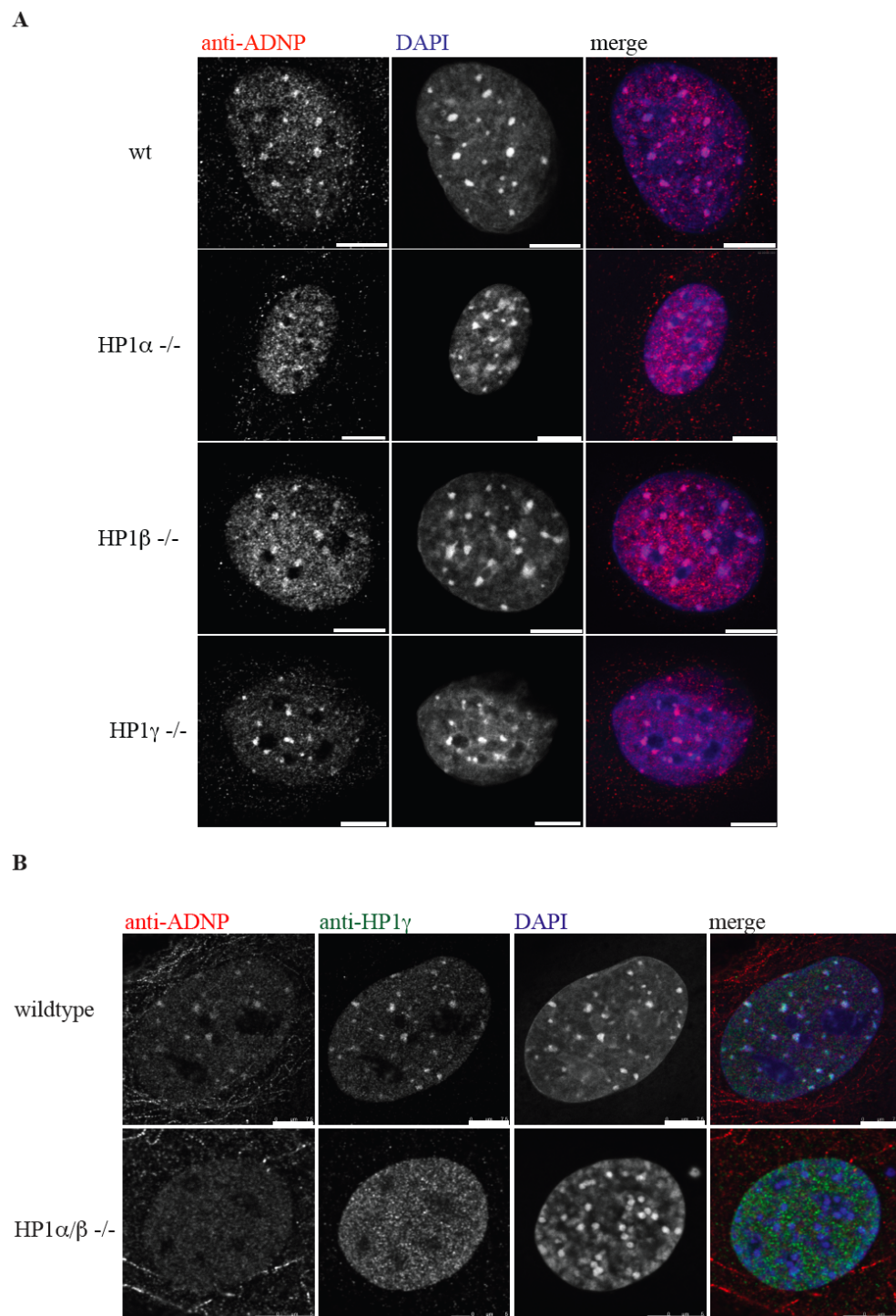


Figure 3-10: ADNP localization to pericentromeric heterochromatin is HP1 dependent.

A, Immunofluorescence. MEF wildtype and HP1 α , β or γ single knock-out cells were stained with an anti-ADNP antibody. **B**, Immunofluorescence. MEF wildtype and HP1 α/β double knock-out cells were stained with the indicated antibodies. DNA was visualized using DAPI. Bars represent 7.5 μ m.

To verify that ADNP displacement in HP1 α/β double knockout cells is not an effect of H3K9me3, ADNP or HP1 γ misregulation their expression levels were assessed by Western Blot. Total cell extracts of wild type and HP1 α/β knockout MEF cells were separated by SDS-PAGE and probed with anti-ADNP, anti-HP1 γ and anti-H3K9me3 antibodies. β -tubulin and H4 were used as a loading control. No significant changes in the expression / modification levels could be detected. Immunostaining of H3K9me3 and counterstaining with DAPI in the HP1 α/β double knockout cells did not indicate an effect on H3K9me3 localization (Figure 3-11).

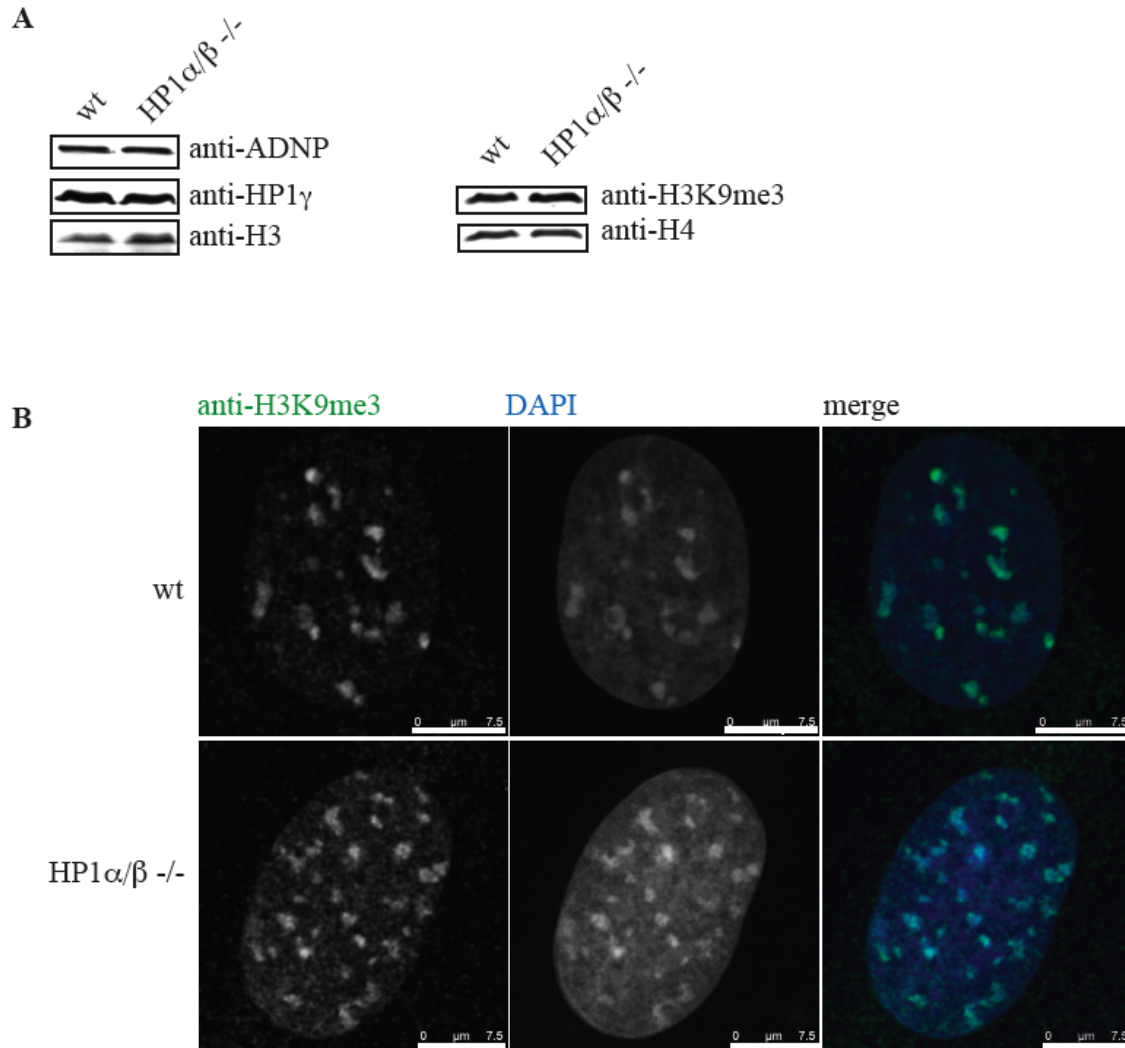


Figure 3-11: levels of HP1 γ , ADNP and H3K9me3 as well as H3K9me3 distribution are not affected by HP1 α/β knockout

A, Western Blot. Total cell extracts of wild type and HP1 α/β knockout MEF cells were analyzed by Western Blot using the indicated antibodies. **B**, Immunofluorescence. MEF wildtype and HP1 α/β double knockout cells were stained with anti-H3K9me3 antibodies. DNA was visualized using DAPI. Bars represent 7.5 μ m.

From these results, I concluded that ADNP does not bind to H3K9me3 directly but is recruited to pericentromeric heterochromatin by HP1. This behavior is not dependent on one particular isoform of HP1.

3.3.3 ADNP localization to chromocenters mainly depends on HP1 binding to the PxVxL motif within the homeodomain

To further characterize the ADNP – HP1 interaction, the homeodomain was mutated at the putative HP1 interaction sites. The lysine in the ARKS motif was mutated to arginine to prevent a possible methylation event, which might be bound by the HP1 chromo domain. In the PxVxL motif the valine was mutated to a glutamate. This mutation has been shown to strongly reduce binding of the HP1 chromoshadow domain (Figure 3-12 A). Wild type ADNP, the single point mutants and the double mutant were fused to YFP and introduced into NIH3T3 cells. Because the transfection efficiency of the full-length protein was below 1 % and strong overexpression caused aggregation of YFP-ADNP (data not shown) inducible stable cell-lines were established. Figure 3-12 B shows Western Blot analysis of two cell-lines for each of the mutations using an anti-ADNP antibody. The upper band represents the YFP-ADNP fusion protein whereas the lower band shows the endogenous ADNP. For comparison, extracts of untransfected NIH3T3 cells were loaded. Only moderate overexpression levels were detected (Figure 3-12 B). Live cell imaging revealed that the ARKS point mutation had no effect on ADNP localization. The mutation within the PxVxL motif lead to a strong reduction of the ADNP signal at chromocenters. Only the K767K/V821E double mutant was completely displaced. These results were confirmed *in vitro*. Wild type and mutant FLAG-tagged ADNP was expressed in TNT reticulocyte extract and used for H3K9me3 peptide pulldown experiments. In the presence of recombinant HP1 β wild type and K767R mutated ADNP were bound to H3K9me3 peptide bound beads. However, only minimal amounts of the PxVxL mutant proteins and no double mutant protein could be detected (Figure 3-12 D).

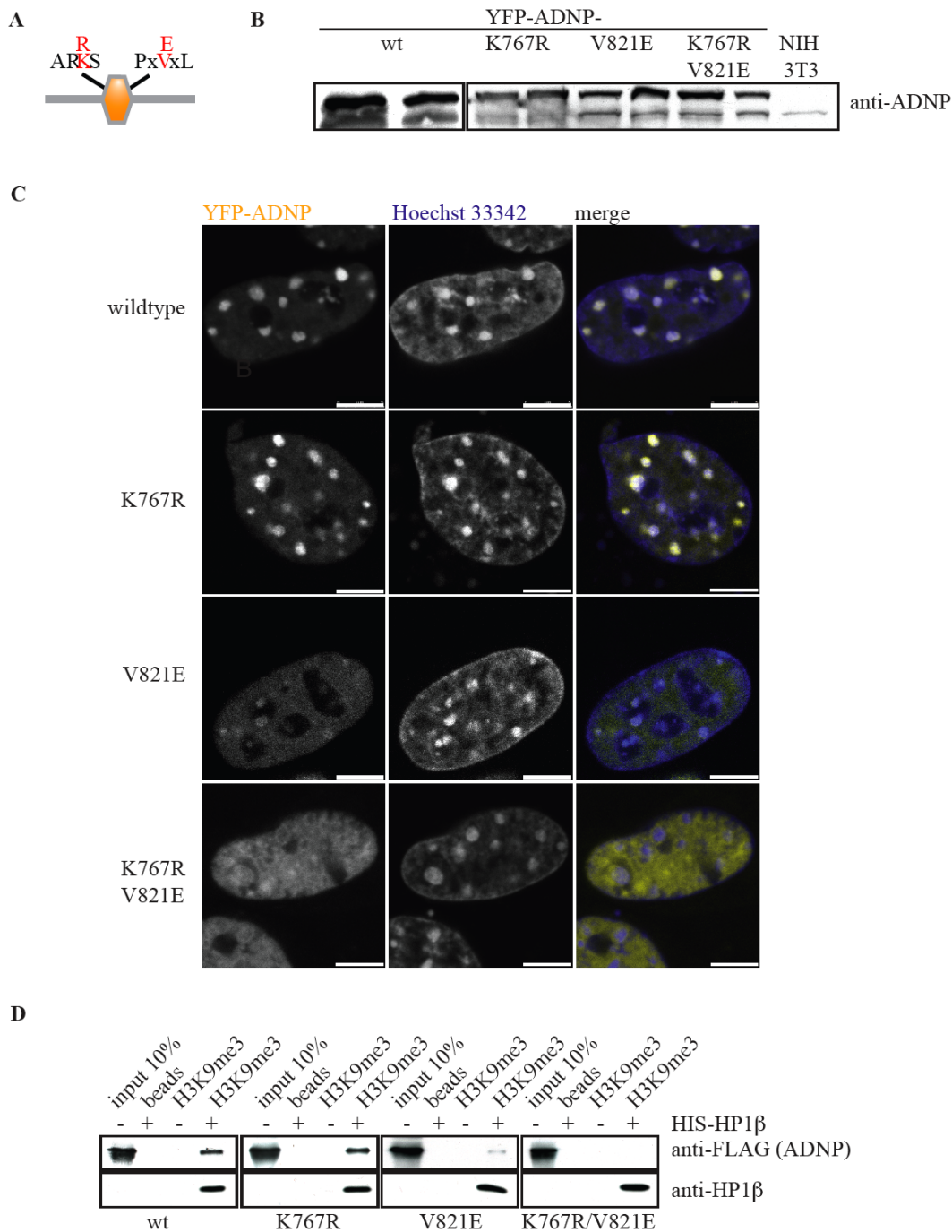


Figure 3-12: The PxVxL and ARKS motifs are involved in ADNP localization.

A, Schematic representation of the ADNP-homeodomain, containing a K to R mutation in the ARKS and a V to E mutation in the PxVxL motif. **B**, Two clones of inducible NIH3T3 cells, expressing YFP-ADNP, wild-type or carrying one or both of these mutations were analyzed by Western Blot using an anti-ADNP antibody. **C**, Live cell imaging. DNA was stained with Hoechst 33342 dye. Bars represent 5 μ m. **D**, Pull-down experiment with H3K9me3-peptides, immobilized on magnetic beads using TNT-reticulocyte-extract expressed ADNP-FLAG (wt and point mutants) and recombinant 6xHIS-HP1 β , analyzed by Western Blot.

To test whether ADNP dimerization/multimerization rather than HP1 interaction is involved in recruitment of the ADNP mutants, YFP-ADNP was immunoprecipitated using an anti-GFP antibody. All forms of YFP-ADNP including the double mutant, which does not localize to pericentromeric heterochromatin, co-immunoprecipitated endogenous ADNP.

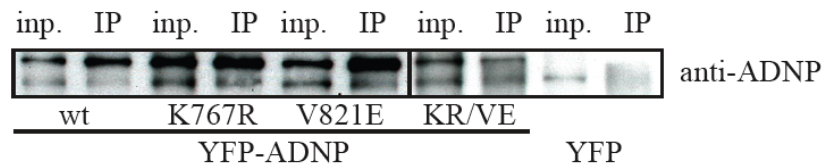


Figure 3-13: The AKRS and PxVxL point mutations have no influence on ADNP multimerization.

Immunoprecipitation. Nuclear extract was prepared from inducible NIH3T3 cells, expressing YFP-ADNP, wild-type or carrying a K to R mutation in the ARKS (K767R) and a V to E mutation in the PxVxL (V821E) motif. YFP expressing inducible NIH3T3 cells were used as control. Immunoprecipitation was performed with anti-GFP antibody and analyzed by Western Blot using anti-ADNP antibody.

If the interaction between the HP1 chromoshadow domain and the ADNP PxVxL motif is the main mechanism for its recruitment to H3K9me3, then association of ADNP with H3K9me3 should be strongly reduced by a mutation within the chromoshadow domain. A mutation of tryptophan 170 to alanine (W170A) of HP1 β had been described to abolish HP1-PxVxL interaction without affecting HP1 dimerization and H3K9me3 binding (Thiru et al., 2004). This mutant as well as wild type HP1 β were used in a peptide pull-down experiment with wild type FLAG-tagged ADNP. The W170A mutation had no effect on HP1 binding to H3K9me3 peptide bound beads. However, only background levels of ADNP were detected with HP1 β (W170A).

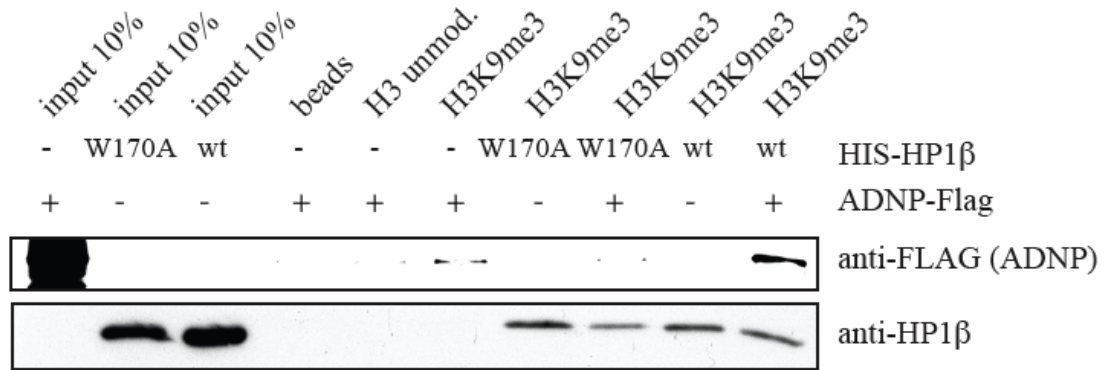


Figure 3-14: HP1 chromoshadow domain mutation strongly reduces binding of ADNP

Pulldown experiment with H3K9me3-peptides, immobilized on magnetic beads using TNT-reticulocyte-extract expressed ADNP-FLAG and recombinant 6xHIS-HP1β (wt and W170A mutants), analyzed by Western Blot.

3.3.4 A possible lysine methylation in the ADNP ARKS motif is not involved in HP1 binding

The results of the previous section showed a severe effect of PxVxL mutation on ADNP recruitment. This effect was enhanced by a mutation within the ARKS motif (Figure 3-12). Thus, a minor effect of a possible lysine methylation of the ADNP ARKS motif could not be excluded so far. Therefore, I tested whether ADNP is methylated in nuclei and HP1 would bind trimethylated lysine 767.

To test if ADNP is methylated, nuclei were isolated from NIH3T3 cells and incubated with adenosyl-L-methionine S-[methyl-³H]. Subsequently ADNP was immunoprecipitated with an anti-ADNP antibody. 15% of the sample was used to confirm the immunoprecipitation by Western Blot. The remaining sample was used for SDS-PAGE followed by autoradiography. After 6 months detection time a signal at the expected size of ADNP was detected in the IP. Compared to the signal of non-specifically precipitated histones in the IP, and the control the possible ADNP signal was very weak.

The possibility of HP1 binding to trimethylated lysine 767 of ADNP was assessed by pull-down experiments using unmethylated ADNP peptides or peptides trimethylated at lysine 767. Histone H3 peptides unmodified or trimethylated at lysine 9 served as positive controls. Using HeLaS3 nuclear extracts in the peptide pull-down experiment all isoforms of HP1 bound to H3K9me3 but not detectably to ADNPK767me3 peptide bound beads. The same result was observed for ADNP itself and for CDYL (Fischle et al., 2008), another chromodomain protein.

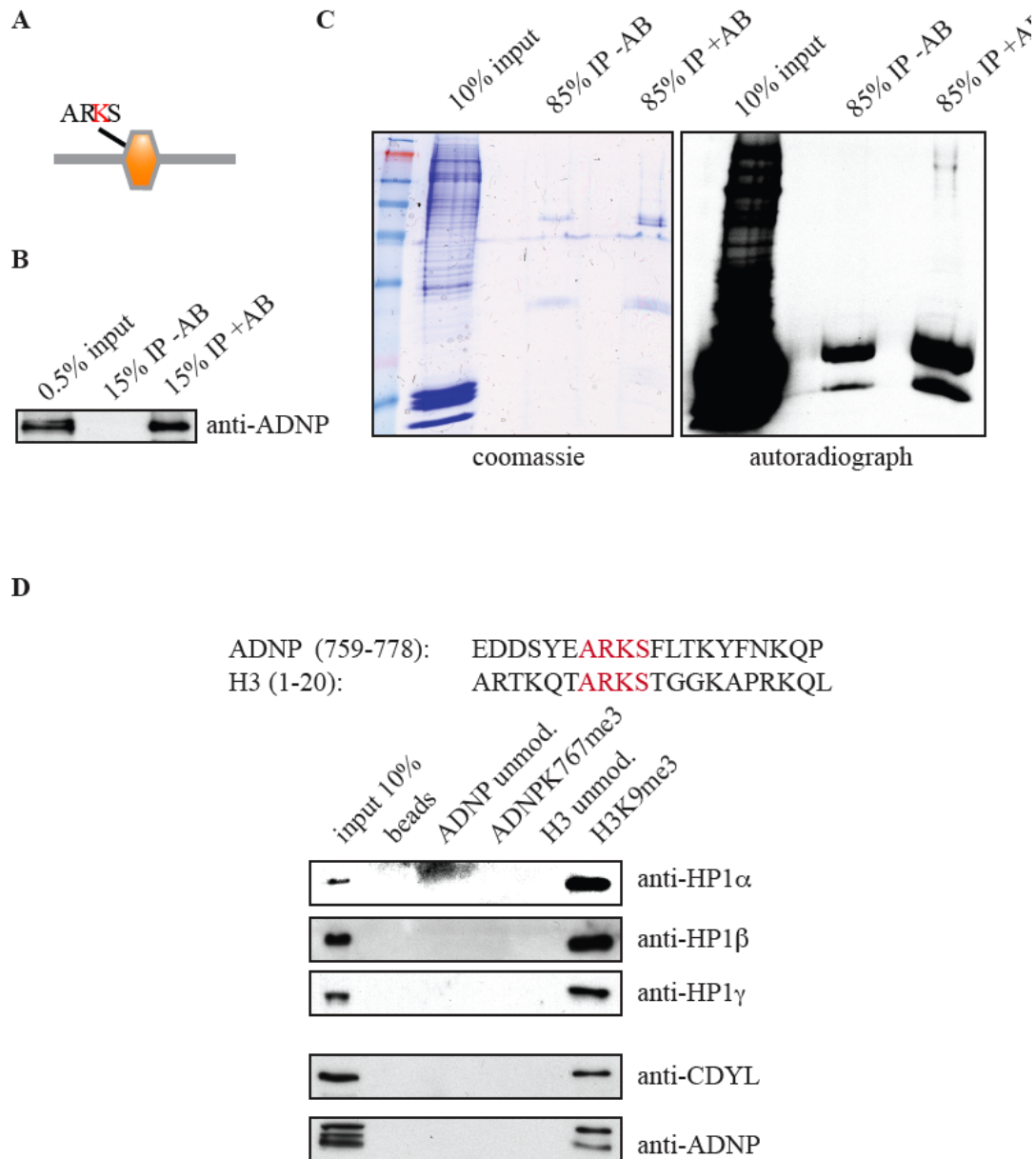


Figure 3-15: The ARKS motif of ADNP is not involved in HP1 binding

A, Schematic representation of the ADNP homeodomain containing the ARKS motif. **B** and **C**, Immunoprecipitation. Isolated nuclei of NIH3T3 cells were incubated with adenosyl-L-methionin S-[methyl-³H]. Immunoprecipitation was performed with anti-ADNP antibody and analyzed by **B**, Western Blot with anti-ADNP antibody and **C**, autoradiography. Coomassie staining and the autoradiograph after 6 months exposure are shown. **D**, Peptide pulldown. ADNP peptides and histone H3 peptides unmodified or trimethylated at lysine 767 or 9 respectively, were bound to magnetic beads and incubated with HeLa S3 nuclear extract. Beads without immobilized peptides served as a control. A Western Blot with the indicated antibodies anti-ADNP antibody is shown.

Taken together, these results indicate that ADNP is recruited to pericentromeric heterochromatin by HP1 interacting with H3K9me3 via its chromo domain on one hand and with the homeodomain of ADNP on the other hand. The HP1 – ADNP interaction is mainly mediated by binding of the HP1 chromoshadow domain to the PxVxL motif within the ADNP homeodomain. Although the effect of a PxVxL mutation is enhanced by an additional mutation in the ARKS motif, there is no evidence that methylation of the ARKS motif is involved in that process.

3.4 ADNP function at pericentromeric heterochromatin

ADNP had been shown to be involved in up- and down-regulation of a diverse set of genes during embryogenesis (Mandel et al., 2007). Other chromatin functions have not been described so far. Known interaction partners of ADNP however lead to testable hypotheses of ADNP function at pericentromeric heterochromatin. Brg1, an interaction partner of ADNP, has recently been shown to be involved in structure and organization of pericentromeric heterochromatin (Bourgo et al., 2009). In addition, ADNP is displaced from chromocenters in Suv39h1/h2 knockout cells. An ADNP loss-of-function phenotype at pericentromeric heterochromatin should also be reflected in those cells. Therefore, I tested whether ADNP knockdown results in one of the phenotypes described for the Suv39h1/h2 knockout cells: (I) change of global levels and distribution of histone modifications, (II) reduction of DNA methylation and (III) transcriptional silencing of major satellite repeats (Lehnertz et al., 2003; Peters et al., 2003; Peters et al., 2001; Schotta et al., 2004).

3.4.1 ADNP knockdown does not phenocopy the Brg1 knockout phenotype

Deletion of Brg1 in mouse fibroblasts results in dissolution of pericentromeric heterochromatin domains and a redistribution of trimethylated H3K9 and H4K20 (Bourgo et al., 2009). Involvement of ADNP in these Brg1 functions was tested by knockdown of ADNP by siRNA. Two different siRNAs, 71 and 68, were used to knock down ADNP. A scrambled siRNA served as control. The knockdown of ADNP was confirmed by immunofluorescence staining using an anti-ADNP antibody. DAPI staining of DNA did not show dissolution of pericentromeric heterochromatin (Figure 3-16, Figure 3-17). The distribution of H3K9me3 and H4K20me3 remained unchanged in the ADNP knockdown cells as well (Figure 3-16, Figure 3-17).

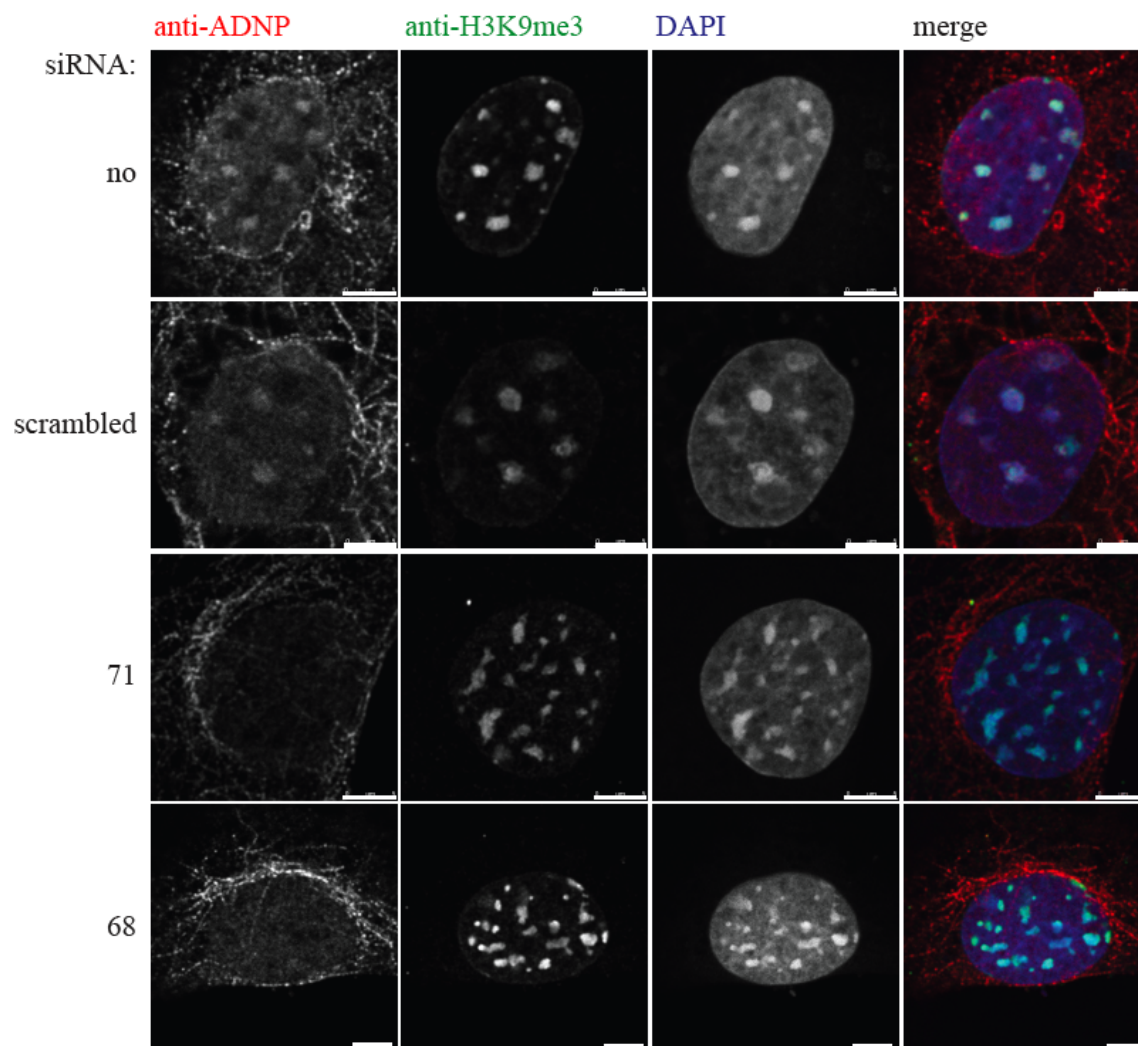


Figure 3-16: ADNP knockdown does not influence H3K9me3 localization.

Immunofluorescence. NIH3T3, transfected with siRNA against ADNP (68 and 71), scrambled siRNA or untransfected (no) were stained with the indicated antibodies. DNA was visualized with DAPI. Bars represent 5 μ m.

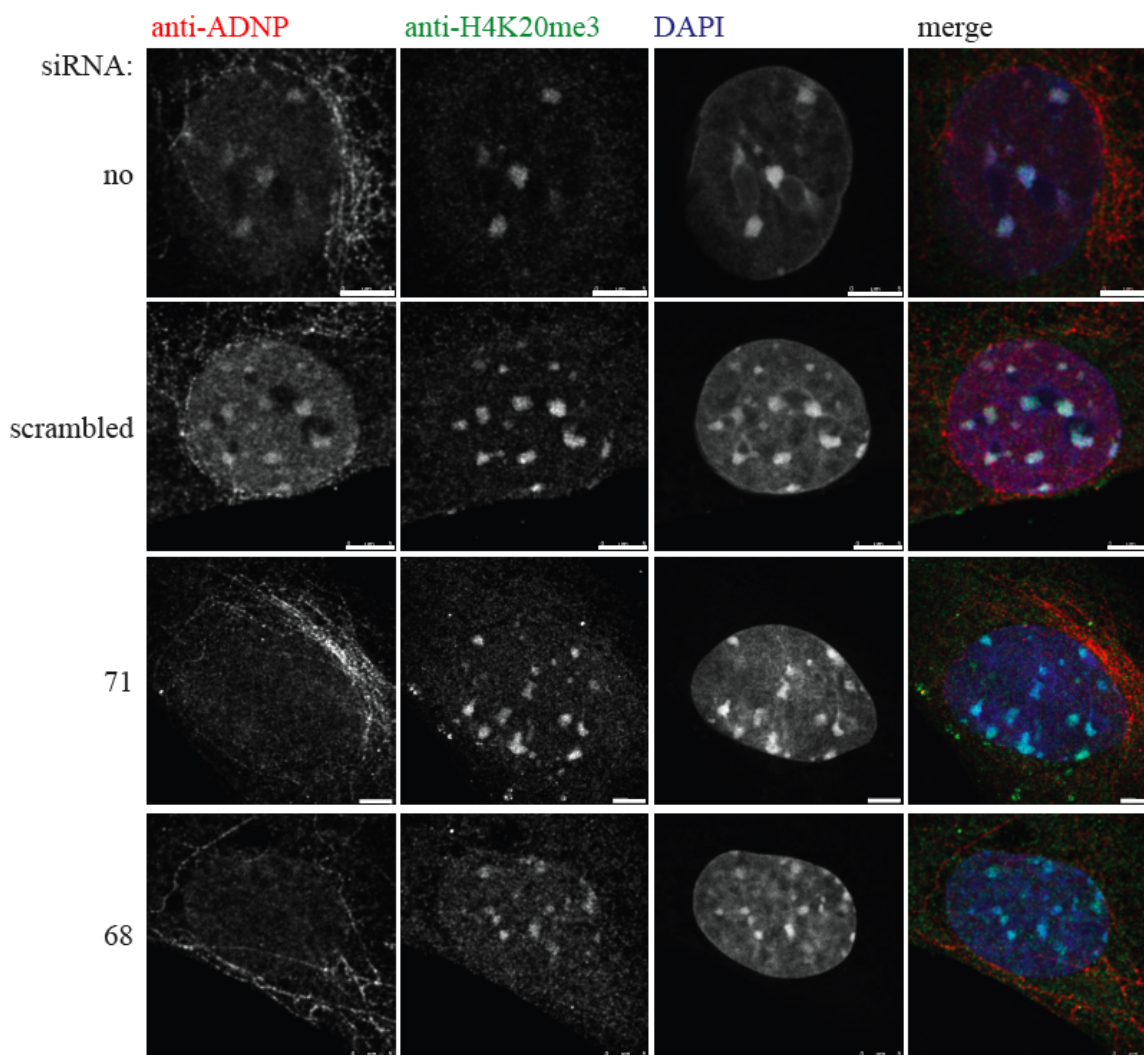


Figure 3-17: ADNP knockdown does not influence H4K20me3 distribution.

Immunofluorescence. NIH3T3, transfected with siRNA against ADNP (68 and 71), scrambled siRNA or untransfected (no) were stained with the indicated antibodies. DNA was visualized with DAPI. Bars represent 5 μ m.

3.4.2 Knockdown of ADNP does not influence the global level of histone modifications

Functional analysis of ADNP was carried out by siRNA knockdown. From a single knockdown cell preparation, I assessed the knockdown efficiency on protein level as shown in the representative Western Blot in Figure 3-18. The knockdown efficiency for all subsequent experiments is shown except for immunofluorescence analysis. A reduction of ADNP could be achieved with both siRNAs. However, the knockdown was most efficient for siRNA 71.

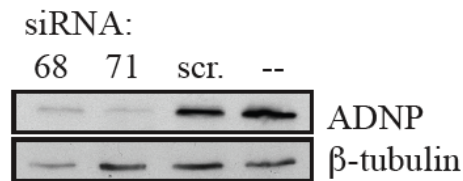


Figure 3-18: ADNP knockdown.

Western Blot. NIH3T3 cells were transfected with siRNA against ADNP (68 and 71). As controls NIH3T3 cells transfected with a scrambled siRNA and untransfected cells were used. The knockdown was verified by Western Blot using anti-ADNP and anti β -tubulin (loading control) antibodies.

Suv39h1 is a methyltransferase specific for H3K9me_{2/3}. Its knockout however does not only reduce H3K9me₃ levels but also related (H3K9me₃/S10ph decrease and H3K9ac increase) and indirectly affected (H4K20me₃ decrease) histone modification levels (Schotta et al., 2004). To test if ADNP has an effect on global histone modification levels total cell extract of the ADNP knockdown NIH3T3 cells (Figure 3-18) as well as Suv39h1/h2 knockout and wild type MEF cells (positive control) was analyzed by Western Blot. Histone H3 and H4 antibodies were used as loading controls. For H3K9me₃/S10ph, two different exposures are shown to detect the combined modification in the control MEF cells (upper panel) without overexposing the siRNA NIH3T3 cells

(lower panel). The positive control MEF cells showed the expected result described above. Conversely, no effect of ADNP knockdown could be observed. For completion, H3K27me1, which is also associated with pericentromeric heterochromatin (Peters et al., 2003) was analyzed. For H3K27me1, there was no effect of Suv39 knockout and ADNP knockdown was detected.

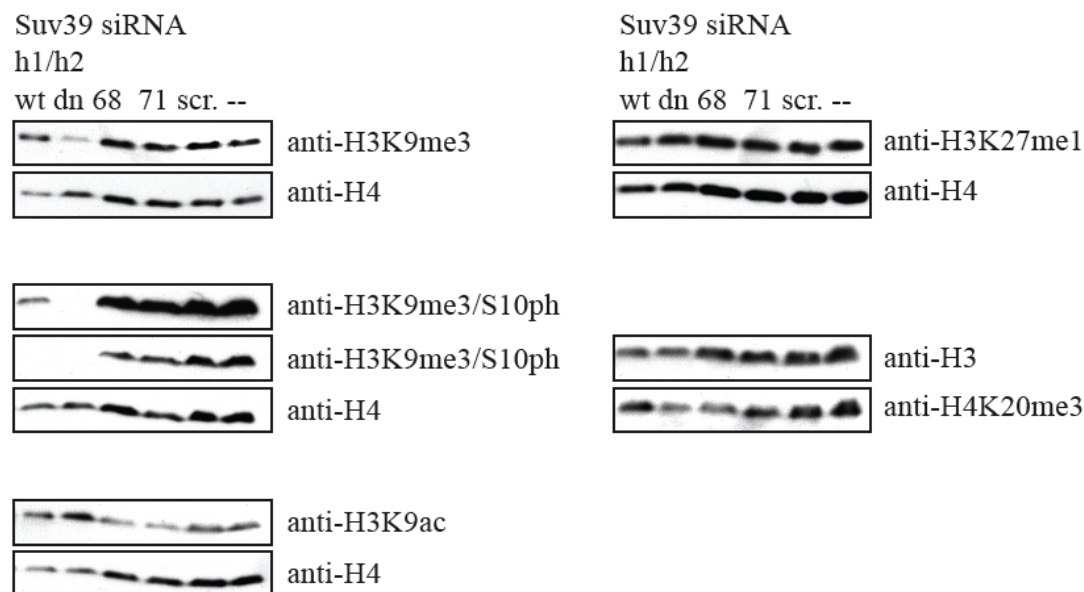


Figure 3-19: ADNP knockdown does not influence global histone modifications

Western Blot. Aliquots of the cells shown in Figure 3-18 were analyzed by Western Blotting using the indicated antibodies. The anti-H4 and anti-H3 antibodies were used to verify equal loading. Suv39h1/h2 wildtype (wt) and double knockout (dn) MEF cells served as experimental controls.

3.4.3 ADNP knockdown has no influence on the localization of HP1 and repressive histone modifications

Not only the global level of modifications but also the localization of certain histone modifications, H4K20me3 and H3K27me1 as well as HP1 are affected by Suv39h1/h2 knockout (Harnicarova Horakova et al., 2009; Peters et al., 2003; Schotta et al., 2004). With my experiments, I could exclude an effect of ADNP on H3K9me3 and H4K20me3 (3.4.1). To further investigate a role of ADNP on HP1 and H3K27me1 localization, the HP1 isoforms and H3K27me1 were stained with the respective antibodies as in (3.4.1). Suv39h1/h2 knockout and wild type MEF cells were used as experimental controls. None of the HP1 isoforms localized to pericentromeric heterochromatin in the Suv39h1/h2 knockout cells whereas the distribution of HP1 remained unchanged in the ADNP knockdown cells (Figure 3-20Figure 3-21Figure 3-22). In contrast to the literature (Peters et al., 2003), I observed a mixed population of about 50% of the cells exhibiting diffuse or heterochromatic H3K27me1 signals in all MEF and NIH3T3 cells analyzed. A representative image is shown in Figure 3-23 A, upper panel. (Peters et al., 2003) described a complete loss of H3K27me1 from pericentromeric heterochromatin. To show that Suv39h1/h2 knockout and ADNP knock-down had no such effect in my experiments, only cells showing H3K27me1 signals at pericentromeric heterochromatin are depicted. Differences in the staining intensity were within a variability also observed in the wild type cells. This variability could be seen in untransfected and scrambled siRNA transfected cells as well.

In conclusion, knock-down of ADNP had no detectable effect on HP1 and H3K27me1 distribution.

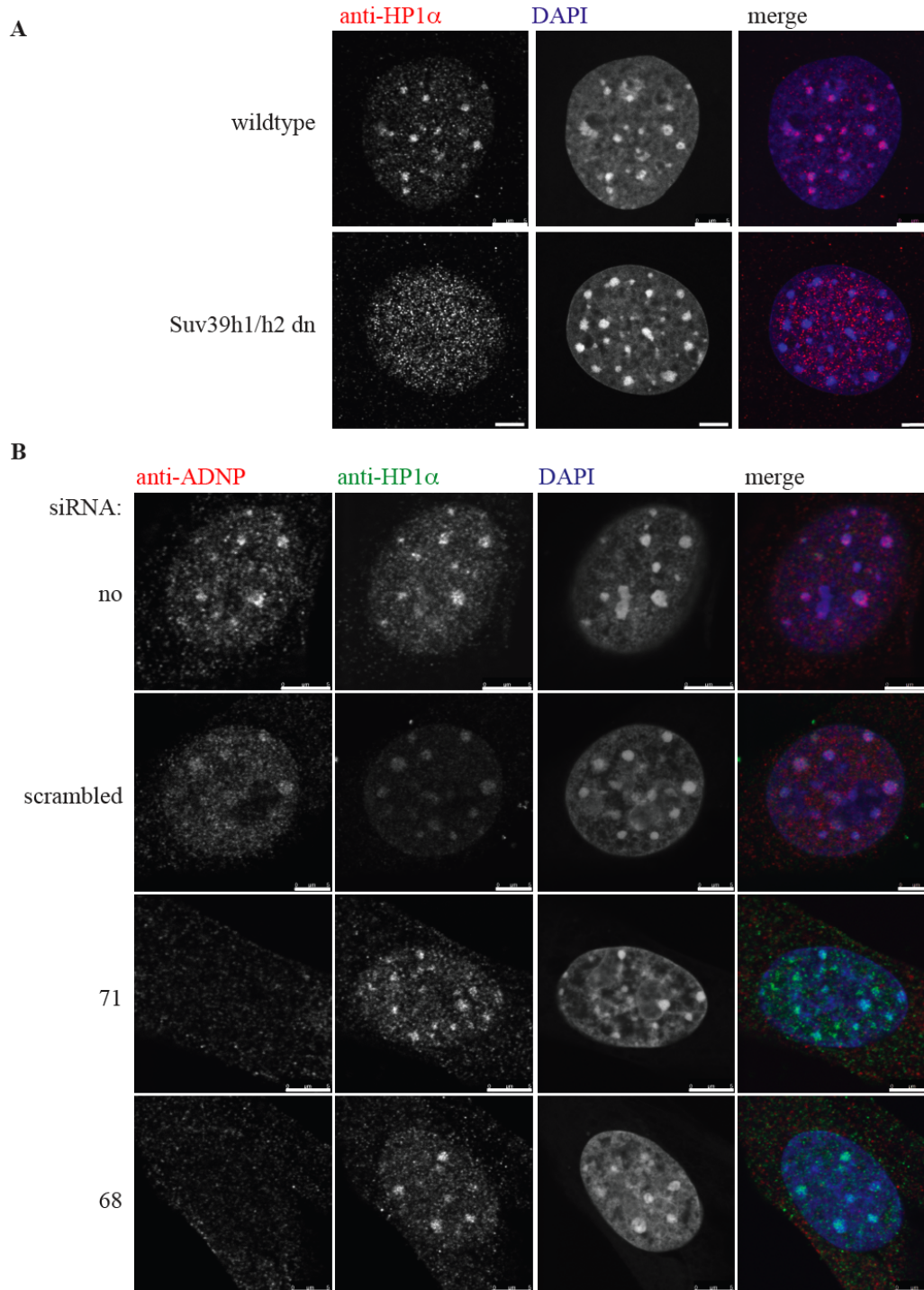


Figure 3-20: ADNP knockdown does not influence HP1 α localization.

Immunofluorescence. **A**, As an experimental control Suv39h1/h2 wildtype and double knockout (dn) MEF cells were stained with an anti-HP1 α antibody. **B**, NIH3T3 cells, transfected with siRNA against ADNP (68 and 71) scrambled siRNA or untransfected (no) were stained with the indicated antibodies. DNA was visualized with DAPI. Bars represent 5 μ m.

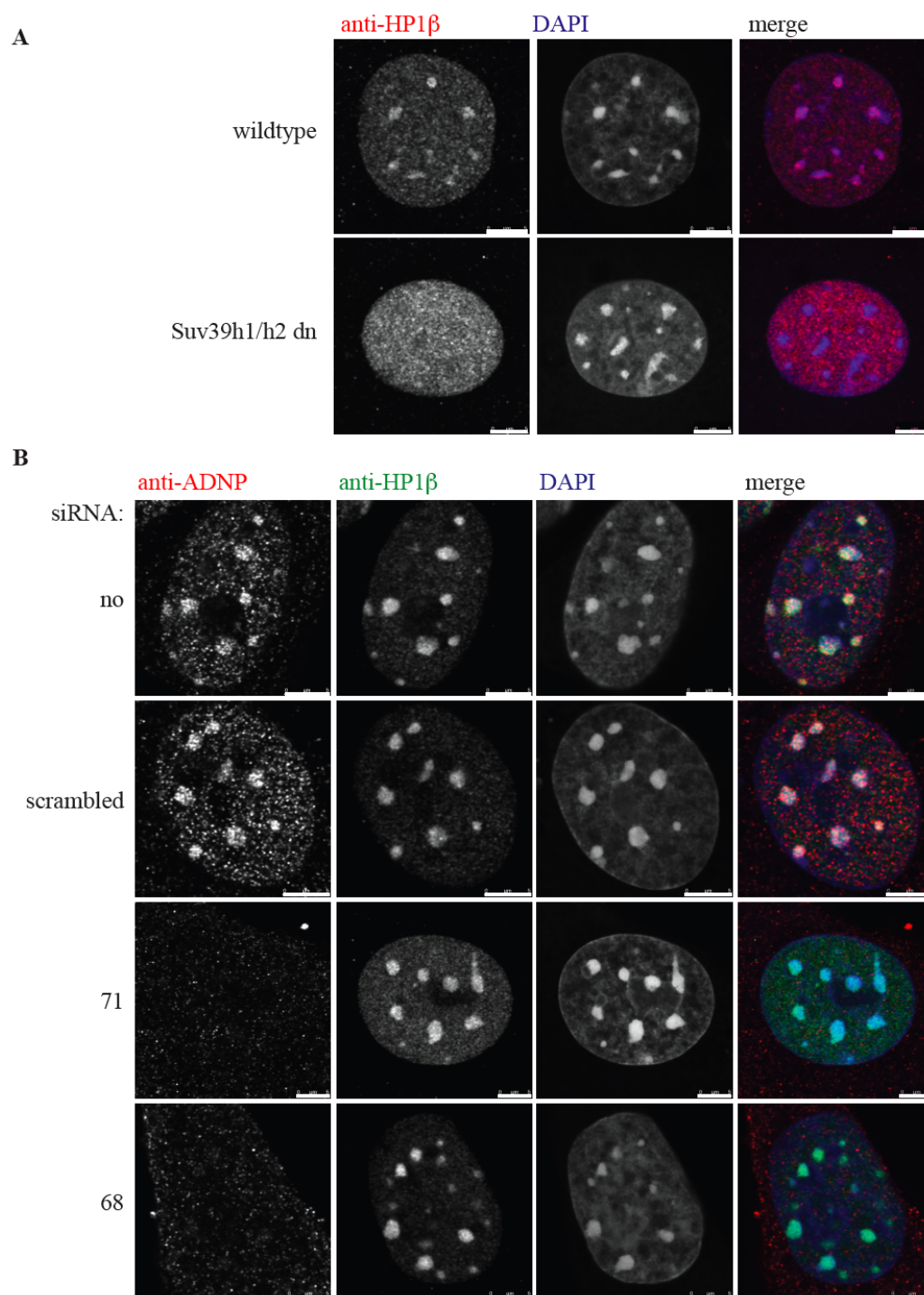


Figure 3-21: ADNP knockdown does not influence HP1 β localization.

Immunofluorescence. **A**, As an experimental control Suv39h1/h2 wildtype and double knockout (dn) MEF cells were stained with an anti-HP1 β antibody. **B**, NIH3T3 cells, transfected with siRNA against ADNP (68 and 71) scrambled siRNA or untransfected (no) were stained with the indicated antibodies. DNA was visualized with DAPI. Bars represent 5 μ m.

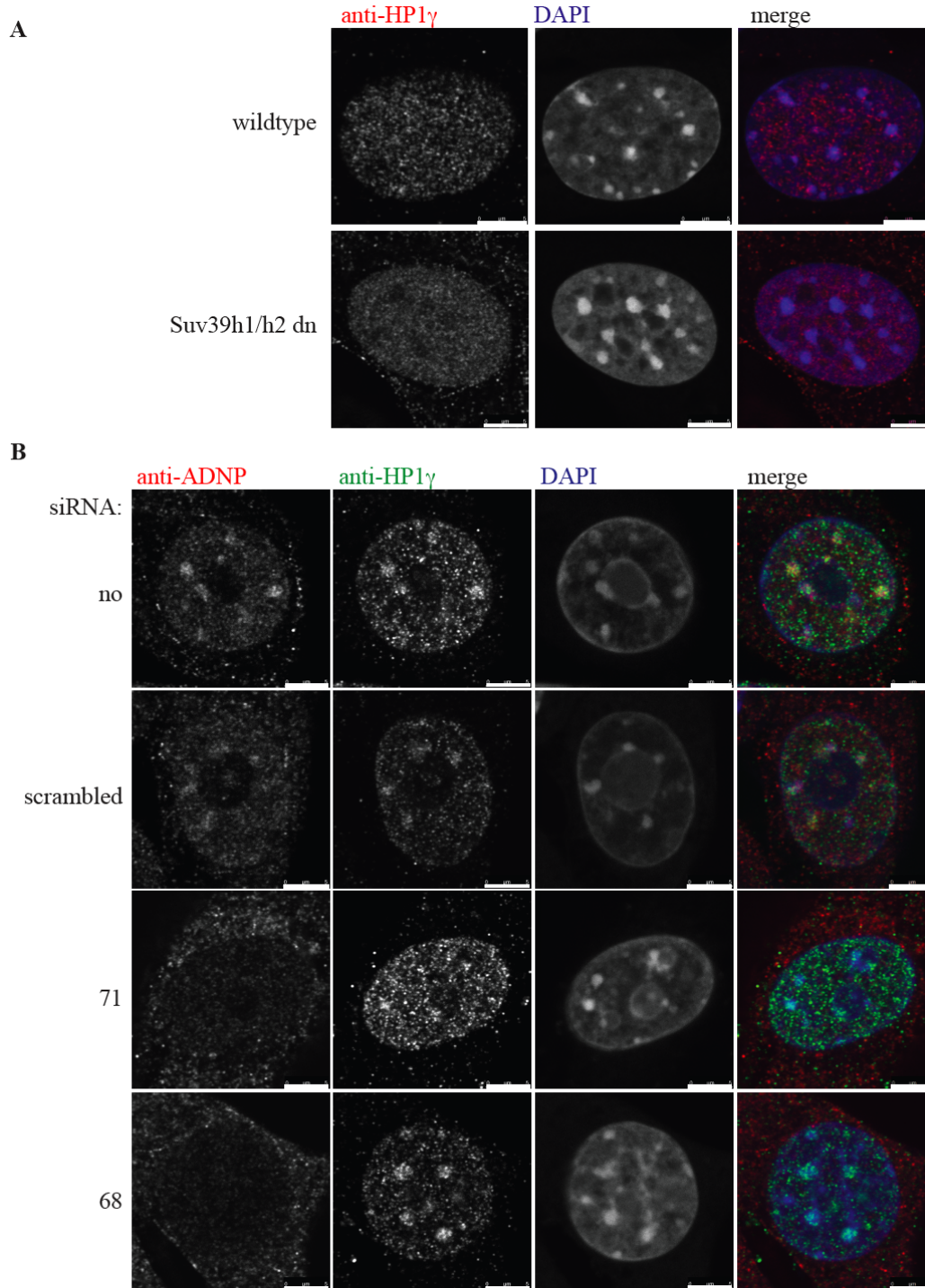


Figure 3-22: ADNP knockdown does not influence HP1 γ localization.

Immunofluorescence. **A**, As an experimental control Suv39h1/h2 wildtype and double knockout (dn) MEF cells were stained with an anti-HP1 γ antibody. **B**, NIH3T3 cells, transfected with siRNA against ADNP (68 and 71) scrambled siRNA or untransfected (no) were stained with the indicated antibodies. DNA was visualized with DAPI. Bars represent 5 μ m.

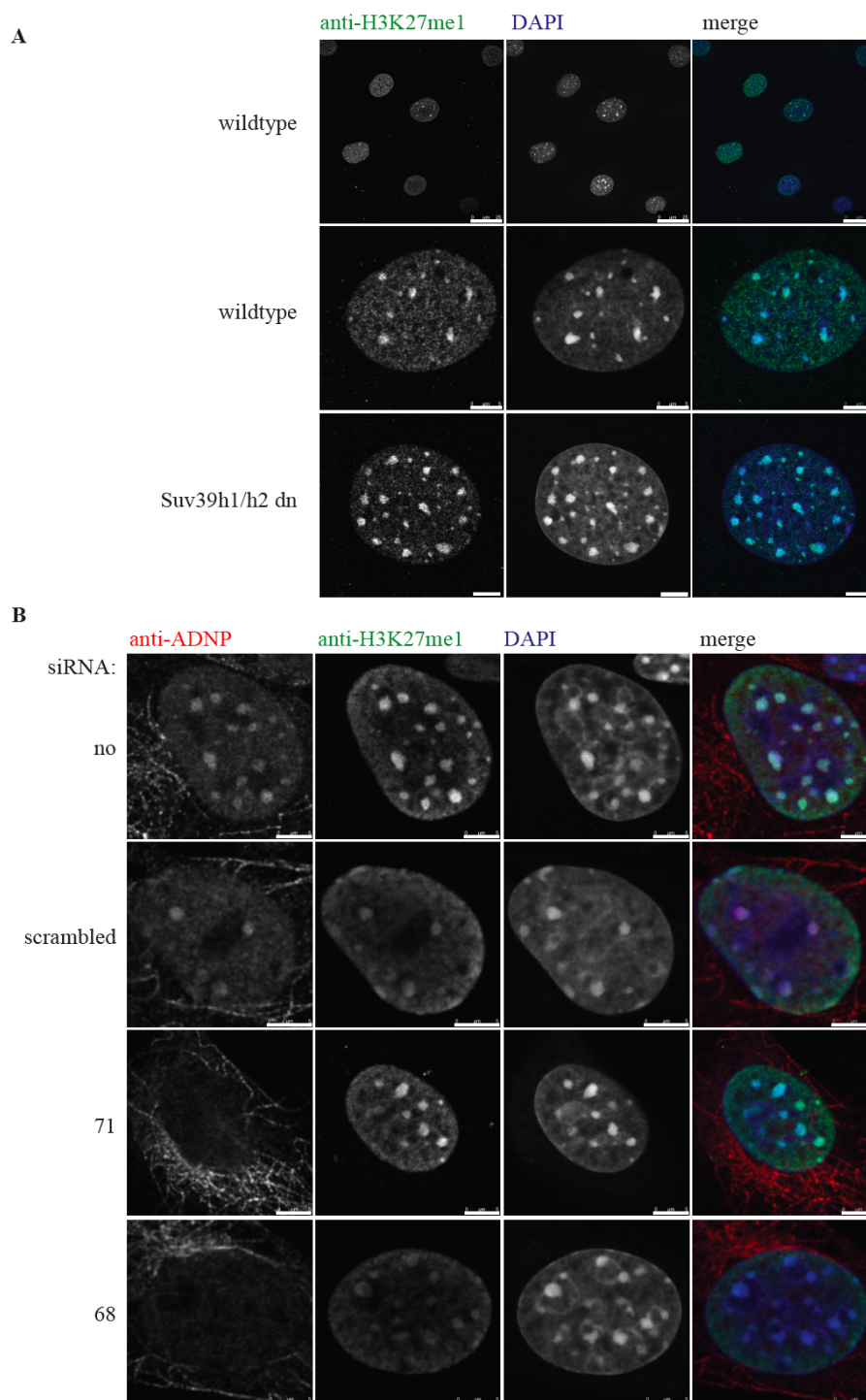


Figure 3-23: ADNP knockdown does not influence H3K27me1 distribution.

Immunofluorescence. **A**, As an experimental control Suv39h1/h2 wildtype and double knockout (dn) MEF cells were stained with an anti-H3K27me1 antibody. **B**, NIH3T3 cells, transfected with siRNA against ADNP (68 and 71) scrambled siRNA or untransfected (no) were stained with the indicated antibodies. DNA was visualized with DAPI. Bars represent 5 μ m and 25 μ m in A, upper panel.

3.4.4 ADNP is not involved in GpG methylation

To determine whether ADNP is involved in the Suv39h1/h2 dependent DNA methylation at major satellite repeats, genomic DNA was extracted from ADNP knockdown and control NIH3T3 cells (Figure 3-18) as well as Suv39h1/h2 knockout and wild type MEF cells. DNA was digested with the methylation sensitive restriction enzyme Tail (5'-ACGT-3') and separated on a 1% agarose gel. By ethidium bromide staining, digested DNA could already be detected in the absence of Suv39h1/h2 indicating a global loss of CpG methylation in these cells (Figure 3-24 A). A subsequent southern blot followed by hybridization with a major satellite probe confirmed the enhanced digestion of major satellite DNA in Suv39h1/h2 knockout cells. In contrast, no enhanced digestion of global DNA or major satellite repeats was found after knockdown of ADNP (Figure 3-24).

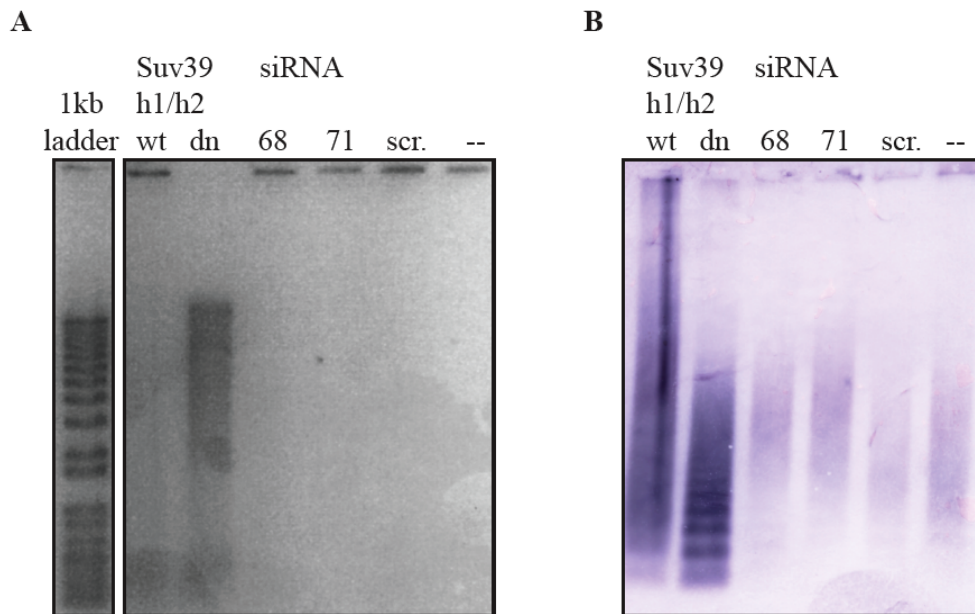


Figure 3-24: ADNP knockdown has no influence on CpG-methylation.

A and **B**, Genomic DNA was prepared from aliquots of the cells shown in Figure 3-19 A, digested with Tail and separated on an 1% agarose gel. As experimental control Suv39h1/h2 wildtype (wt) and double knockout (dn) MEF cells were used. **A**, Ethidiumbromide staining and **B**, Southern blot of the agarose gel shown in A using a major satellite repeat probe are shown.

3.4.5 ADNP functions in silencing of major satellite repeats

ADNP has been demonstrated to be involved in transcriptional activation as well as repression during embryogenesis (Mandel et al., 2007). To analyze whether ADNP plays a role in the Suv39h1 mediated silencing of major satellite repeats (Lehnertz et al., 2003) I addressed the activating or repressive potential of ADNP. I applied a luciferase reporter assay where the firefly luciferase is under the control of a weak promoter (TK-promoter). This setup allows the detection of enhanced as well as reduced transcription depending on the activity of the protein that is targeted to the UAS in front of the promoter (Figure 3-25 A). I used this construct either after transient transfection into HEK 293 cells or stably integrated and thereby chromatinized in HEK 293 cells (HEK TK22) (Ishizuka and Lazar, 2003). Gal4 tagged ADNP was transfected into these cells together with a plasmid containing the renilla luciferase gene controlled by the CMV promoter to measure the transfection efficiency. The transcriptional repressor (SMRT) fused to Gal4 served as an experimental control. Luciferase expression levels were measured by substrate turnover, which results in luminosity. Firefly luciferase luminosity was first normalized to the renilla luciferase signal and second to the untransfected control cells.

Transfection of Gal4-SMRT strongly reduced the firefly luciferase signal in a dose-dependent manner. Although the reduction in luminosity after transfection of increasing amounts of Gal4-ADNP was not as strong as that of Gal4-SMRT a silencing activity of ADNP was clearly observed in both cell lines after transient transfection of the reporter gene cassette or in a stably integrated, chromatinized context.

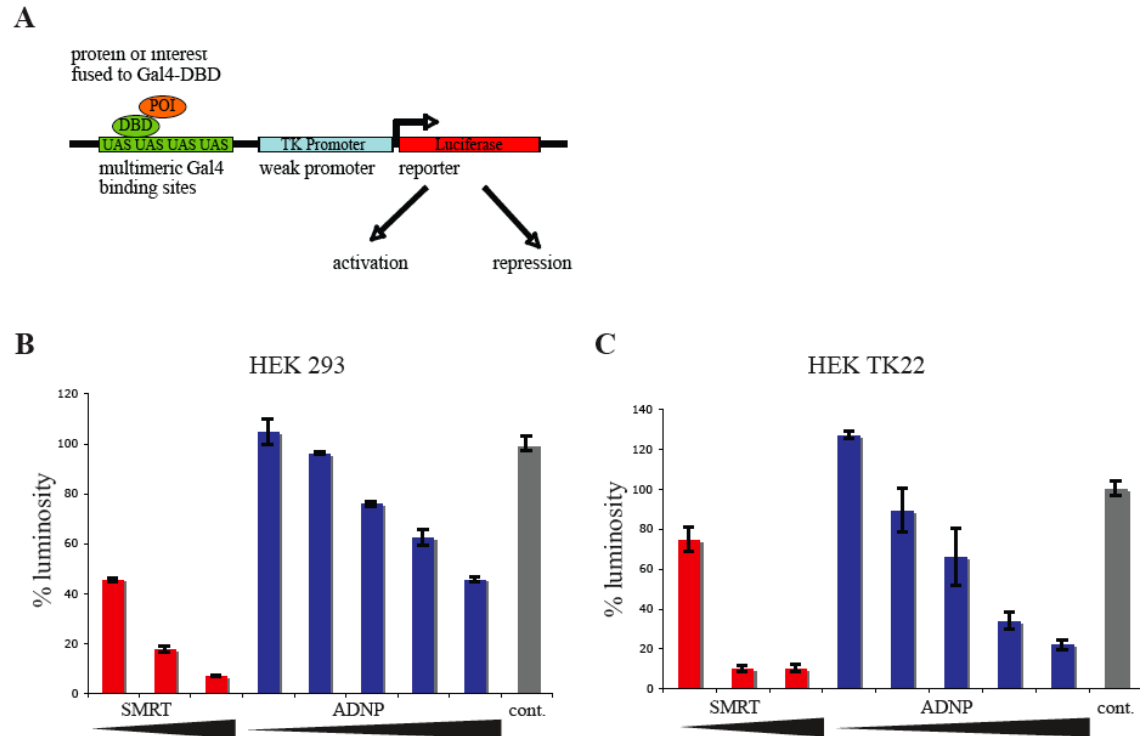


Figure 3-25: ADNP has silencing activity.

A, Schematic representation of the construct used for the luciferase reporter assay. The protein of interest (POI) is fused to the Gal4-DNA binding domain (DBD) and thus recruited to the Gal4-binding site (UAS) upstream of the TK-promoter. The TK-promoter allows a basal transcription of the Firefly-luciferase, which is used as a reporter. Depending on the properties of the POI, luciferase expression can be up or down regulated. **B**, The reporter construct was transiently transfected or **C**, stably integrated in HEK 293 cells. Increasing concentrations of SMRT (positive control) or ADNP were transfected. pCDNA3.1 was used as control. Luciferase activity was measured 1dpt (HEK 293) or 2dpt (HEK TK22).

To test whether ADNP has a silencing function at pericentromeric heterochromatin I determined the transcriptional status of major satellite repeats. I performed RT-PCR analyses on total RNA that had been reverse transcribed with random oligo-dT primers. Using specific primers the abundance of major satellite transcripts relative to GAPDH mRNA was determined by real-time PCR. The relative major satellite expression is displayed in Figure 3-26 as the $2^{-\Delta ct}$ value. The Suv39h1/h2 knockout as well as the HP1 α/β knockout cells showed a clear increase in major satellite transcription compared to the respective wild type MEFs. In the ADNP knockdown cells the level of these transcripts was only elevated after treatment with siRNA 71 but not with siRNA 68. To

analyze whether this is a consequence of the stronger reduction of ADNP with siRNA 71 or is due to an off-target effect of this particular siRNA I repeated the experiment with two YFP-ADNP or YFP overexpressing cell-lines. ADNP expression levels of these cells were analyzed by Western Blot. Compared to the YFP expressing controls YFP-ADNP overexpression reduced major satellite expression significantly. (Figure 3-26)

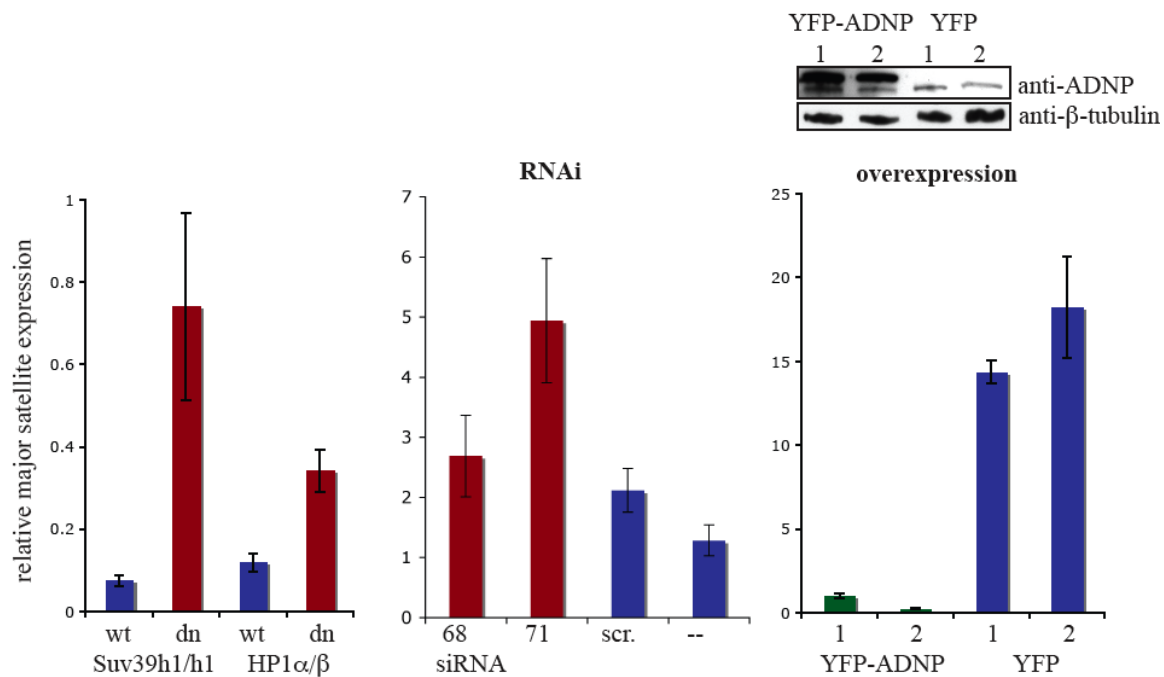


Figure 3-26: ADNP influence on major satellite repeat expression

A, Western Blot. ADNP expression levels of two YFP-ADNP and YFP (control) overexpressing cell lines were analyzed by Western Blot. The upper band represents YFP-ADNP, the lower band the endogenous protein. Tubulin served as loading control. B, quantitative RT-PCR. Total RNA was extracted from Suv39h1/h2 and HP1α/β double knockout MEF (red), ADNP knockdown (red) and YFP-ADNP overexpressing (green) NIH3T3 cells. The respective wild type and YFP cells served as control (blue). Reverse transcription was followed by real-time PCR. Relative major satellite expression, normalized to GAPDH is shown. Error bars represent the standard deviation of a triplicate experiment.

Summing up, analysis of ADNP knockdown in NIH3T3 cells did not indicate an ADNP function in Brg1 mediated organization of pericentromeric heterochromatin, Also, effects on histone modifications, HP1 distribution and DNA methylation as observed in the

Suv39h1/h2 knockout were not detected. Although up-regulation of major satellite transcription was only detected with one of the two siRNAs, additional results from luciferase assays and ADNP overexpression suggest that ADNP is involved in transcriptional silencing at pericentromeric heterochromatin.

4 Discussion

4.1 Identification of H3K9me3 associated proteins

A scientific challenge in chromatin research is trying to understand how factors and enzymes that set or recognize histone modifications and other factors/components interplay to establish and maintain distinct functional domains of chromatin in higher eukaryotes. Genetic approaches have identified sets of proteins, e.g. suppressors and enhancers of variegation (Su(var) and E(var)) that led to first insights into chromatin organization pathways. Recent advances in mass spectrometry introduced proteomic techniques to compile a list of factors that is necessary (and sufficient) to mediate distinct states of chromatin. One such method to discover chromatin associated factors is a pulldown assay using histone tail peptides modified at distinct residues (Wysocka et al., 2005). However proteins that require chromatin as a substrate for interaction may not bind peptides immobilized on beads. Using oligonucleosomes instead of peptides facilitates binding of factors that depend on additional contacts with histones, DNA or chromatin structure. A single amino acid modification such as trimethylation of histone H3 lysine 9 used in this study may cause a change in affinity for that site rather than a completely bound or unbound state of some proteins. To detect such quantitative differences stable isotope labeling by amino acids in cell culture (SILAC) was used. These differences are displayed as the ratio between the isotope labeled (heavy) and unlabeled (light) form of the proteins in the samples, in this case pulldowns of H3K9me3 or unmodified oligonucleosomes respectively. To exclude differences resulting from the heavy and light nuclear extracts a reversed biological replicate was conducted (light extract for H3K9me3 and heavy extract for unmodified oligonucleosomes). Most proteins have a ratio between 0.5 and 2, indicating no enrichment in both samples. Such proteins bind either to chromatin independent of the histone methylation state or unspecifically to the beads. The overlap of proteins enriched at least 2-fold at H3K9me3 in replicate experiments consisted of only 20 proteins. Among these proteins were known

heterochromatin factors such as all isoforms of HP1, UHRF1/2 as well as POGZ, which was recently described to interact with HP1 (Brasher et al., 2000; Karagianni et al., 2008; Nozawa et al., 2010). One of the factors, DNA methyltransferase 1 (DNMT1) was indeed only identified in the oligonucleosome but not in the peptide context (Franz et al., 2009). This indicates specificity of the method. However, the total number of proteins was not higher than that of the peptide pulldown method. Possibly, binding of larger complexes or additional factors requires not only one modification for interaction but rather a combination of different heterochromatin marks such as histone modifications and DNA methylation. Another reason for the low number of factors found in the chromatin pulldown experiment might be, that the dodecameric oligonucleosomes are too short to form higher order structures resembling those within a cell nucleus. Therefore, the structures or the local density of the H3K9me3 mark required for binding of larger complexes could not be achieved with this experimental setup.

4.2 ADNP is a novel component of pericentromeric heterochromatin

ADNP was originally discovered as a gene product associated with neuroprotection/neuroglia interactions (Bassan et al., 1999). In the nucleus, it has been shown to be involved in transcriptional regulation of genes that are associated with e.g. lipid metabolism and organogenesis (Mandel et al., 2007). ADNP has also been identified as an interaction partner of the SWI/SNF chromatin-remodeling complex. Association of ADNP with specific histone modifications and pericentromeric heterochromatin had not been described before. Therefore, I decided to focus my thesis work on characterizing the properties and functions of this protein in relation to heterochromatin.

The identification of ADNP as an H3K9me3 associated factor by mass spectrometry was verified by Western-blot (Figure 3-3). In vivo, H3K9me3 is enriched at pericentromeric heterochromatin that can be visualized in mouse cells as DAPI-dense regions. Antibody staining of ADNP revealed that ADNP co-localizes with H3K9me3 at heterochromatin in

mouse fibroblasts (Figure 3-4). A speckled staining in the nucleus and a tubulin-like staining in the cytoplasm were also observed. Ectopic expression of YFP-ADNP results in a diffuse signal within the nucleus and enrichment at DAPI-dense regions (Figure 3-8). These results suggest that ADNP is localized to pericentromeric heterochromatin but is not restricted to these areas. Like other heterochromatin associated factors such as HP1 and CDYL, ADNP is displaced from chromatin during mitosis. The majority of nucleosomes containing histone H3 methylated on lysine 9 are then phosphorylated on serine 10, a double-modification that evicts HP1 from mitotic chromatin. However, a small number of H3 nucleosomes at centromeric/pericentromeric regions still bind HP1 α and these might serve as the foundation or could regulate the association of the KMN network (the structural core of the kinetochore, named after its constituents: the protein KNL-1/Spc105/Blinkin, and the Mis12 and the Ndc80 subcomplexes) with the centromere (Przewloca and Glower, 2009). The behavior of ADNP in that context could not be determined because of the cross-reactivity of the antibody with tubulin-like structures (Figure 3-5). The cytoplasmic staining is in contrast to reports that ADNP is excluded from the cytoplasm in fibroblasts (Divinski et al., 2006). Subcellular fractionation and expression of YFP-ADNP did not show cytosolic signals (Figure 3-4, Figure 3-8). Therefore, I consider the cytoplasmic staining as an artifact of unspecific binding of the anti-ADNP antibody.

Next, I investigated whether ADNP requires modified chromatin context instead of H3K9me3 peptides for interaction. The oligonucleosomes used for the pull-down are identical except for the methylation of histone H3 lysine 9, suggesting that the specificity is conferred by this modification. Protein structure predictions however show that ADNP consists of zinc-fingers and a homeobox, which are domains involved in DNA binding. ADNP chromatin immunoprecipitation showed interaction with multiple gene promoters, which confirm DNA binding capability of ADNP (Mandel et al., 2007). There are two possible hypothesis how DNA binding could be involved in ADNP association with heterochromatin: unspecific DNA binding might be necessary to stabilize ADNP at chromatin after recruitment by H3K9me3 or specific DNA and H3K9me3 binding may act synergistically to recruit ADNP to pericentromeric heterochromatin. For the

chromatin pull-down an artificial nucleosome positioning sequence was used (Lowary and Widom, 1998; Thastrom et al., 1999). In this experimental setting only unspecific DNA binding might play a role. To test this a peptide pulldown was performed. Here only unmodified and methylated histone tail peptides were used. ADNP association with the H3K9me3 peptide bound beads excludes that DNA binding is needed for recruitment to this modification in vitro. However, a weak affinity of ADNP for DNA might stabilize the binding to chromatin after recruitment. The specific binding of DNA at pericentromeric heterochromatin cannot be excluded. However, in the Suv39h1/h2 double knockout cells where H3K9me3 is not enriched at pericentromeric heterochromatin, ADNP is displaced from these areas as well (Figure 3-6). If specific DNA binding occurs at pericentromeric heterochromatin, it is not sufficient for ADNP recruitment.

4.3 ADNP is targeted to pericentromeric heterochromatin by HP1

I observed that ADNP localizes to pericentromeric heterochromatin. How is ADNP then targeted to these regions? Structural prediction algorithms did not detect known methyl-lysine binding domains such as a chromo domain, a plant homeo domain, a tudor domain or a malignant brain tumor domain. The only domains predicted in ADNP are a homeodomain and zinc fingers. For the majority of the 1108 amino acids protein the structure is completely unknown. Still, the possibility that ADNP binds directly to H3K9me3 by a domain that lacks sufficient homology for structural prediction can not be excluded by computational analysis. However, *in vitro* results from peptide pulldowns using ADNP expressed in reticulocyte lysate showed no binding of ADNP to H3K9me3 peptides (Figure 3-9). Immunofluorescence analysis in HP1 α/β knockout cells where the level and distribution of H3K9me3 remained unaffected revealed delocalization of ADNP from chromocenters in these cells (Figure 3-10). These results suggest that ADNP is not recruited to pericentromeric heterochromatin by direct binding to H3K9me3.

A likely candidate for indirect ADNP recruitment is HP1. During these studies the interaction of ADNP with HP1 α was suggested (Mandel et al., 2007). The ADNP homeodomain contains a PxVxL and an ARKS motif. PxVxL motifs in general are binding motifs of the HP1 chromoshadow domain (Thiru et al., 2004). ARKS is a motif in the histone H3 tail that encompasses of lysines 9 and 27. When lysine 9 of histone H3 is trimethylated it is recognized by the HP1 chromo domain. Trimethylated lysine 27 is also bound by HP1 but with a lower affinity. ADNP has also been shown to interact with the SWI/SNF complex via interaction of Brg1 most likely with the C-terminus of ADNP (Mandel and Gozes, 2007). Although Brg1 does not localize to DAPI dense regions, its knockout causes misorganization of pericentromeric heterochromatin (Bourgo et al., 2009). In ADNP deletion mutants the homeodomain was necessary and sufficient for targeting to heterochromatin (Figure 3-8). This result and the delocalization of ADNP in the HP1 α/β knockout cells indicate that HP1 is the main mediator of ADNP heterochromatin recruitment. Interestingly, knockout of single HP1 isoforms did not affect ADNP localization, suggesting that ADNP interaction with HP1 is not limited to a particular isoform (Figure 3-10). Peptide pulldown experiments confirmed that all isoforms of HP1 are indeed able to target ADNP to H3K9me3 peptides (Figure 3-9).

4.4 Mapping of the HP1 – ADNP interaction interface

To further map the HP1 – ADNP interaction point mutants were introduced into the ARKS and the PxVxL motifs. A lysine to arginine mutation in the ARKS motif prevents its putative trimethylation. This mutation in a histone H3 peptide context has been described to prevent HP1 binding. Therefore I introduced this mutation into the ADNP ARKS sequence (K767R). For the PxVxL motif a valine to glutamate mutation has been shown to abolish the interaction with HP1. Thus, valine 821 in the ADNP homeodomain was mutated to glutamate (V821A). Live cell imaging as well as peptide pulldowns showed no effect of the K767R mutation on ADNP targeting. In contrast, the V821A mutation resulted in ADNP highly reduced signals at DAPI dense regions and H3K9me3 peptides in these experiments. Interestingly, only in the K767R/V821E double mutant

recruitment to pericentromeric heterochromatin and H3K9me3 peptides was completely abolished (Figure 3-12). In agreement with these results, W170A mutation in the HP1 chromoshadow domain, which has no influence on H3K9me3 binding and HP1 dimerization but eliminates PxVxL binding, strongly reduced ADNP recruitment to H3K9me3 (Figure 3-14). Obviously, HP1 binding and subsequent targeting of ADNP mainly depends on the PxVxL motif. Nevertheless, an additional effect of the K767R mutation was detected. This effect could be explained by (i) an influence on ADNP dimerization/multimerization preventing recruitment of the non HP1 bound ADNP mutant by endogenous ADNP, (ii) stabilization of the HP1 binding to the PxVxL motif by synergistically binding to a hypothetical ADNP K767me3 or (iii) disruption of the homeodomain structure. Hypothesis (i) was excluded by endogenous ADNP co-precipitating with wild type and all point mutants of YFP-ADNP (Figure 3-13). To address possibility (ii) I tested whether ADNP can be methylated and whether K767me3 would be bound by HP1. The result shown in Figure 3-15 C suggests that ADNP might indeed be methylated. However, *in vitro* HP1 did not bind to ADNPK767me3 peptides (Figure 3-15 D). A potential reason for that behavior lies in the residues surrounding the ARKS motif. The structure of a histone tail bound HP1 chromo domain has been published. If the threonine preceding the ARKS in the H3 sequence is replaced by a glutamate as in the ADNP sequence, a steric inhibition of peptide binding seems likely (Figure 4-1).

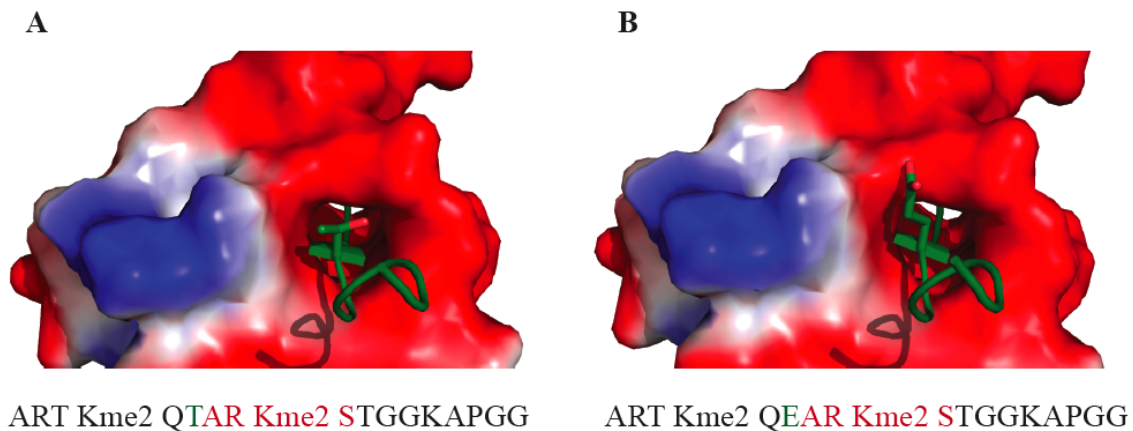


Figure 4-1: Structure of mouse HP1 β chromo domain.

A. Crystal structure of mouse HP1 β chromo domain in complex with the lysine 9 methyl H3 N-terminal peptide (1GUW) as a cartoon. The surface charge is represented ranging from red (acidic) to blue (basic). The histone tail peptide is shown as sticks. **B.** Threonine 6 was replaced by a glutamate as in the ADNP sequence in silico (Nielsen et al., 2002).

The remaining hypothesis is that K767R causes disruption of the ADNP homeodomain structure. Since HP1 has been shown to bind several different proteins having different domains / structures via their PxVxL motif, this type of interaction seems not to require a certain structure. Any remaining PxVxL independent interaction that might be mediated by the homeodomain could be abolished by the K767R mutation.

4.5 Nuclear function of ADNP

Complete deficiency of ADNP in mouse embryos results in dramatic changes in gene expression (Mandel et al., 2007). Up-regulated transcripts were clustered into a family encoding proteins enriched in the visceral endoderm such as apolipoproteins, cathepsins and metallothioneins. In contrast, a down-regulated gene cluster consisted of organogenesis markers including neurogenesis and heart development (Mandel et al., 2007). ADNP functions at pericentromeric heterochromatin have not yet been described.

Interaction between ADNP and three members of the SWI/SNF chromatin-remodeling complex (BAF250a, BAF170 and Brg1) has been shown by co-immunoprecipitation (Mandel and Gozes, 2007). Although Brg1 does not localize to DAPI dense regions its deficiency results in dissolution of pericentromeric heterochromatin and delocalization of the heterochromatin markers H3K9me3 and H4K20me3 (Bourgo et al., 2009). ADNP could be involved in that process by recruiting Brg1 or by modulating the activity of the SWI/SNF complex. By immunofluorescence analysis however, no effect of ADNP knockdown on the integrity of chromocenters and the distribution of trimethylated H3K9 and H4K20 were detected (Figure 3-16; Figure 3-17).

Since ADNP loss of function phenotypes should also be observed in Suv39h1/h2 knockout cells, where HP1 and ADNP are delocalized from pericentromeric heterochromatin (Figure 3-6; Figure 3-20; Figure 3-21; Figure 3-22), I tested ADNP knockdown cells for several described Suv39h1/h2 knockout phenotypes.

Suv39h1/h2 are methyltransferases specific for lysine 9 of histone H3 at pericentromeric heterochromatin. Therefore, its depletion results in a reduction of H3K9me3 and the loss of this modification from pericentric heterochromatin. Reduction of H3K9me3 levels leads to a decrease of combination H3K9me3 with serine 10 phosphorylation and an increase of lysine 9 acetylation. These are primary effects of the Suv39h1/h2 knockout. However, ADNP might be involved in Suv39h1/h2 targeting to or stabilization at heterochromatin or it may influence Suv39h1/h2 enzymatic activity. Another heterochromatin marker, H4K20me3 is also mislocalized after loss of Suv39h1/h2. H4K20me3 has been proposed to be mediated by H3K9me3-bound HP1 recruiting Suv4-20, the H4K20 methyltransferase (Schotta et al., 2004). Since ADNP interacts with HP1, an influence on that process seems plausible. A reported loss of H3K27 monomethylation in Suv39h1/h2 knockout cells (Peters et al., 2003) could neither be reproduced with a commercial antibody nor with the antibody used in the original report. Immunofluorescence and Western Blot analysis however did not show any differences in the described histone modifications (Figure 3-16; Figure 3-17; Figure 3-19; Figure 3-23).

Both histone modifications and HP1 are displaced from pericentromeric heterochromatin in Suv39h1/h2 knockout cells (Harnicarova Horakova et al., 2009). This result is most likely an effect of the loss of H3K9me3. Nevertheless ADNP might mediate the specificity of HP1 α and/or HP1 β for these areas. *In vitro*, no specificity of ADNP for a certain HP1 isoform was detected (Figure 3-9). Consistently ADNP knockdown did not result in relocalization of HP1.

DNA methylation at major satellite repeats has been reported to occur either by the DNA methyltransferase DNMT1 in a Suv39h1/h2 independent manner (Chuang et al., 1997; Rountree et al., 2000) or by DNMT3a/b dependent on Suv39h1/h2 (Lehnertz et al., 2003). DNMT3a and DNMT3b were shown to interact with HP1 α and HP1 β (Lehnertz et al., 2003), raising the possibility that ADNP might play a role in that process. Digestion with a methylation sensitive restriction enzyme, however, did not reveal any influence of ADNP knockdown on global DNA methylation or DNA methylation of major satellite repeats.

Finally, Suv39h1/h2 have been reported to be involved in transcriptional silencing of major satellite repeats (Lehnertz et al., 2003). Depletion of Suv39h1/h2 results in loss of markers for transcriptional repression such as histone modifications, DNA methylation and HP1 localization (as described in the previous section) yet the exact mechanism to reach a silent state remains unknown. In Suv39h1/h2 as well as in HP1 α/β knockout cells transcription of major satellite repeats was increased. Enhanced major satellite repeat transcription was also observed after transfection with one of the two siRNAs (siRNA 71) against ADNP (Figure 3-26). siRNA 71 induced a stronger reduction of ADNP than siRNA 68 (~85% vs. ~60% of scrambled siRNA control) (Figure 3-18). The knockdown efficiency of siRNA 68 might not be sufficient to cause an effect on transcription. On the other hand, the enhanced transcription after transfection of siRNA 71 could be due to an off-target effect of that particular siRNA. Additional results from luciferase assays and YFP-ADNP overexpression however indicate, that ADNP is indeed involved in silencing of major satellite repeats (Figure 3-25, Figure 3-26).

These results lead to the proposal of the following model for ADNP recruitment to and function at pericentromeric heterochromatin: Histone H3 is trimethylated at lysine 9 by Suv39h1/h2. The H3K9me3 modification is bound by the HP1 chromo domain. HP1 recruits ADNP via interaction of its chromoshadow domain with the PxVxL motif in the ADNP homeodomain. Finally, ADNP induces transcriptional silencing of major satellite repeats. Further experiments are required to elucidate the exact mechanism of how silencing is mediated.

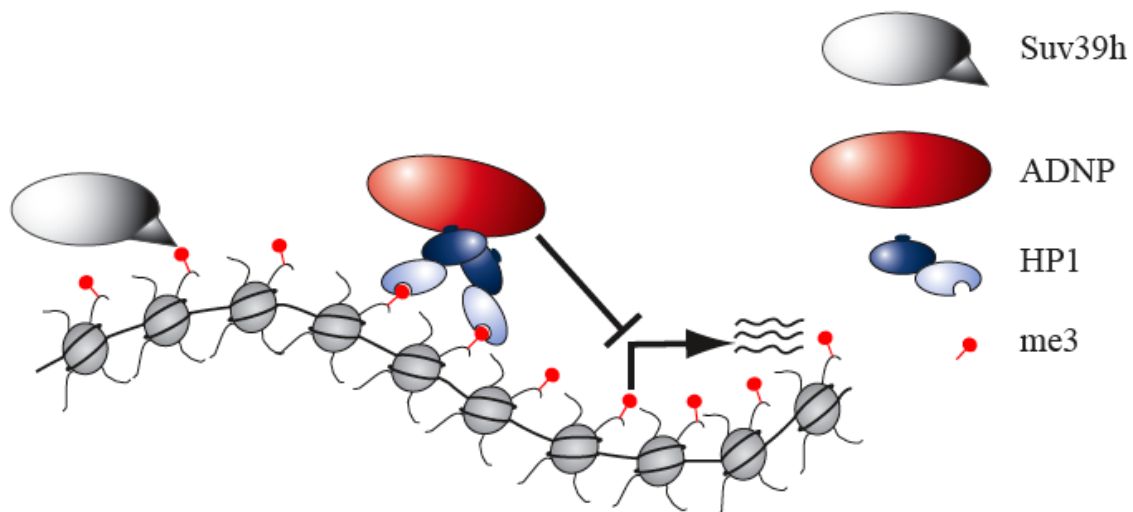


Figure 4-2: Model for ADNP recruitment and function

Suv39h (grey) trimethylates histone H3 at lysine 9 (H3K9me3; small red circle). HP1 via its chromo domain (light blue) to chromatin. HP1 recruits ADNP (red) via binding of the dimeric HP1 chromoshadow domain (dark blue) to a PxVxL motif. Upon recruitment to chromatin, ADNP silences major satellite transcription by an unknown mechanism.

5 References

- Aagaard, L., Laible, G., Selenko, P., Schmid, M., Dorn, R., Schotta, G., Kuhfittig, S., Wolf, A., Lebersorger, A., Singh, P.B., *et al.* (1999). Functional mammalian homologues of the *Drosophila* PEV-modifier Su(var)3-9 encode centromere-associated proteins which complex with the heterochromatin component M31. *Embo J* 18, 1923-1938.
- Adams-Cioaba, M.A., and Min, J. (2009). Structure and function of histone methylation binding proteins. *Biochem Cell Biol* 87, 93-105.
- Agalioti, T., Chen, G., and Thanos, D. (2002). Deciphering the transcriptional histone acetylation code for a human gene. *Cell* 111, 381-392.
- Agalioti, T., Lomvardas, S., Parekh, B., Yie, J., Maniatis, T., and Thanos, D. (2000). Ordered recruitment of chromatin modifying and general transcription factors to the IFN-beta promoter. *Cell* 103, 667-678.
- Agger, K., Christensen, J., Cloos, P.A., and Helin, K. (2008). The emerging functions of histone demethylases. *Curr Opin Genet Dev* 18, 159-168.
- Ahmad, K., and Henikoff, S. (2002). Epigenetic consequences of nucleosome dynamics. *Cell* 111, 281-284.
- Allis, C.D., Bowen, J.K., Abraham, G.N., Glover, C.V., and Gorovsky, M.A. (1980). Proteolytic processing of histone H3 in chromatin: a physiologically regulated event in *Tetrahymena* micronuclei. *Cell* 20, 55-64.
- Allis, C.D., Jenuwein, T., and Reinberg, D. (2007). *Epigenetics*. Cold Spring Harbor: Cold Spring Harbor Laboratory Press.
- Angelov, D., Vitolo, J.M., Mutskov, V., Dimitrov, S., and Hayes, J.J. (2001). Preferential interaction of the core histone tail domains with linker DNA. *Proc Natl Acad Sci U S A* 98, 6599-6604.
- Arents, G., Burlingame, R.W., Wang, B.C., Love, W.E., and Moudrianakis, E.N. (1991). The nucleosomal core histone octamer at 3.1 Å resolution: a tripartite protein assembly and a left-handed superhelix. *Proc Natl Acad Sci U S A* 88, 10148-10152.
- Ausubel, F.M., Brent, R., Kingston, R.E., Moore, D.D., Seidman, J.G., Smith, J.A., and Struhl, K. (1998). *Current Protocols in Molecular Biology* (John Wiley & Sons, Inc.).
- Avery, O.T., Macleod, C.M., and McCarty, M. (1944). Studies on the Chemical Nature of the Substance Inducing Transformation of Pneumococcal Types : Induction of Transformation by a Desoxyribonucleic Acid Fraction Isolated from *Pneumococcus* Type Iii. *J Exp Med* 79, 137-158.
- Bannister, A.J., Zegerman, P., Partridge, J.F., Miska, E.A., Thomas, J.O., Allshire, R.C., and Kouzarides, T. (2001). Selective recognition of methylated lysine 9 on histone H3 by the HP1 chromo domain. *Nature* 410, 120-124.
- Barski, A., Cuddapah, S., Cui, K., Roh, T.Y., Schones, D.E., Wang, Z., Wei, G., Chepelev, I., and Zhao, K. (2007). High-resolution profiling of histone methylations in the human genome. *Cell* 129, 823-837.

- Bassan, M., Zamostiano, R., Davidson, A., Pinhasov, A., Giladi, E., Perl, O., Bassan, H., Blat, C., Gibney, G., Glazner, G., *et al.* (1999). Complete sequence of a novel protein containing a femtomolar-activity-dependent neuroprotective peptide. *J Neurochem* 72, 1283-1293.
- Beni-Adani, L., Gozes, I., Cohen, Y., Assaf, Y., Steingart, R.A., Brenneman, D.E., Eizenberg, O., Trembolver, V., and Shohami, E. (2001). A peptide derived from activity-dependent neuroprotective protein (ADNP) ameliorates injury response in closed head injury in mice. *J Pharmacol Exp Ther* 296, 57-63.
- Bernstein, B.E., Mikkelsen, T.S., Xie, X., Kamal, M., Huebert, D.J., Cuff, J., Fry, B., Meissner, A., Wernig, M., Plath, K., *et al.* (2006). A bivalent chromatin structure marks key developmental genes in embryonic stem cells. *Cell* 125, 315-326.
- Bertin, A., Renouard, M., Pedersen, J.S., Livolant, F., and Durand, D. (2007). H3 and H4 histone tails play a central role in the interactions of recombinant NCPs. *Biophys J* 92, 2633-2645.
- Bestor, T.H. (2000). The DNA methyltransferases of mammals. *Hum Mol Genet* 9, 2395-2402.
- Bourgo, R.J., Siddiqui, H., Fox, S., Solomon, D., Sansam, C.G., Yaniv, M., Muchardt, C., Metzger, D., Chambon, P., Roberts, C.W., *et al.* (2009). SWI/SNF deficiency results in aberrant chromatin organization, mitotic failure, and diminished proliferative capacity. *Mol Biol Cell* 20, 3192-3199.
- Brasher, S.V., Smith, B.O., Fogh, R.H., Nietlispach, D., Thiru, A., Nielsen, P.R., Broadhurst, R.W., Ball, L.J., Murzina, N.V., and Laue, E.D. (2000). The structure of mouse HP1 suggests a unique mode of single peptide recognition by the shadow chromo domain dimer. *Embo J* 19, 1587-1597.
- Burkhardt, C.A., Kavallaris, M., and Band Horwitz, S. (2001). The role of beta-tubulin isoforms in resistance to antimitotic drugs. *Biochim Biophys Acta* 1471, O1-9.
- Chang, B., Chen, Y., Zhao, Y., and Bruick, R.K. (2007). JMJD6 is a histone arginine demethylase. *Science* 318, 444-447.
- Chen, S., and Charness, M.E. (2008). Ethanol inhibits neuronal differentiation by disrupting activity-dependent neuroprotective protein signaling. *Proc Natl Acad Sci U S A* 105, 19962-19967.
- Chuang, L.S., Ian, H.I., Koh, T.W., Ng, H.H., Xu, G., and Li, B.F. (1997). Human DNA-(cytosine-5) methyltransferase-PCNA complex as a target for p21WAF1. *Science* 277, 1996-2000.
- Clements, A., Poux, A.N., Lo, W.S., Pillus, L., Berger, S.L., and Marmorstein, R. (2003). Structural basis for histone and phosphohistone binding by the GCN5 histone acetyltransferase. *Mol Cell* 12, 461-473.
- Collins, R.E., Northrop, J.P., Horton, J.R., Lee, D.Y., Zhang, X., Stallcup, M.R., and Cheng, X. (2008). The ankyrin repeats of G9a and GLP histone methyltransferases are mono- and dimethyllysine binding modules. *Nat Struct Mol Biol* 15, 245-250.
- Cosma, M.P., Tanaka, T., and Nasmyth, K. (1999). Ordered recruitment of transcription and chromatin remodeling factors to a cell cycle- and developmentally regulated promoter. *Cell* 97, 299-311.
- Cowieson, N.P., Partridge, J.F., Allshire, R.C., and McLaughlin, P.J. (2000). Dimerisation of a chromo shadow domain and distinctions from the chromodomain as revealed by structural analysis. *Curr Biol*, 517-525.

- Daujat, S., Zeissler, U., Waldmann, T., Happel, N., and Schneider, R. (2005). HP1 binds specifically to Lys26-methylated histone H1.4, whereas simultaneous Ser27 phosphorylation blocks HP1 binding. *J Biol Chem*, 38090-38095.
- Davey, C.A., Sargent, D.F., Luger, K., Maeder, A.W., and Richmond, T.J. (2002). Solvent mediated interactions in the structure of the nucleosome core particle at 1.9 a resolution. *J Mol Biol* 319, 1097-1113.
- Delattre, M., Spierer, A., Tonka, C.H., and Spierer, P. (2000). The genomic silencing of position-effect variegation in *Drosophila melanogaster*: interaction between the heterochromatin-associated proteins Su(var)3-7 and HP1. *J Cell Sci*, 4253-4261.
- Dhalluin, C., Carlson, J.E., Zeng, L., He, C., Aggarwal, A.K., and Zhou, M.M. (1999). Structure and ligand of a histone acetyltransferase bromodomain. *Nature* 399, 491-496.
- Divinski, I., Holtser-Cochav, M., Vulih-Schultzman, I., Steingart, R.A., and Gozes, I. (2006). Peptide neuroprotection through specific interaction with brain tubulin. *J Neurochem* 98, 973-984.
- Divinski, I., Mittelman, L., and Gozes, I. (2004). A femtomolar acting octapeptide interacts with tubulin and protects astrocytes against zinc intoxication. *J Biol Chem* 279, 28531-28538.
- Dormann, H. (2009). REGULATION OF HETEROCHROMATIN PROTEIN 1 BY PHOSPHORYLATION OF HISTONE H3 AND THE HP1 HINGE DOMAIN (New York, The Rockefeller University).
- Duncan, E.M., Muratore-Schroeder, T.L., Cook, R.G., Garcia, B.A., Shabanowitz, J., Hunt, D.F., and Allis, C.D. (2008). Cathepsin L proteolytically processes histone H3 during mouse embryonic stem cell differentiation. *Cell* 135, 284-294.
- Eroglu, B., Wang, G., Tu, N., Sun, X., and Mivechi, N.F. (2006). Critical role of Brg1 member of the SWI/SNF chromatin remodeling complex during neurogenesis and neural crest induction in zebrafish. *Dev Dyn* 235, 2722-2735.
- Felsenfeld, G., and Groudine, M. (2003). Controlling the double helix. *Nature* 421, 448-453.
- Fischle, W. (2005). In nucleosome enzymatic assays for the identification and characterization of histone modifying activities. *Methods* 36, 362-367.
- Fischle, W., Franz, H., Jacobs, S.A., Allis, C.D., and Khorasanizadeh, S. (2008). Specificity of the chromodomain Y chromosome family of chromodomains for lysine-methylated ARK(S/T) motifs. *J Biol Chem* 283, 19626-19635.
- Fischle, W., Tseng, B.S., Dormann, H.L., Ueberheide, B.M., Garcia, B.A., Shabanowitz, J., Hunt, D.F., Funabiki, H., and Allis, C.D. (2005). Regulation of HP1-chromatin binding by histone H3 methylation and phosphorylation. *Nature* 438, 1116-1122.
- Fischle, W., Wang, Y., and Allis, C.D. (2003a). Binary switches and modification cassettes in histone biology and beyond. *Nature* 425, 475-479.
- Fischle, W., Wang, Y., and Allis, C.D. (2003b). Histone and chromatin cross-talk. *Curr Opin Cell Biol* 15, 172-183.
- Fischle, W., Wang, Y., Jacobs, S.A., Kim, Y., Allis, C.D., and Khorasanizadeh, S. (2003c). Molecular basis for the discrimination of repressive methyl-lysine marks in histone H3 by Polycomb and HP1 chromodomains. *Genes Dev* 17, 1870-1881.

- Francis, N.J., Kingston, R.E., and Woodcock, C.L. (2004). Chromatin compaction by a polycomb group protein complex. *Science* **306**, 1574-1577.
- Franz, H., Mosch, K., Soeroes, S., Urlaub, H., and Fischle, W. (2009). Multimerization and H3K9me3 binding is required for CDYL1b heterochromatin association. *J Biol Chem* **5**, 5.
- Furman, S., Steingart, R.A., Mandel, S., Hauser, J.M., Brenneman, D.E., and Gozes, I. (2004). Subcellular localization and secretion of activity-dependent neuroprotective protein in astrocytes. *Neuron Glia Biol* **1**, 193-199.
- Gaudin, V., Libault, M., Pouteau, S., Juul, T., Zhao, G., Lefebvre, D., and Grandjean, O. (2001). Mutations in LIKE HETEROCHROMATIN PROTEIN 1 affect flowering time and plant architecture in Arabidopsis. *Development* **128**, 4847-4858.
- Gozes, I., and Brenneman, D.E. (2000). A new concept in the pharmacology of neuroprotection. *J Mol Neurosci* **14**, 61-68.
- Gozes, I., Morimoto, B.H., Tiong, J., Fox, A., Sutherland, K., Dangoor, D., Holser-Cochav, M., Vered, K., Newton, P., Aisen, P.S., *et al.* (2005). NAP: research and development of a peptide derived from activity-dependent neuroprotective protein (ADNP). *CNS Drug Rev* **11**, 353-368.
- Gozes, I., Zamostiano, R., Pinhasov, A., Bassan, M., Giladi, E., Steingart, R.A., and Brenneman, D.E. (2000). A novel VIP responsive gene. Activity dependent neuroprotective protein. *Ann N Y Acad Sci* **921**, 115-118.
- Grewal, S.I., and Elgin, S.C. (2007). Transcription and RNA interference in the formation of heterochromatin. *Nature* **447**, 399-406.
- Grunstein, M. (1997). Molecular model for telomeric heterochromatin in yeast. *Curr Opin Cell Biol* **9**, 383-387.
- Guccione, E., Bassi, C., Casadio, F., Martinato, F., Cesaroni, M., Schuchlautz, H., Luscher, B., and Amati, B. (2007). Methylation of histone H3R2 by PRMT6 and H3K4 by an MLL complex are mutually exclusive. *Nature* **449**, 933-937.
- Hansen, J.C. (2002). Conformational dynamics of the chromatin fiber in solution: determinants, mechanisms, and functions. *Annu Rev Biophys Biomol Struct* **31**, 361-392.
- Hansen, J.C. (2006). Linking genome structure and function through specific histone acetylation. *ACS Chem Biol* **1**, 69-72.
- Hansen, J.C., Tse, C., and Wolffe, A.P. (1998). Structure and function of the core histone N-termini: more than meets the eye. *Biochemistry* **37**, 17637-17641.
- Harnicarova Horakova, A., Galiova, G., Legartova, S., Kozubek, S., Matula, P., and Bartova, E. (2009). Chromocentre integrity and epigenetic marks. *J Struct Biol* **169**, 124-133.
- Hassa, P.O., Haenni, S.S., Elser, M., and Hottiger, M.O. (2006). Nuclear ADP-ribosylation reactions in mammalian cells: where are we today and where are we going? *Microbiol Mol Biol Rev* **70**, 789-829.
- Heintzman, N.D., Hon, G.C., Hawkins, R.D., Kheradpour, P., Stark, A., Harp, L.F., Ye, Z., Lee, L.K., Stuart, R.K., Ching, C.W., *et al.* (2009). Histone modifications at human enhancers reflect global cell-type-specific gene expression. *Nature* **459**, 108-112.

- Heitz, E. (1928). Das Heterochromatin der Moose. *Jahrb Wiss Botainik* 69, 762-818.
- Hill, D.A., Chiosea, S., Jamaluddin, S., Roy, K., Fischer, A.H., Boyd, D.D., Nickerson, J.A., and Imbalzano, A.N. (2004). Inducible changes in cell size and attachment area due to expression of a mutant SWI/SNF chromatin remodeling enzyme. *J Cell Sci* 117, 5847-5854.
- Hofmann, K. (2009). Ubiquitin-binding domains and their role in the DNA damage response. *DNA Repair (Amst)* 8, 544-556.
- Holbert, M.A., and Marmorstein, R. (2005). Structure and activity of enzymes that remove histone modifications. *Curr Opin Struct Biol* 15, 673-680.
- Huynh, V.A., Robinson, P.J., and Rhodes, D. (2005). A method for the in vitro reconstitution of a defined "30 nm" chromatin fibre containing stoichiometric amounts of the linker histone. *J Mol Biol* 345, 957-968.
- Iberg, A.N., Espejo, A., Cheng, D., Kim, D., Michaud-Levesque, J., Richard, S., and Bedford, M.T. (2008). Arginine methylation of the histone H3 tail impedes effector binding. *J Biol Chem* 283, 3006-3010.
- Ishizuka, T., and Lazar, M.A. (2003). The N-CoR/histone deacetylase 3 complex is required for repression by thyroid hormone receptor. *Mol Cell Biol* 23, 5122-5131.
- Jacobs, S.A., and Khorasanizadeh, S. (2002). Structure of HP1 chromodomain bound to a lysine 9-methylated histone H3 tail. *Science* 295, 2080-2083.
- Jacobs, S.A., Taverna, S.D., Zhang, Y., Briggs, S.D., Li, J., Eissenberg, J.C., Allis, C.D., and Khorasanizadeh, S. (2001). Specificity of the HP1 chromo domain for the methylated N-terminus of histone H3. *EMBO J* 20, 5232-5241.
- Jenuwein, T., and Allis, C.D. (2001). Translating the histone code. *Science* 293, 1074-1080.
- Johansen, K.M., and Johansen, J. (2006). Regulation of chromatin structure by histone H3S10 phosphorylation. *Chromosome Res* 14, 393-404.
- Johnson, A., Li, G., Sikorski, T.W., Buratowski, S., Woodcock, C.L., and Moazed, D. (2009). Reconstitution of heterochromatin-dependent transcriptional gene silencing. *Mol Cell* 35, 769-781.
- Kalakonda, N., Fischle, W., Boccuni, P., Gurvich, N., Hoya-Arias, R., Zhao, X., Miyata, Y., Macgrogan, D., Zhang, J., Sims, J.K., *et al.* (2008). Histone H4 lysine 20 monomethylation promotes transcriptional repression by L3MBTL1. *Oncogene* 27, 4293-4304.
- Karagianni, P., Amazit, L., Qin, J., and Wong, J. (2008). ICBP90, a novel methyl K9 H3 binding protein linking protein ubiquitination with heterochromatin formation. *Mol Cell Biol* 28, 705-717.
- Katsetos, C.D., Legido, A., Perentes, E., and Mork, S.J. (2003). Class III beta-tubulin isotype: a key cytoskeletal protein at the crossroads of developmental neurobiology and tumor neuropathology. *J Child Neurol* 18, 851-866; discussion 867.
- Koester-Eiserfunke, N. (2010). Characterization of Lin-61 methyl mark binding and its function in *C. elegans* vulva development. In Group of Chromatin Biochemistry (Goettingen, Max Planck Institute for Biophysical Chemistry).

- Koonin, E.V., Zhou, S., and Lucchesi, J.C. (1995). The chromo superfamily: new members, duplication of the chromo domain and possible role in delivering transcription regulators to chromatin. *Nucleic Acids Res* 23, 4229-4233.
- Kornberg, R.D. (1974). Chromatin structure: a repeating unit of histones and DNA. *Science* 184, 868-871.
- Kouzarides, T. (2007). Chromatin modifications and their function. *Cell* 128, 693-705.
- L. Vandel, E.N., O. Vaute, R. Ferreira, S. Ait-Si-Ali and D. Trouche (2001). Transcriptional repression by the retinoblastoma protein through the recruitment of a histone methyltransferase. *Mol Cell Biol* 21, 6484-6494.
- Lachner, M., O'Carroll, D., Rea, S., Mechtler, K., and Jenuwein, T. (2001). Methylation of histone H3 lysine 9 creates a binding site for HP1 proteins. *Nature* 410, 116-120.
- Laemmli, U.K. (1970). Cleavage of structural proteins during the assembly of the head of bacteriophage T4. *Nature* 227, 680-685.
- Lander, E.S., Linton, L.M., Birren, B., Nusbaum, C., Zody, M.C., Baldwin, J., Devon, K., Dewar, K., Doyle, M., FitzHugh, W., *et al.* (2001). Initial sequencing and analysis of the human genome. *Nature* 409, 860-921.
- Lee, B.M., and Mahadevan, L.C. (2009). Stability of histone modifications across mammalian genomes: implications for 'epigenetic' marking. *J Cell Biochem* 108, 22-34.
- Lehnertz, B., Ueda, Y., Derijck, A.A., Braunschweig, U., Perez-Burgos, L., Kubicek, S., Chen, T., Li, E., Jenuwein, T., and Peters, A.H. (2003). Suv39h-mediated histone H3 lysine 9 methylation directs DNA methylation to major satellite repeats at pericentric heterochromatin. *Curr Biol* 13, 1192-1200.
- Linder, B., Gerlach, N., and Jackle, H. (2001). The Drosophila homolog of the human AF10 is an HP1-interacting suppressor of position effect variegation. *EMBO Rep* 2, 211-216.
- Lowary, P.T., and Widom, J. (1998). New DNA sequence rules for high affinity binding to histone octamer and sequence-directed nucleosome positioning. *J Mol Biol* 276, 19-42.
- Luger, K., Mader, A.W., Richmond, R.K., Sargent, D.F., and Richmond, T.J. (1997). Crystal structure of the nucleosome core particle at 2.8 Å resolution. *Nature* 389, 251-260.
- Luger, K., Rechsteiner, T.J., and Richmond, T.J. (1999). Preparation of nucleosome core particle from recombinant histones. *Methods Enzymol* 304, 3-19.
- Maison, C., Bailly, D., Peters, A.H., Quivy, J.P., Roche, D., Taddei, A., Lachner, M., Jenuwein, T., and Almouzni, G. (2002). Higher-order structure in pericentric heterochromatin involves a distinct pattern of histone modification and an RNA component. *Nat Genet* 30, 329-334.
- Mandel, S., and Gozes, I. (2007). Activity-dependent neuroprotective protein constitutes a novel element in the SWI/SNF chromatin remodeling complex. *J Biol Chem* 282, 34448-34456.
- Mandel, S., Rechavi, G., and Gozes, I. (2007). Activity-dependent neuroprotective protein (ADNP) differentially interacts with chromatin to regulate genes essential for embryogenesis. *Dev Biol* 303, 814-824.
- Mangenot, S., Leforestier, A., Vachette, P., Durand, D., and Livolant, F. (2002). Salt-induced conformation and interaction changes of nucleosome core particles. *Biophys J* 82, 345-356.

- Martens, J.H., O'Sullivan, R.J., Braunschweig, U., Opravil, S., Radolf, M., Steinlein, P., and Jenuwein, T. (2005). The profile of repeat-associated histone lysine methylation states in the mouse epigenome. *EMBO J* 24, 800-812.
- Melcher, M., Schmid, M., Aagaard, L., Selenko, P., Laible, G., and Jenuwein, T. (2000). Structure-function analysis of SUV39H1 reveals a dominant role in heterochromatin organization, chromosome segregation, and mitotic progression. *Mol Cell Biol* 20, 3728-3741.
- Metzger, E., Wissmann, M., Yin, N., Muller, J.M., Schneider, R., Peters, A.H., Gunther, T., Buettnner, R., and Schule, R. (2005). LSD1 demethylates repressive histone marks to promote androgen-receptor-dependent transcription. *Nature* 437, 436-439.
- Mikkelsen, T.S., Ku, M., Jaffe, D.B., Issac, B., Lieberman, E., Giannoukos, G., Alvarez, P., Brockman, W., Kim, T.K., Koche, R.P., *et al.* (2007). Genome-wide maps of chromatin state in pluripotent and lineage-committed cells. *Nature* 448, 553-560.
- Mujtaba, S., Zeng, L., and Zhou, M.M. (2007). Structure and acetyl-lysine recognition of the bromodomain. *Oncogene* 26, 5521-5527.
- Muller, H.J., and Altenburg, E. (1930). The Frequency of Translocations Produced by X-Rays in *Drosophila*. *Genetics* 15, 283-311.
- Nathan, D., Ingvarsdottir, K., Sterner, D.E., Bylebyl, G.R., Dokmanovic, M., Dorsey, J.A., Whelan, K.A., Krsmanovic, M., Lane, W.S., Meluh, P.B., *et al.* (2006). Histone sumoylation is a negative regulator in *Saccharomyces cerevisiae* and shows dynamic interplay with positive-acting histone modifications. *Genes Dev* 20, 966-976.
- Nelson, C.J., Santos-Rosa, H., and Kouzarides, T. (2006). Proline isomerization of histone H3 regulates lysine methylation and gene expression. *Cell* 126, 905-916.
- Nielsen, A.L., Oulad-Abdelghani, M., Ortiz, J.A., Remboutsika, E., Chambon, P., and Losson, R. (2001a). Heterochromatin formation in mammalian cells: interaction between histones and HP1 proteins. *Mol Cell* 7, 729-739.
- Nielsen, P.R., Nietlispach, D., Mott, H.R., Callaghan, J.M., Bannister, A.J., Kouzarides, T., Murzin, A.G., Murzina, N.V., and Laue, E.D. (2002). Structure of the HP1 chromodomain bound to histone H3 methylated at lysine 9. *Nature* 416, 103-107.
- Nielsen, S.J., Schneider, R., Bauer, U.M., Bannister, A.J., Morrison, A., O'Carroll, D., Firestein, R., Cleary, M., Jenuwein, T., Herrera, R.E., *et al.* (2001b). Rb targets histone H3 methylation and HP1 to promoters. *Nature* 412, 561-565.
- Nowak, S.J., and Corces, V.G. (2004). Phosphorylation of histone H3: a balancing act between chromosome condensation and transcriptional activation. *Trends Genet* 20, 214-220.
- Nozawa, N.S., K., N., H.T., M., O., I., T., H., N., N., H., K., and C., O. (2010). Human POGZ modulates dissociation of HP1alpha from mitotic chromosome arms through Aurora B activation. *Nat Cell Biol*.
- Olins, A.L., and Olins, D.E. (1974). Spheroid chromatin units (v bodies). *Science* 183, 330-332.
- Ong, S.E., and Mann, M. (2005). Mass spectrometry-based proteomics turns quantitative. *Nat Chem Biol* 1, 252-262.

- Ong, S.E., and Mann, M. (2006). A practical recipe for stable isotope labeling by amino acids in cell culture (SILAC). *Nat Protoc* *1*, 2650-2660.
- Peters, A.H., Kubicek, S., Mechtler, K., O'Sullivan, R.J., Derijck, A.A., Perez-Burgos, L., Kohlmaier, A., Opravil, S., Tachibana, M., Shinkai, Y., *et al.* (2003). Partitioning and plasticity of repressive histone methylation states in mammalian chromatin. *Mol Cell* *12*, 1577-1589.
- Peters, A.H., O'Carroll, D., Scherthan, H., Mechtler, K., Sauer, S., Schofer, C., Weipoltshammer, K., Pagani, M., Lachner, M., Kohlmaier, A., *et al.* (2001). Loss of the Suv39h histone methyltransferases impairs mammalian heterochromatin and genome stability. *Cell* *107*, 323-337.
- Peterson, C.L., and Laniel, M.A. (2004). Histones and histone modifications. *Curr Biol* *14*, R546-551.
- Pinhasov, A., Mandel, S., Torchinsky, A., Giladi, E., Pittel, Z., Goldsweig, A.M., Servoss, S.J., Brenneman, D.E., and Gozes, I. (2003). Activity-dependent neuroprotective protein: a novel gene essential for brain formation. *Brain Res Dev Brain Res* *144*, 83-90.
- Platero J.S., H.T., and Eissenberg J.C. (1995). Functional analysis of the chromo domain of HP1. *EMBO J*, 3977-3986.
- Platero, J.S., Hartnett, T., and Eissenberg, J.C. (1995). Functional analysis of the chromo domain of HP1. *EMBO J*, 3977-3986.
- Prigent, C., and Dimitrov, S. (2003). Phosphorylation of serine 10 in histone H3, what for? *J Cell Sci* *116*, 3677-3685.
- Przewloca, M.R., and Glower, M.G. (2009). The Kinetochores and the Centromere: A Working Long Distance Relationship. *Annu Rev Genet* *43*, 439-465.
- Qian, C., and Zhou, M.M. (2006). SET domain protein lysine methyltransferases: Structure, specificity and catalysis. *Cell Mol Life Sci* *63*, 2755-2763.
- Qu, J.H., Cheng, J., Zhang, L.X., Zhong, Y.W., Liu, Y., Wang, L., and Dai, J.Z. (2005). [Screening of binding proteins to interferon-alpha promoter DNA by phage display technique]. *Zhonghua Gan Zang Bing Za Zhi* *13*, 520-523.
- Quintana, F.J., Zaltzman, R., Fernandez-Montesinos, R., Herrera, J.L., Gozes, I., Cohen, I.R., and Pozo, D. (2006). NAP, a peptide derived from the activity-dependent neuroprotective protein, modulates macrophage function. *Ann N Y Acad Sci* *1070*, 500-506.
- Reik, W., Dean, W., and Walter, J. (2001). Epigenetic reprogramming in mammalian development. *Science* *293*, 1089-1093.
- Reuter, G., Gausz, J., Gyurkovics, H., Friede, B., Bang, R., Spierer, A., Hall, L.M., and Spierer, P. (1987). Modifiers of position-effect variegation in the region from 86C to 88B of the *Drosophila melanogaster* third chromosome. *Mol Gen Genet* *210*, 429-436.
- Rosenfeld, J.A., Wang, Z., Schones, D.E., Zhao, K., DeSalle, R., and Zhang, M.Q. (2009). Determination of enriched histone modifications in non-genic portions of the human genome. *BMC Genomics* *10*, 143.
- Rosson, G.B., Bartlett, C., Reed, W., and Weissman, B.E. (2005). BRG1 loss in MiaPaCa2 cells induces an altered cellular morphology and disruption in the organization of the actin cytoskeleton. *J Cell Physiol* *205*, 286-294.

Rountree, M.R., Bachman, K.E., and Baylin, S.B. (2000). DNMT1 binds HDAC2 and a new co-repressor, DMAP1, to form a complex at replication foci. *Nat Genet* 25, 269-277.

Sambrook, J., and Russel, D. (2001). *Molecular Cloning. A laboratory Manual*, 3rd edn (Cold Spring Harbor, New York, Cold Spring Harbor Laboratory Press).

Sampath, S.C., Marazzi, I., Yap, K.L., Sampath, S.C., Krutchinsky, A.N., Mecklenbrauker, I., Viale, A., Rudensky, E., Zhou, M.M., Chait, B.T., *et al.* (2007). Methylation of a histone mimic within the histone methyltransferase G9a regulates protein complex assembly. *Mol Cell* 27, 596-608.

Sari, Y., and Gozes, I. (2006). Brain deficits associated with fetal alcohol exposure may be protected, in part, by peptides derived from activity-dependent neurotrophic factor and activity-dependent neuroprotective protein. *Brain Res Rev* 52, 107-118.

Schotta, G., Lachner, M., Sarma, K., Ebert, A., Sengupta, R., Reuter, G., Reinberg, D., and Jenuwein, T. (2004). A silencing pathway to induce H3-K9 and H4-K20 trimethylation at constitutive heterochromatin. *Genes Dev* 18, 1251-1262.

Schultz, D.C., Ayyanathan, K., Negorev, D., Maul, G.G., and Rauscher, F.J., 3rd (2002). SETDB1: a novel KAP-1-associated histone H3, lysine 9-specific methyltransferase that contributes to HP1-mediated silencing of euchromatic genes by KRAB zinc-finger proteins. *Genes Dev* 16, 919-932.

Seet, B.T., Dikic, I., Zhou, M.M., and Pawson, T. (2006). Reading protein modifications with interaction domains. *Nat Rev Mol Cell Biol* 7, 473-483.

Selmi, C., Lleo, A., Zuin, M., Podda, M., Rossaro, L., and Gershwin, M.E. (2006). Interferon alpha and its contribution to autoimmunity. *Curr Opin Investig Drugs* 7, 451-456.

Seo, S., Richardson, G.A., and Kroll, K.L. (2005). The SWI/SNF chromatin remodeling protein Brg1 is required for vertebrate neurogenesis and mediates transactivation of Ngn and NeuroD. *Development* 132, 105-115.

Sharma, K., Weber, C., Bairlein, M., Greff, Z., Kéri, G., Cox, J., Olsen, J.V., and Daub, H. (2009). Proteomics strategy for quantitative protein interaction profiling in cell extracts. *Natue Methods* 6, 741-744.

Shevchenko, A., Wilm, M., Vorm, O., and Mann, M. (1996). Mass spectrometric sequencing of proteins silver-stained polyacrylamide gels. *Anal Chem* 68, 850-858.

Shogren-Knaak, M., Ishii, H., Sun, J.M., Pazin, M.J., Davie, J.R., and Peterson, C.L. (2006). Histone H4-K16 acetylation controls chromatin structure and protein interactions. *Science* 311, 844-847.

Shogren-Knaak, M.A., and Peterson, C.L. (2004). Creating designer histones by native chemical ligation. *Methods Enzymol* 375, 62-76.

Sigalov, E., Fridkin, M., Brenneman, D.E., and Gozes, I. (2000). VIP-Related protection against Iodoacetate toxicity in pheochromocytoma (PC12) cells: a model for ischemic/hypoxic injury. *J Mol Neurosci* 15, 147-154.

Simone, C. (2006). SWI/SNF: the crossroads where extracellular signaling pathways meet chromatin. *J Cell Physiol* 207, 309-314.

Smothers, J.F., and Henikoff, S. (2000). The HP1 chromo shadow domain binds a consensus peptide pentamer. *Curr Biol*, 27-30.

- Soeroes, S. (2010). H3K9me3 dependent HP1 chromatin association and its consequences for chromatin packaging. In Group of Chromatin Biochemistry (Goettingen, Max Planck Institute for Biophysical Chemistry).
- Steingart, R.A., and Gozes, I. (2006). Recombinant activity-dependent neuroprotective protein protects cells against oxidative stress. *Mol Cell Endocrinol* 252, 148-153.
- Sterner, D.E., and Berger, S.L. (2000). Acetylation of histones and transcription-related factors. *Microbiol Mol Biol Rev* 64, 435-459.
- Stewart, M.D., Li, J., and Wong, J. (2005). Relationship between histone H3 lysine 9 methylation, transcription repression, and heterochromatin protein 1 recruitment. *Mol Cell Biol* 25, 2525-2538.
- Strahl, B.D., and Allis, C.D. (2000). The language of covalent histone modifications. *Nature* 403, 41-45.
- Struhl, K. (1998). Histone acetylation and transcriptional regulatory mechanisms. *Genes Dev* 12, 599-606.
- Taverna, S.D., Li, H., Ruthenburg, A.J., Allis, C.D., and Patel, D.J. (2007). How chromatin-binding modules interpret histone modifications: lessons from professional pocket pickers. *Nat Struct Mol Biol* 14, 1025-1040.
- Thastrom, A., Lowary, P.T., Widlund, H.R., Cao, H., Kubista, M., and Widom, J. (1999). Sequence motifs and free energies of selected natural and non-natural nucleosome positioning DNA sequences. *J Mol Biol* 288, 213-229.
- Thiru, A., Nietlispach, D., Mott, H.R., Okuwaki, M., Lyon, D., Nielsen, P.R., Hirshberg, M., Verreault, A., Murzina, N.V., and Laue, E.D. (2004). Structural basis of HP1/PXVXL motif peptide interactions and HP1 localisation to heterochromatin. *Embo J* 23, 489-499.
- Thomas, J.O. (1999). Histone H1: location and role. *Curr Opin Cell Biol* 11, 312-317.
- van Attikum, H., and Gasser, S.M. (2009). Crosstalk between histone modifications during the DNA damage response. *Trends Cell Biol* 19, 207-217.
- Vassallo, M.F., and Tanese, N. (2002). Isoform-specific interaction of HP1 with human TAFII130. *Proc Natl Acad Sci U S A* 99, 5919-5924.
- Vermeulen, M., Mulder, K.W., Denissov, S., Pijnappel, W.W., van Schaik, F.M., Varier, R.A., Baltissen, M.P., Stunnenberg, H.G., Mann, M., and Timmers, H.T. (2007). Selective anchoring of TFIID to nucleosomes by trimethylation of histone H3 lysine 4. *Cell* 131, 58-69.
- Wang, H., An, W., Cao, R., Xia, L., Erdjument-Bromage, H., Chatton, B., Tempst, P., Roeder, R.G., and Zhang, Y. (2003). mAM facilitates conversion by ESET of dimethyl to trimethyl lysine 9 of histone H3 to cause transcriptional repression. *Mol Cell* 12, 475-487.
- Wang, Z., Schones, D.E., and Zhao, K. (2009). Characterization of human epigenomes. *Curr Opin Genet Dev* 19, 127-134.
- Weake, V.M., and Workman, J.L. (2008). Histone ubiquitination: triggering gene activity. *Mol Cell* 29, 653-663.
- Weiler, K.S., and Wakimoto, B.T. (1995). Heterochromatin and gene expression in *Drosophila*. *Annu Rev Genet* 29, 577-605.

Wustmann, G., Szidonya, J., Taubert, H., and Reuter, G. (1989). The genetics of position-effect variegation modifying loci in *Drosophila melanogaster*. *Mol Gen Genet* 217, 520-527.

Wysocka, J., Swigut, T., Milne, T.A., Dou, Y., Zhang, X., Burlingame, A.L., Roeder, R.G., Brivanlou, A.H., and Allis, C.D. (2005). WDR5 associates with histone H3 methylated at K4 and is essential for H3 K4 methylation and vertebrate development. *Cell* 121, 859-872.

Zamostiano, R., Pinhasov, A., Gelber, E., Steingart, R.A., Seroussi, E., Giladi, E., Bassan, M., Wollman, Y., Eyre, H.J., Mulley, J.C., *et al.* (2001). Cloning and characterization of the human activity-dependent neuroprotective protein. *J Biol Chem* 276, 708-714.

Zeng, L., and Zhou, M.M. (2002). Bromodomain: an acetyl-lysine binding domain. *FEBS Lett* 513, 124-128.

Zhang, Y., and Reinberg, D. (2001). Transcription regulation by histone methylation: interplay between different covalent modifications of the core histone tails. *Genes Dev* 15, 2343-2360.

Zhao, T., Heyduk, T., Allis, C.D., and Eissenberg, J.C. (2000). Heterochromatin protein 1 binds to nucleosomes and DNA in vitro. *J Biol Chem* 275, 28332-28338.

6 Curriculum vitae

Personal Details

Name: Kerstin Mosch
Date of birth: August 14, 1970
Place of birth: Dresden, Germany
Nationality: German

Work Experience:

10.2005 – 12.2005 Biotechnological Centre of the TU Dresden, Proteomics group
/Genomics group; Student assistant

08.2004 – 11.2004 Biotechnological Centre of the TU Dresden, Proteomics group;
Student assistant

05.2004 – 08.2004 Biotechnological Centre of the TU Dresden, Bioinformatics group;
Student assistant

08.2002 – 09.2002 Institut of Polymer Research, Dresden; Internship

08.2001 – 09.2001 TU Dresden, Institut of Zoology; Student assistant

02.1994 – 04.2000 Dresdner Bank AG in Dresden; Bank employee

education

since 07/2006 GGNB “Molecular Biology of Microbial, Animal and Plant Cells”,
Georg-August-University Göttingen

PhD studies, Thesis: “Identification and characterization of ADNP as a novel heterochromatin component”

03.2005 – 09.2005 Biotechnological Centre of the TU Dresden
Master studies, Thesis: “Generation of recombinant adenoviruses for functional analysis of osteoclasts”

04.2003 – 08.2003 TU Dresden, Institut of Zoology
Bachelor studies, Thesis: “Nachweis von Varianten der Östrogenrezeptoren α und β in Gebärmutterkarzinomzelllinien”

09.1997 – 07.2000 Abendgymnasium Dresden; Abitur

Stipends

2006 - 2008 Max-Planck-Institute stipend

Publications

Franz, H., Sörös, S., Mosch, K., Urlaub, H., and W. Fischle, Multimerization and H3K9me3 binding is required for CDYL1b heterochromatin association. *J Biol Chem*, 2009; Dec 11;284(50):35049-59

Heckel T, Czupalla C, Expirto Santo AI, Anitei M, Arantzazu Sanchez-Fernandez M, Mosch K, Krause E and Hoflack B., Src-dependent repression of ARF6 is required to maintain podosome-rich sealing zones in bone-digesting osteoclasts. *Proc Natl Acad Sci USA*, 2009 Feb 3; 106(5):1451-6

Zhang K, Mosch K, Fischle W and Grewal SI., Roles of the Ctr4 methyltransferase complex in nucleation, spreading and maintenance of heterochromatin. *Nat Struct Mol Biol*. 2008 Apr; 15(4):381-8.